



This is to certify that the

thesis entitled

SCAPULAR DISPLACEMENT BY DIFFERENTIAL MOIRE METHODS

presented by

Paul John Moga

has been accepted towards fulfillment of the requirements for

M.S. degree in Biomechanics

Major professor

Gary L. Cloud, Ph.D.

Date 15 May 1992

# LIBRARY Michigan State University

PLACE IN RETURN BOX to remove this checkout from your record. TO AVOID FINES return on or before date due.

DATE DUE	DATE DUE	DATE DUE

MSU Is An Affirmative Action/Equal Opportunity Institution c:circidatedus.pm3-p.1

## SCAPULAR DISPLACEMENT BY DIFFERENTIAL MOIRE METHODS

Ву

Paul John Moga

#### A THESIS

Submitted to
Michigan State University
in partial fulfillment of the requirements
for the degree of

MASTER OF SCIENCE

Department of Biomechanics

1992

#### **ABSTRACT**

### SCAPULAR DISPLACEMENT BY DIFFERENTIAL MOIRE METHODS

By

#### Paul John Moga

In this pilot study, non-contact, non-invasive differential moire methods were applied in order to quantify the displacement of the human inferior scapular angle. The technique utilizes moire fringes, which are produced by the optical interference of two superimposed gratings consisting of equidistant, alternating lines and spaces. Here, they were created by double-exposing thirty-five millimeter black and white film. The first exposure of the scapular region was taken with the parascapular muscles at rest and the second during incremented percentages of maximum voluntary contraction in isometric arm adduction. The frontal plane (inplane, x-axis) shift of the scapular reference mark relative to the midline was determined from the photographic data. Sequential fringe order values, N, when coupled with factors as projected grating pitch and the geometric relationships of the experimental apparatus were then used to calculate the sagittal plane (out-ofplane, z-axis) displacement of the inferior angle of the scapula. The in-plane, medial displacement averaged 9.8mm, ±0.9mm, and the out-of-plane, posterior displacement averaged 22.97mm, ±0.9mm, both at 70% of maximal voluntary scapular adduction.

Key Words: Moire, Scapula, Displacement.

Copyright by:
PAUL JOHN MOGA
1992

To the Creator Who guides us all along the Path.

#### **ACKNOWLEDGEMENTS**

I would first like to thank my Committee members for their guidance and support throughout the course of my graduate program. My Major Professor, Gary L. Cloud, Ph.D., Department of Mechanics and Materials Science, demonstrated great patience in his countless reviews of this thesis. The other two members, H.M. Reynolds, Ph.D. and J.J. Rechtien, D.O., Ph.D., both from the Department of Biomechanics, College of Osteopathic Medicine, continually gave invaluable input. "Mac" Reynolds helped me to wade through the early years of graduate study, generally being right in the advise he would give. Jim Rechtien added his clinical expertise to my coursework.

Various other faculty, staff, and fellow grad students of the Department were all more than happy to give of their time, particularly Bob Hubbard, Ph.D., R.W. Soutas-Little, Ph.D., and Roger Haut, Ph.D. For their contributions to my background in Biomechanics, I am thankful. Staffers Brenda, Sharon, and LeAnn made it easier to muddle through the administrative glitches. Students as Joia, Mike, Kathy, "Molson", Steve, and Klemens, and especially my office-mate and friend Ray Fredericksen, provided the comraderie that

kept everything from getting too serious.

Shae Schoefelt did a superb job in her processing of the photographic negatives. The folks at Quicksilver Photographic provided excellent photo lab results and, together with others as Photomart of Lansing, were always able to give good technical pointers.

I would like to give my heartfelt thanks to my family for the integral part that they played in this thesis.

First, to the memory of my grandparents - Pavel Nestor and Raveica Tamaş Moga, Ioniţa "Teischleru" and Cristina Cicalé Sakula (Secula), who taught us Faith and hard work. Thanks to the "eager" pilot study assistants, brother Tom, Gary, and Dean, who gave of their time in the early phases of the project. Debbie trekked through the first hand-written drafts, converting them into a logical sequence. Brother John (and Yehudit) expertly laboured to prepare some of the graphics for presentation. A special thanks goes out to my parents, Traian and Anna, who, as they always have, supported the efforts of their children, in this case, helping to design and build the apparatus, collect the data, and present the early results in a recognizable form.

Finally, I would like to recognize the tolerance of my wife, Kris, who has stood by throughout the lean times and "ups and downs" of my graduate career, helping me to see the rays of light seeping down through the trees.

#### TABLE OF CONTENTS

			Page
LIST OF F	IGURE	S	ix
LIST OF T	ABLES	• • • • • • • • • • • • • • • • • • • •	.xii
KEY TO SY	MBOLS	AND NOMENCLATURE	xiii
CHAPTER			
I. I	NTROD	UCTION	1
	1.1 1.2 1.3 1.4 1.5	Applied Problem	1
II.		DEVELOPMENT OF A DIFFERENTIAL MOIRE FOR USE IN HUMAN SUBJECTS	
	2.1 2.2 2.3	Abstract Introduction Literature Review	8
	2.4	2.3.2 Biological Applications  Materials and Methods	17
	2.5 2.6 2.7	Results Discussion Summary	23
III.		References for Chapter II  ULAR INFERIOR ANGLE OUT-OF-PLANE DISPLAC G DIFFERENTIAL MOIRE METHODS	EMENT
	3.1 3.2 3.3	Abstract	31
		3.4.1 Apparatus	41

TABLE OF	CONT	ENTS (con'd)	Page
		3.4.4 Photographic Methods	
		3.4.5 Data Processing	
		3.4.6 Displacement Calculations	
	3.5	Results	
		3.5.1 Fringe Patterns	
		3.5.2 Displacement Graphs	
	3.6	Discussion	
		3.6.1 Apparatus and Protocol	
		3.6.2 Graphs	
		3.6.3 Measurement Variation	
		3.6.4 Reassignment of N	62
	3.7		65
		3.7.1 Suggestions: Further Stud	y66
	3.8		69
	3.9	References for Chapter III	74
	002		D. 1.
IV.		PULAR OUT-OF-PLANE DISPLACEMENT IN LATE	
	BRNI	DING USING DIFFERENTIAL MOIRE	75
		93s was one was	
	4.1		
	4.2		
	4.3		
		4.3.1 Protocol	
	4.4		
		4.4.1 Fringe Patterns	84
		4.4.2 Displacement Values	
	4.5		
	4.6	Conclusions	97
v.	CONC	LUDING REMARKS AND SUMMARY	100
	5.1		
	5.2		
	5.3		
	5.4		109
	5.5		111
	5.6	Applications	114
A DOGMOTO	P.C		115
APPENDIC	BD	• • • • • • • • • • • • • • • • • • • •	113
	A.	Anatomy	115
		A.1 Osteology	
		A.2 Musculature	
	в.	Pathology	
	c.	Human Use Committee Consent Forms	
	D.	Proposed Budget	
	J.	rroposed budget	133
LIST OF	REFERI	ences	136
	Con	eral References	120
	\ <b>7</b> ₩116	C.A.L. N.C.L.C.L.C.L.C.C.C.C.C.C.C.C.C.C.C.C.C.	

#### LIST OF FIGURES

Figure	
CHAPTI	R II
2.1	Watered Silk (adapted from Oster & Nishijima, 1963)9
2.2	Two Superimposed Grating Patterns & Grating Pitch, p (adapted from Oster & Nishijima, 1963)9
2.3	Shadow Moire Method (adapted from Rogers, et al, 1979) Copyright 1991 Society for Experimental Mechanics, with permission
2.4	Projection Moire Method (adapted from Rogers, et al, 1979) Copyright 1991 Society for Experimental Mechanics, with permission
2.5	Grating Jig19
2.6	Experimental Apparatus (Copyright 1991 Society for Experimental Mechanics, with permission)20
2.7	Projected Grating Pattern24
2.8	Moire Fringe Pattern25
CHAPTI	R III
3.1	Geometry (adapted from Roger, et al., 1979)34
3.2	Geometry (adapted from Khetan, 1975) Copyright 1991 Society for Experimental Mechanics, with permission
3.3	Test Apparatus-Aluminum Bar/Strain Gage38
3.4	Subject Labelling and Landmark "Pairs"43
3.5	Fringe Progression and Fringe Values (N)53
2 (	\$161G

Figure	Page
3.7	x vs. %MVC56
3.8	w vs. %MVC57
3.9	w <sub>d</sub> vs. %MVC57
3.10	N vs. %MVC58
3.11	d vs. %MVC58
3.12	N (Re-estimated) vs. %MVC64
3.13	d(new) vs. %MVC64
3.8.1	Clavicular Ligaments (adapted from Goss, 1974 and Warfel, 1974)70
3.8.2	Shoulder Complex Axes (adapted from Nordin & Frankel, 1989)71
3.8.3	Inferior Angle Displacement and Z-axis Motion in Abduction (adapted from Dvir & Berme, 1978 and Nordin & Frankel, 1989)
CHAPTER	IV
4.1 G	oniometer80
4.2 F	ringe Progression in Flexion85
4.3 F	ringe Progression in Extension86
4.4 F	ringe Progression in Rotation87
	ringe Progression in Left Lateral Bending, with endulum Goniometer89
4.6 F	ringe Appearance in a Combination of Postures91
4.7 N	vs. %MVC (Lateral Bending)94
4.8 d	vs. %MVC (Lateral Bending)94

Parascapular Muscles (adapted from Goss,

A.2

#### LIST OF TABLES

Table	Page
СНАРТ	ER II
2.1	Dimensions and Methods from Previous Studies21
СНАРТ	ER III
3.1	<b>%MVC Values</b> (in Pounds)45
3.2	Raw Data Scaling Factor48
3.3	$\mathbf{x}_{so}$ , $\mathbf{x}$ , and N Values49
3.4	Formulae50
3.5	w, $w_d$ , d, and d/N Values51
3.6	d vs. Force, Height, Weight, Age, and Moment Arm Length68
СНАРТ	ER IV
4.1	$x_{so}$ , $x$ , and N Values82
4.2	N (Re-estimated to 0.05), $w_d$ , d, and d/N Values83
4.3	x <sub>so</sub> , x Values: Neutral vs. Lateral Bending96
APPEN	DICES
A.1	Scapular Adductors119
B.1	Neuropathies126
B 2	Myonathies 127

#### KEY TO COMMONLY USED NOMENCLATURE

- p = Pitch, distance between grating lines, center to center
- N = Fringe Order
- w = z-axis coordinate value undisplaced
- $w_d$  = z-axis coordinate of the point P displaced
- $d = Displacement, or w_d w$
- $x_{\infty}$  = x-axis coordinate of point P undisplaced
- x = x-axis coordinate of point P displaced
- $\theta$  = Angle between camera and projector optical axes
- MVC = Maximum Voluntary Contraction
- C = Cervical
- T = Thoracic
- L = Left
- R = Right
- Note. Other symbols are explained in their context at the time of their use.

#### CHAPTER I

#### INTRODUCTION

#### 1.1 APPLIED PROBLEM

The shoulder apparatus is a complex mechanism, moving about several axes in many planes throughout its range of motion (Dvir & Berme, 1978; Inman, 1944). The scapula plays an integral role in the overall function of this complex. Its normal activity may be influenced by trauma, developmental defects, or pathological processes (Appendix B, page 122), including changes in neuromuscular function (Beeson & McDermott, 1975). The quantification of normal function - range of motion, displacement, and even muscle activation sequence may be helpful in assessing the amount of dysfunction, in diagnosing disease processes, or in monitoring rehabilitation and gauging therapeutic regimens.

#### 1.2 THEORETICAL PROBLEM

Moire fringe methods are non-invasive and non-contact techniques that have had applications to biological systems (Takasaki, 1970; Adair, et al., 1977; Andonian, 1984).

These methods have been refined for quantitative use in determining surface point displacement (Khetan, 1975). For

practicality and clinical usefulness, it is necessary to adapt these approaches to a protocol which will allow ease of subject application and simplicity of data acquisition. Furthermore, data reduction methods must also be improved to permit efficient handling of the data. These methods, with the aforementioned improvements, may be applied to the shoulder complex to assist in defining scapular kinematics.

#### 1.3 THESIS STATEMENT

This thesis has several hypotheses:

- Moire fringe methods may be developed to enable reliable and reproduceable study of human topography to quantify surface landmark motion.
- 2). The adaptation of the method may result in a quantification of surface point movement.
- 3). The graded, out-of-plane displacement of the inferior scapular angle corresponds to incremented muscular contraction of the parascapular and shoulder complex musculature.
- 4). To a limited extent, spurious positioning of the subject in the same plane as the scapular movement in "neutral" should do little to affect the data.

5). The reduced data may ultimately supply information which helps to define scapular motion and potentially lend itself to clinical application.

#### 1.4 RESEARCH OBJECTIVES

It naturally follows that the thesis research objectives are:

- To develop a single-source, projection moire protocol to be used in studying landmark motion of the human subject.
- To apply this method to an investigation of scapular movement.
- 3). To determine the in-plane and out-of-plane displacement of the inferior scapular angle.
- 4). To develop a second protocol to partially define scapular landmark displacement in postures other than the upright "neutral" position.
- 5). To attempt to determine if the data from this postural variation has a large impact on scapular inferior angle displacement.

#### 1.5 THESIS ORGANIZATION

The thesis is written partly as a collection of distinct papers or Chapters. Chapter II outlines the development of the moire technique for use on human subjects. Chapter III reviews the application of the differential moire method toward the delineation of the inplane and out-of-plane displacement of the inferior scapular angle. In an effort to differentiate true displacement from contaminated data, Chapter IV describes an additional study in which the subject's test position is purposefully altered to determine what, if any, changes in the results come from postural shifts. Finally, assumptions, limitations, concluding remarks, and recommendations for further study are set forth in Chapter V.

In addition to the chapters, several appendices serve to augment the text with information on basic anatomy, pathology, and kinematics. All of these sections contain figures and/or tables, which are generally presented either on the page of their citation or on the page following.

For each chapter, any outside sources cited are listed separately in Reference sections found at the ends of the chapters and collectively at the end of the thesis. Those sources used for general knowledge and not specifically cited are also listed in the Cumulative Reference section under the title General References.

#### CHAPTER II

# THE DEVELOPMENT OF A DIFFERENTIAL MOIRE FRINGE METHOD FOR USE IN HUMAN SUBJECTS

#### 2.1 ABSTRACT

Moire fringe techniques have been used in engineering to study strain and the deformation of objects under load. Formulae based upon geometrical and stress/strain relationships permit quantification of these parameters. Biological applications are largely limited to absolute topographical methods, used primarily to screen for scoliosis and to monitor the progress of scoliosis therapy. Little work has been done to numerically quantify displacement of landmark points. This paper discusses the adaptation of differential moire techniques to biological studies, with human subjects in two states of muscular contraction. Projection methods were chosen for the inherent simplicity and portability of the apparatus. grating slide was projected onto a subject at rest and with back muscles contracted to provide the contrast of projected grating patterns which, when superimposed, would yield moire fringes. Superimposition was accomplished using black and white 35mm double-exposure photography. The moire fringes on the developed, printed, and enlarged negatives were the the raw data that were digitized. The digitized fringes could then be processed using formulae that would ultimately provide the basis for the calculation of the out-of-plane displacement of human subject surface landmarks in a non-contact, non-invasive manner.

Key Words: Optical metrology, moire, out-of-plane
displacement.

#### 2.2 INTRODUCTION

Moire fringe topography is an optical method by which surface deformation may be studied. Overlapping two gratings of equidistant, alternating lines and spaces yields a "fringe pattern", or third set of lines and spaces. Superimposition of the two gratings gives moire fringe patterns which vary in spacing and shape according to the changes (strains) of the surface onto which the originals are, in this case, projected. For topographical analysis, a master grating may be conviently projected onto the object of interest.

As noted by the literature, the fringe technique has been quantitatively used primarily in the engineering realm

to study material deformation and strain. This optical technique has been applied to studying surface changes caused by rotational stress, tension, compression, and inplane or out-of-plane displacement. Biomedical applications have basically been for surface topography and scoliosis screening, with very little quantitative use noted. These more commonly used methods are absolute topography and are largely a qualitative evaluation.

In contrast, differential moire is the technique of comparing the fringe pattern changes during the progression of surface variation. In this study, it is hypothesized that a quantitative method can be developed to permit the investigation of sequential motion and the in-plane and outof-plane displacement of a landmark on the human subject. The aim is to refine a single-source, differential moire technique as a non-contact, non-invasive approach to explore the musculoskeletal elements responsible for surface deformation and to quantify the movement of landmarks on the human subject. Accurate photogrammetric techniques could provide early, cost-effective confirmation of pathologic conditions, including muscular wasting processes or neurologic deficits leading to atrophy. Indeed, the severity of musculoskeletal injury, as incurred in athletic or industrial settings, may be quantified. Likewise, the progress of rehabilitation might also be monitored using such methods.

#### 2.3 LITERATURE REVIEW

#### 2.3.1 Engineering Applications

As early as 1874, Lord Rayleigh described his observations of moire fringe production, noting that if two patterns "containing the same number of (parallel) lines to the inch" were superimposed, a "system of parallel lines develops itself, whose (thickness) increases as the angle of inclination (between the two patterns) diminishes."

Oriental silks exhibit the appearance of these patterns, but not the exact phenomenon. As the silken surface contour varies, the concentric, ovoid shapes change, relative to the contour. The French noted this, and applied the name

"moire" or "watered silk" (Figure 2.1, Oster & Nishijima, 1963).

Theocaris (1962) explains that the phenomenon may be adapted to metrology. He discussed the effect created by the use of gratings having less than 1000 lines per inch. A grating is a series of alternating parallel lines and spaces, all of equal width. Moire fringes result when two such sets of lines are out of alignment and superimposed. During this positioning, light that would be transmitted through both gratings is obstructed. This occurs where the lines of one crosses the space of another and where lines intersect (Figure 2.2). Theocaris further stated that fringe production is based upon the "rectilinear propagation of

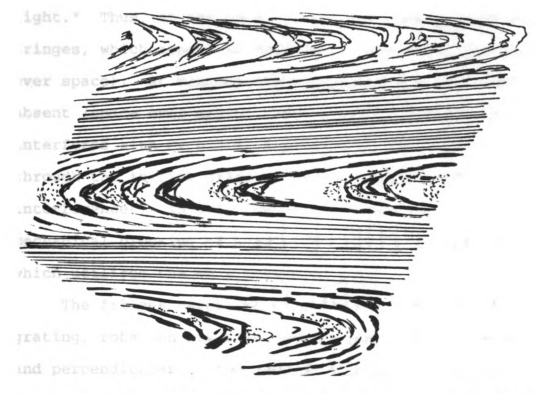


Figure 2.1 Watered Silk (adapted from Oster & Nishijima, 1963)

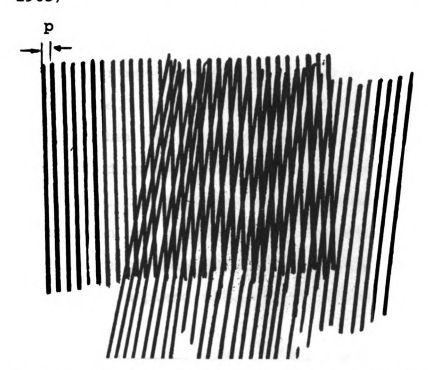


Figure 2.2 Two Superimposed Grating Patterns & Grating Pitch, p (adapted from Oster & Nishijima, 1963)

light." Thus, at the point of minimum light transmission, fringes, which appear as dark lines, are most intense (bar over space). At maximum light transmission, fringes are absent (space over space). So, the superimposed grating interferes with or blocks a portion of the light transmitted through the initial grating, hence the term "optical interference". In this context, interference refers to the mechanical blocking of light, in contrast to interferometry, which utilizes the wave nature of light.

The fringes resulting from subject, and therefore grating, rotation are also roughly parallel to one another, and perpendicular to the general grating orientation.

During the in-plane rotation of two superimposed gratings, the fringes approach one another and decrease in width as the angle between the gratings decreases. With two gratings of equal pitch, the fringes are perpendicular to the bisector of this angle. This fringe "closeness" or density is defined as the number of undeformed grating lines per unit inch, as measured center to center, with pitch, p, as its reciprocal. Thus, the distance between fringes depends upon the angle between the orientation of the lines of the two gratings. Because of this relationship, given the interfringe distance, in-plane rotation of two gratings may be measured.

When specimen displacement occurs under tension or compression (that is, stretching and shortening) in a

direction perpendicular to the grating line orientation ("the primary direction"), fringes move across the plane perpendicular to themselves. In contrast, the "secondary direction" is parallel to the grating orientation (Dally & Riley, 1978).

In 1945, Tollenaar described observations and suggestions for interpretating the geometry of fringe relationships, developing formulae and measurement techniques to determine strain based on the optical interference phenomenon. Morse, Durelli and Sciammarella (1960) further discussed the correlation of fringe pattern geometry with material strain and rotation. These relationships permit the quantification of the deformation of objects under stress by measuring fringe pattern displacement. From this, strain may be calculated (Dally & Riley, 1978).

Methods of fringe production for engineering applications are by projection of a grating directly onto the subject, illumination of a grating with its shadow cast onto the subject, or affixing the grating to object (Martin & Ju, 1970). The physically affixed grating must also be "distortable - etched or engraved parallel lines, or a flexible applique to allow for aberrations and distortions" (Theocaris, 1962). The grating pattern is then recorded for both stressed and unstressed states. By taking a photograph of both conditions, and by superimposing the negatives, the

investigator can "create" fringe patterns. This assumes, however, that camera angles and positions are constant, and that motion is only of the structure/grating combination.

The gratings must then be compared optically to produce the desired fringe patterns. Counting the shift of fringe position of an unfixed grating relative to a point on a fixed grating allows calculation of relative displacement in terms of grating pitch. This is because the number of fringes moving past the point is proportional to (if not equal to) the number of rulings of the moving grating, relative to the same point (Theocaris, 1962).

One method of optical comparison is by superimposition of individual negatives or by double-exposure photography (Khetan, 1975). The unstressed or less-stressed grating would be one half of the exposure, with the more stressed as the other half. Thus, a single negative would contain fringe patterns, as opposed to the necessity of carefully aligning the two separate negatives. Indeed, with electronic recording, a television monitor, and analog-to-digital (A:D) processing equipment, the need for a darkroom is removed altogether (Yatagai, et al., 1982).

#### 2.3.2 Biological Applications

Moire fringe techniques have also been used to study the topography of biological surfaces. A surface "contour map" may be produced as a result of interference between a grating placed close to an object and the grating's shadow (Andonian, 1984). When the grating (master) is interposed between a source of high-intensity illumination and a subject, a shadow of the master is cast upon the subject. At the same time, that shadow is distorted relative to contour changes of the subject's surface. Viewing in a direction normal to the subject automatically superimposes the undistorted master and the shadow of the distorted subject gratings, with resulting fringe production. A photographic record of the fringe pattern, when used as in the work of Adair, et al. (1977), on the human back, "will permit assessment of the overall body shape and symmetry."

Two methods are commonly used in biological applications. As previously described, these are shadow moire and projection moire (Figure 2.3 & 2.4). In the shadow method, the grating is constructed using a large frame. A light source is on one side of the grating, and the subject on the other, with the light projecting a grating shadow onto the object of interest. The photographic recording device (camera) used to view the object is aligned with its axis normal to the subject. One problem with shadow moire is that a grating must be

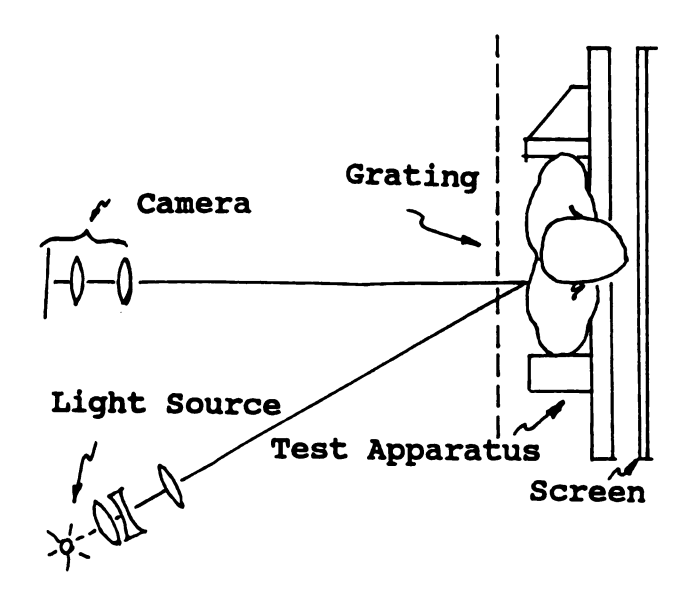


Figure 2.3 Shadow Moire Method (adapted from Rogers, et al, 1979) Copyright 1991 Society for Experimental Mechanics, with permission.

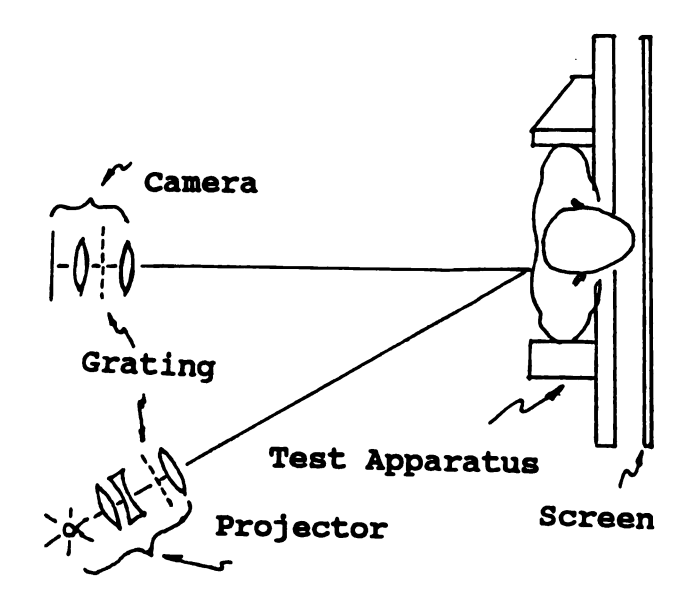


Figure 2.4 Projection Moire Method (adapted from Rogers, et al, 1979) Copyright 1991 Society for Experimental Mechanics, with permission.

fabricated large enough to be placed in front of the entire subject. Some grating screens are frames with dark line threaded taut on pins set at equal intervals.

Understandably, these frames must be firm enough to prevent distortion under tension. On the other hand, projection moire does away with the large screen, as a grating is projected onto the subject and viewed with camera aligned similar to the shadow method. In this application, the grating is etched on a slide or prepared on a photographic plate.

Early work by Brooks and Heflinger (1969) demonstrated the use of a double-beam laser projection method with an interferometer to study real-time moire gaging. At about the same time, Meadows, et al. (1970), used the shadow method to show how surface moire patterns corresponded with planar contours. Hiroshi Takasaki, however, performed perhaps some of the most significant early work on medical applications, as described in his initial article of 1970. He suggested that the Brooks and Heflinger technique had more "freedom" than his early work, and that the projection method allowed a "neater" observation of deformation. used monochromatic, incoherent xenon light, whereas Brooks and Heflinger used a coherent laser source. The former type was thought to be better for more well-defined fringe production. Others, as Adair, et al. (1977), Van Wijk (1980), and Andonian (1984) used quartz lamps as a source of

illumination for their moire application to scoliosis screening. In a subsequent work of 1973, Takasaki recommended using a blue light source to improve grating clarity and a coarse grating with oblique illumination to raise fringe contrast. He likewise suggested that use of a fast shutter speed, high film speed, and high sensitivity film processing would also improve fringe contrast.

One problem with the coarser grating pitch is that along with a decrease in fineness comes a decrease in sensitivity to detect fine displacements. In contrast, an exceedingly fine grating results in poor fringe formation, when using standard photographic technique. Too large of an illumination angle will make the master grating's shadow wider at the distal aspect of the subject's field. address this, Miles and Speight (1975) described a technique for the preparation of a special grating to give equispaced lines on the target screen. Their non-uniform grating compensates for the progressively widening spaces occurring on the far side of the screen in the oblique projection of a standard grating. The team likewise used projection moire, but on animals to record surface contours. Benoit, et al. (1975), made suggestions for determining the sign of these contour lines. An elevation in contour was labelled as positive, and a depression marked as negative. Their suggestions were to include any double-projection fringe system shift or displacement in a portion of the grating

itself. Either of these techniques would provide an additional "reference plane" to permit contour sign definition.

Adair, et al. (1977), felt moire topography would satisfy the requirements of a "rapid, reliable, inexpensive, easily reproducible, and non-invasive technique needed for scoliosis screening. In their work, photographs were made of the fringe patterns from superimposed gratings projected onto the backs of school children. Any asymmetry of these resulting patterns was the criterion for further diagnostic workup, such as confirmatory roentgenography. Andonian (1984) expanded upon this use, citing not only its benefit for early scoliosis detection, but also as a means for "monitoring progress of an established curve and its response to treatment". He used topography to identify "muscle contraction and structural changes" produced by surface electrodes placed on the paravertebral musculature. This muscle stimulation technique, incidentally, has been investigated as a treatment of scoliosis.

#### 2.4 MATERIALS AND METHODS

#### 2.4.1 Projection Moire Methods

The single projector/grating, single-beam projection moire method was selected for this study, as the equipment was relatively simple and portable, in contrast to the

requisite master grating screen of the shadow technique.

Recall that the former method uses a projector to imprint
the grating on the subject whereas the latter uses a light
source to illuminate the screen and cast a shadow of the
grating on the subject. As suggested earlier, the
projection method can cover an area as large as the
projector's cone of light, while the shadow method requires
a grating as large as the subject. Using the projection
method, the surface may be photographed more "conveniently
even in situations of dynamic deflections", while with
shadow moire, "fringes are contour lines of deflection, that
don't correspond to equal deflection differences" (Khetan,
1975).

The method of grating reproduction was after the work of J. Nokes and G.L. Cloud, Ph.D., Department of Metallurgy, Mechanics, and Materials Science, Michigan State University (Figure 2.5). In a darkroom, a jig was set up such that an unexposed photographic glass plate was placed beneath a master grating. Equidistant grooves were cut in the master, giving alternating lines and spaces. The gratings in the jig were covered with a clear glass plate, a "weight" that assured contact with the film plate and permitted light transmission and plate exposure. The film plate was exposed with light and developed, giving the line/space pattern from the master. Initially, the plates were processed using HRP developer with a water to developer ratio of 4:1. As an

improvement, D-19 developer for Kodak 131 plates at f16 for twenty seconds with 150 watt bulb was substituted. Finally, these were trimmed (2" x 2", "slide size") for use in the projector.

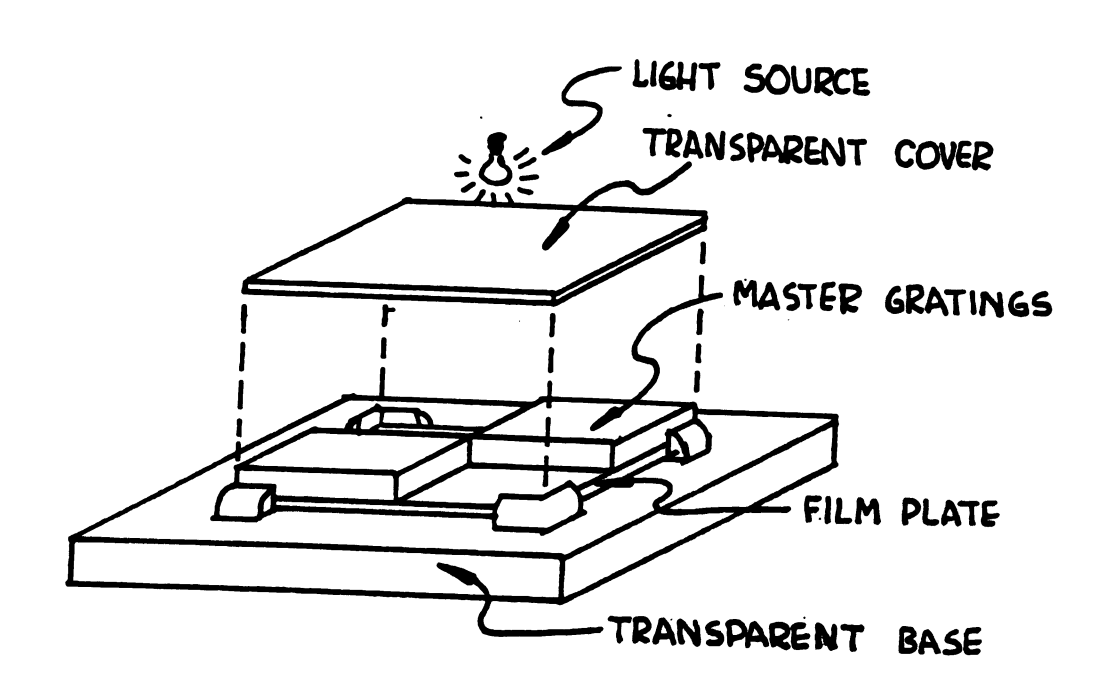


Figure 2.5 Grating Jig

The camera was arranged so that its optical axis was normal to the subject, perpendicular to the plane of the surface landmark. The slide projector used to project the grating slide was placed with its projecting axis oblique to the subject plane. The resulting relationship was a right angle triangle, with the base as the camera-to-subject distance and the hypotenuse as the projector-to-subject distance (Figure 2.6). Angle theta, at the intersection

between camera axis and projector axis, was determined trigonometrically. In earlier pilot work (Moga, 1986 & 1988, unpublished), the camera-to-subject and projector-to-subject distances were varied from 0.5m to approximately 3.5m. The angle between the two axes, theta, was varied incrementally from five degrees to forty-five degrees. Distances ultimately selected were 3.8m from camera to subject, and 1.5m between camera and projector. These were based upon the work of others and the aforementioned, unpublished trials by the author (Table 2.1).

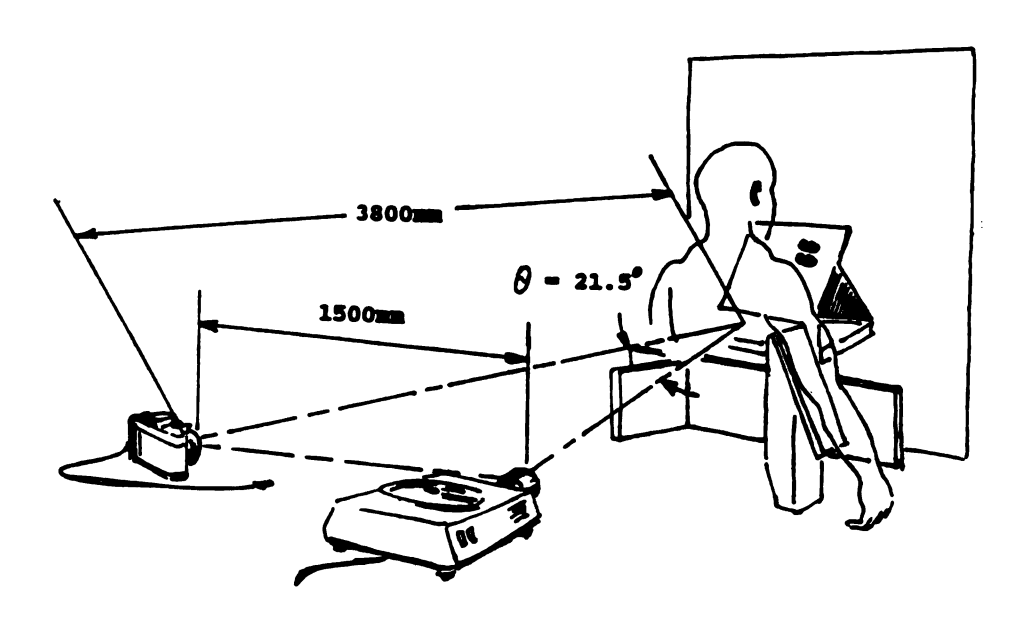


Figure 2.6 Experimental Apparatus (Copyright 1991 Society for Experimental Mechanics, with permission)

Subjects were placed in a test apparatus which restricted motion of the torso in any direction except neutral standing. The testing stand was designed primarily

for use in an experiment investigating the motion of a point on the scapula and permitted isometric adduction of the right arm and adduction of the scapula (Figure 2.6, Moga & Cloud, 1991). For the purpose of developing a moire method, this test stand isolated muscular contraction of a region of the back, providing the topographic contrast necessary for the two half-exposures of the film: one in the resting, uncontracted state and one in the adducted, contracted state.

Table 2.1

Dimensions and Methods from Previous Studies

Roger, et al. (1979) L = 2.8m d = 0.7m p = 10mm

Shinoto, et al. (1981) L = 1.8m d = 0.44m p = 5mm Camera: Fujinon Moire Film: Neopan 400 ASA, B/W f5.6, 1/8 sec.

Pope, et al. (1981)

Camera: Canon F1, 100mm lens
Projector: Leitz Pradovit,
90mm lens
Film: Ilford HP5, 400 ASA
developed to high contrast

index (0.45)

Suzuki (1981) L = 2m p = 5mm Camera: Fujinon Moire 1/2 to 1/8 sec.

Ohtsuka (1981) L = 1.8m

Moga (1986, Unpublished) L = 1.7m, 2.7m

Camera: Minolta X-370, 50mm

lens with 2X extender

Projector: Kodak, 92mm lens

Film: Kodak Plus-X Pan, 125 ASA

f8, 16, 4 sec. (double-exposure)

## 2.4.2 Photographic Methods

The photographic equipment used consisted of a thirtyfive millimeter camera capable of both double-exposure and
manual shutter control, and a carousel slide projector.

Various lenses were used in the developmental stages of the
work and included 100, 200, and 400mm for the camera and 92
and 102mm for the projector. Lens nodal points,
approximated based upon information from various sources
(the manufacturers and Cox, 1971), were important as the
overall optical system dimensions were measured from their
locations. The types of films used included black and white
Plus-X 125 ASA, Technical Pan 100 ASA, T-Max 400 ASA, and
Tri-X-Pan.

To aim the camera, the "built-in", split screen target centrally located on the lens was used. To aim the projector, an overexposed film slide was marked with an 'X', from lines drawn corner to corner across the slide. At the intersection, a hole was punched with a needle. With this method (courtesy of Mr. Martin, Photo-Mart of Lansing, Michigan), the accuracy of alignment of projector lens axis was within one centimeter, according to Khetan (1975).

Double-exposures of the test subjects' backs were obtained first having the shutter set at "B" with a locking plunger attached to the camera shutter release. When the plunger was depressed and locked, the shutter was held open. Thus, the camera shutter and mirror did not reset, as is

required of some SLR cameras for double-exposure work, minimizing vibration and ultimately fringe distortion. The first half of the exposure was taken of the uncontracted or resting back, with the grating projected and focused onto it. The lens cap was manually removed and replaced over a period of approximately two seconds for a half-exposure. The second half of the exposure was obtained in a similar manner, with the subject still in place on the test apparatus now stressing the area of study by contracting back muscles. Throughout the proceedure, focus was maintained at the plane of the back and not at the background screen.

The thirty-five millimeter black and white negatives were developed using high contrast techniques, enlarged to 8" x 10", and printed on glossy high contrast black and white paper, which was air-dried to reduce glossiness. This print finish was chosen over a true matte finish which might have "muddied" the fringe details.

#### 2.5 RESULTS

When the 300 line-per-inch grating was projected onto the subjects' backs and a photograph taken, a series of parallel lines and spaces were noted (Figure 2.7). These were curved along the surface according to its topography. When the same grating was projected and photographed using



Figure 2.7 Projected Grating Pattern

the double-exposure technique, moire fringe "topographical maps" were formed, having a series of concentric rings over the areas of surface elevation or depression (Figure 2.8). If the subject was placed in the test apparatus, designed to restrict anatomic movement and thus topographical change, these patterns became concentrated in the area of greatest movement and surface deformation. Repetition of these photographic exposures using the same methodology reliably gave similar results for all subjects.

#### 2.6 DISCUSSION

In preliminary studies, gratings of 100, 300, and 500 lines per inch were used. Of these, the 100 line per inch

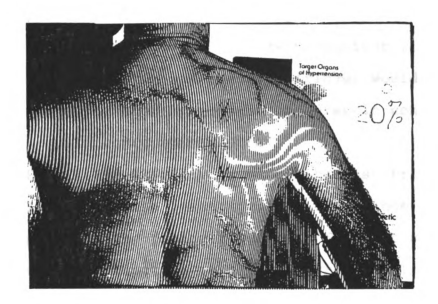


Figure 2.8 Moire Fringe Pattern

grating slide was considered to be "too coarse", as the resulting fringes were neither clear nor continuous. Similarly, the fine, 500 line per inch grating prohibited good line contrast within the experimental-layout distances and thus, did not yield distinct, repeatable, clear fringes. The lack of clarity made fringe observation and any subsequent digitization difficult.

Originally, exposures using both 200 millimeter and 400 millimeter imaging lenses were made at f-stops 16 and 11, respectively. Although the 400mm lens provided a close-up of the area, it did not allow a full field of view of the back. In contrast, the 200mm lens provided a field encompassing the entire subject back, permitting observation of all of the resulting moire fringes in their entirety.

Therefore, this lens served both to gather the data and to provide a large enough field of view to monitor rigid body motion. If such motion was present, fringes would form in areas which had neither motion nor topographic contrast and therefore, would confound the data.

The Plus-X Pan 125 film provided the best fringe pattern clarity and the least "grainy" appearance of the enlarged prints. The faster films were found to be readily overexposed when using the manual shutter control for the double exposures. An automatic iris of higher speed would have perhaps mitigated this and, more importantly, would have standardized exposure times and made the technique even more reproduceable.

#### 2.7 SUMMARY

This chapter discussed the adaptation of a noninvasive, non-contact method of optical metrology to human
study. The single-source, projection moire fringe technique
itself is relatively inexpensive and offers some
portability. A common 35mm slide projector with a 102mm
lens was used to project a 300 line-per-inch grating of
parallel, equidistant lines and spaces onto the subject
surface. A thirty-five millimeter single lens reflex camera
with a 200mm lens and manual shutter control was used to
record the images of the grating patterns on the subject.

Using black and white Plus-X Pan 125 film, double-exposure photography of the subjects' back musculature at rest and during contraction provided the negatives which, when superimposed, produced the moire fringe raw data as a result of the shifted grating patterns.

## 2.7.1 Applications

Surface topography of a region of the back will change in a graduated manner relative to increments of muscle contraction. The fringe patterns over the same contracting region will change in a progressive, quantifiable manner (Moga & Cloud, 1991). It is by using this differential approach that these moire fringes may be identified, numbered, digitized, and processed to yield numeric figures which, when applied to certain formulae, would give in-plane and out-of-plane displacement information of the surface landmarks of human subjects. This might ultimately be useful in monitoring the progress of injury rehabilitation, assessing the severity of injury, or diagnosing processes which might interfere with the normal function of the musculoskeletal system.

#### 2.8 REFERENCES FOR CHAPTER II

- Adair, I.V., Van Wijk, M.C., and Armstrong, G.W.D. Moire topography in scoliosis screening. <u>Clinical Orthopaedics and Related Research</u>. 129: 165-171, 1977.
- Andonian, A.T. Detection of stimulated back muscle contractions by moire topography. <u>J. Biomechanics</u>. 17(9): 653-661, 1984.
- Benoit, P., Mathieu, E., and Thomas, A. Sign determination of contour lines. Optics Communications. 15(3): 392-395, 1975.
- Brooks, R.E. and Heflinger, O. Moire gauging using optical interference patterns. <u>Applied Optics</u>. 8(5): 935-939, 1969.
- Cox, A. <u>Photographic Optics</u>. (pp. 28-40). New York: Focal Press, 1971.
- Dally, J., and Riley, W. <u>Experimental Stress Analysis</u>. (pp. 380-405). New York: McGraw-Hill, 1978.
- Khetan, R.P. <u>Theory and Applications of Projection Moire Methods</u> Doctoral Dissertation, Department of Mechanics, State University of New York at Stony Brook, 1975.
- Lord Rayleigh. On the manufacture and theory of diffraction gratings, in his scientific papers, Cambridge University Press, Vol. 1, p. 209. <u>Philadelphia Magazine</u>. 47: 81-93, 193-205, 1874.
- Martin, L.P., and Ju, F.D. The moire method for measuring large plane, nonhomogeneous deformations. <u>Experimental</u> <u>Mechanics</u>. 10(12): 521-528, 1970.
- Meadows, D.M., Johnson, W.D., and Allen, J.B. Generation of surface contours by moire patterns. <u>Applied Optics</u>. 9(4): 942-947, 1970.
- Miles, C.A., and Speight, B.S. Recording the shape of animals by a moire method. <u>J. Phys. 'E'.</u> 8: 773-776, 1975.
- Moga, P.J. and Cloud, G.L. A study of scapular displacement by differential moire methods. <u>Proc. Soc. Experimental Mech.</u> Milwaukee, WI. Spring, 1991.

Morse, S., Durelli, A.J., and Sciammarella, C.A. Geometry of moire fringes in strain analysis. <u>J. Eng. Mech. Div.,</u> <u>ASCE.</u> 86(EM-4): 105-126, 1960.

Oster, G., and Nishijima, Y. Moire patterns. Sci. Amer. 208(54): 54-63, 1963.

Takasaki, H. Moire topography. Applied Optics. 9(6): 1457-1472, 1970.

Takasaki, H. Moire topography. Applied Optics. 12(4): 845-850, 1973.

Theocaris, P.S. Moire fringes: a powerful measuring device. Applied Mechanics Reviews. 15(5): 333-337, 1962.

Theocaris, P.S. Isopachic patterns by the moire method. <a href="Exp. Mech.">Exp. Mech.</a> 4(6): 153-159, 1964.

Theocaris, P.S. Moire patterns of isopachics. <u>J. Sci.</u> <u>Instrum.</u> 41: 133-138, 1964.

Tollenaar, D. Moire: interferentieverschijnselen bij fasterdruk, <u>Amsterdam Instituut Vour Grafische Techniek</u>, 1945.

Van Wijk, M.C. Moire contourograph - an accuracy analysis. J. Biomechanics. 13: 605-613, 1980.

Yatagai, T., Idesawa, M., Yamaashi, Y., and Suzuki, M. Interactive fringe analysis system: applications to moire contourgram and interferogram. Optical Engineering. 21(5): 901-906, 1982.

#### CHAPTER III

# SCAPULAR INFERIOR ANGLE OUT-OF-PLANE DISPLACEMENT USING DIFFERENTIAL MOIRE METHODS

#### 3.1 ABSTRACT

The amount of in-plane and out-of-plane displacement of the human inferior scapular angle during adduction was determined using differential moire fringe methods. type of optical metrology permits the non-invasive, noncontact quantification of the movement of surface landmarks in a relatively portable and inexpensive manner. subjects (n=3) were placed in an apparatus designed to prohibit motion other than unilateral, isometric arm adduction and scapular adduction in the frontal plane. subjects performed a series of incremented arm contractions up to 70% of the maximum voluntary arm contraction (MVC), with a 300 line-per-inch grating pattern projected onto their backs. Double-exposure photography compared the parascapular topography at rest and during 10% MVC increments of muscular contraction. The superimposition of these two pattern states revealed moire fringes which were subsequently digitized. The processed photographic data were then applied to various formulae to give an in-plane, scapular inferior angle medial displacement average of 9.8mm. and an out-of-plane posterior displacement average of 22.97mm, ±0.9mm, both at 70% of maximal voluntary scapular adduction.

<u>Key Words:</u> Scapular inferior angle, differential moire, projection moire, maximum voluntary contraction, out-of-plane displacement.

#### 3.2 INTRODUCTION

The goal of this study was to examine human scapular motion using differential moire fringe techniques and to quantify the in-plane and out-of-plane displacement of a point on the scapula. It is hypothesized that this area not only displaces posteriorly during adduction, as noted by Nordin & Frankel (1989), but that this displacement may be quantified in a non-contact, remote manner. This was done using single-source, differential projection moire methods previously developed for this application (Moga & Cloud, 1991). The technique depends upon the optical interference between two grating sets, each consisting of a series of parallel, alternating lines and spaces of equal thickness. The grating pattern was projected onto the subject surface, in this case, the parascapular region of the back. Doubleexposure photographs were then taken of the projected patterns, with subjects at rest and contracting at intervals of 10% of maximum voluntary arm adduction. The doubleexposures superimposed the grating patterns, producing moire fringe patterns which were used as the raw data.

The negatives containing the moire patterns were developed, enlarged to 8" by 10", and printed, using high contrast methods. The prints were photocopied, a procedure which enhanced fringe contrast. The midlines of the subjects' backs were marked, along with the point of interest: the inferior scapular angle (Appendix A, Anatomy, page 115). The distances between the two were then measured and, together with other values as fringe order estimations, N, were processed in formulae to yield the in-plane and out-of-plane displacement of the scapular landmark.

The research design is experimental, with submaximal voluntary contractions as the independent variable, and inferior scapular angle point displacement as the dependent variable. The area itself is experimentally readily accessible and near the skin surface.

## 3.3 REVIEW OF THE LITERATURE

Several authors have investigated the geometrical relationships of moire methods in order to derive the calculations for point displacement, surface strain, and so forth. In techniques using moire fringe production, two methods are commonly used, shadow and projection. The former uses a light source to illuminate a grating and cast

a shadow of the line-and-space pattern onto the subject while the latter uses a projector and grating slide to directly illuminate the subject with the pattern (Andonian, 1984; Chapter II, Figure 2.4, page 14). In both instances, the camera or optical recording device is placed with its axis normal to the subject plane, while the light sources are oblique to it. For this study, the projection method was used, as it had more "freedom" than the shadow method and allowed a "neater" observation of deformation (Takasaki, 1970).

## 3.3.1 Geometry

Some authors have developed formulae for slope and topographic mapping, as Livnat and Kafri (1985) and Khetan (1975). The latter author's dual-projection technique was suggested to be effective for a "roughly dynamic" situation.

Roger, et al. (1979), using projected moire in their study of scoliosis, to determine fringe and surface displacement relative to a target screen, offered the following relationship, from Figure 3.1 geometry:

$$z = \frac{\Delta \times L}{(d + \Delta \times)}, \qquad (3.1)$$

where z = fringe distance from target screen

L = distance of nodal point plane from target screen

d = distance between camera and projector
 nodal points

x = (N - 1/2)s, where N = fringe number
s = grating pitch on
target screen

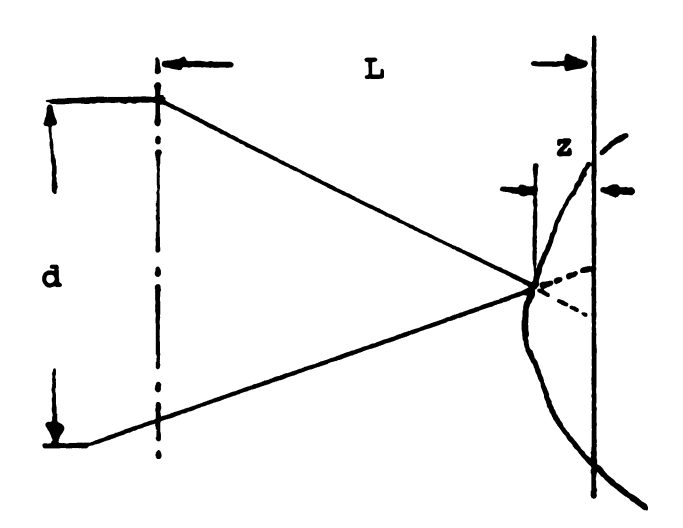


Figure 3.1 Geometry (adapted from Roger, et al, 1979)

Fringes were obtained from photographs by having the subject film overlapping the film of the reference screen.

The resulting fringe formation was digitized, with Cartesian coordinates computed and stored for later processing.

Khetan (1975) cited the work of others which suggested the following "field equation" for surface deflection:

$$w = \frac{Np}{\tan \alpha + \tan \beta - Np/L}, \qquad (3.2)$$

where w = deflection

N = fringe order

p = grating pitch

α = angle between the normal to grating plane and light source

 $\beta$  = angle between the normal to grating plane and center of camera lens

L = distance of light source or camera from grating plane.

Expanding upon earlier efforts, Khetan went on to refine displacement calculations for single and double projection beam methods. For use in this paper, however, Khetan's single beam formula for a curved surface is appropriate. It is:

$$d = w_d - w , \qquad (3.3)$$

where d = displacement

w = z coordinate of point P

 $w_d = z$  coordinate of point P displaced (P').

Separate formulae for  $w_d$  and w are as follows (Figure 3.2):

$$w_{d} = w + \frac{Np}{\sin \theta} \left[ \left( \begin{array}{cccc} 1 - \frac{2w}{s} \cos \theta - \frac{Np}{s \tan \theta} \right) - \frac{x}{s \sin \theta} \\ \left( \begin{array}{cccc} \underline{s} & \cos \theta & -\cos 2 \theta \end{array} \right) \right]$$
 (3.4)

and

$$w = m - x_{so} \tag{3.5}$$

where N = fringe order = # of grating lines in Cone P' SP; Np =  $(n_1 - n_2)p$ ; N =  $(n_1 - n_2)$ 

> p = pitch of projected grating lines on plane FG (assumed parallel to Y-axis)

s = distance from projector to subject reference plane

m = distance from camera to subject
 reference plane

x = x coordinate of point P observed by camera lens

 $\theta$  = angle between camera and projector optical axes

x = x coordinate of point P'

 $x_m = x$  coordinate of point P

x = x

n = # of lines in cone OSP

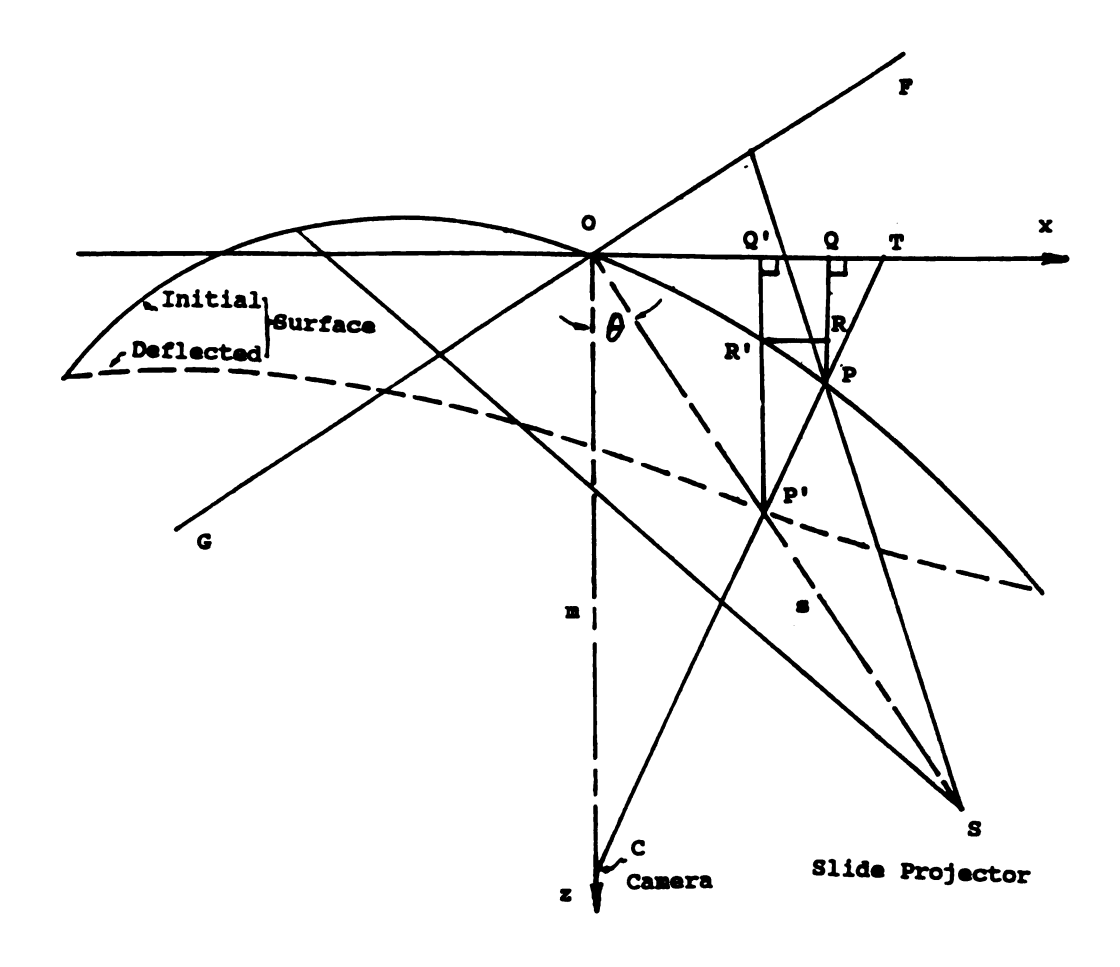


Figure 3.2 Geometry (adapted from Khetan, 1975) Copyright 1991 Society for Experimental Mechanics, with permission.

Khetan (1975) stated that this first order approximation provided "results within 1% of the exact analysis".

He stated that, for curved surfaces, w, the undisplaced z-coordinate of a point on the surface before deflection, equalled  $f(\mathbf{x}_{10})$ . Substituting the formula for  $f(\mathbf{x}_{10})$ , w was calculated in this study using the formula

$$w = - \frac{m \times \sin \theta}{m \cos \theta - x \sin \theta}$$
 (3.6)

#### 3.4 MATERIALS AND METHODS

## 3.4.1 Apparatus

In order to obtain the desired motion of the scapula, a platform was designed to serve as the test jig (Chapter II, Figure 2.6, page 20). Additional thoracic motion, as flexion, extension, rotation and lateral bending, was restricted at the thoracic cage caudad to the scapulae. This restraint was accomplished by sparsely padded blocks which were adjustable in both mediolateral and anteroposterior directions. To restrict shoulder complex activity, provide isometric arm adduction and parascapular muscle contractions and, hence, the necessary scapular displacement, a device was needed. A bar made of aluminum was mounted on the height-adjustable portion of the platform and a Micro Measurements CEA-13-25-OUW-120 strain gage was

affixed to it (Figure 3.3). The gage was connected to a three-wire lead, via a Micro Measurements Bondable Terminal type CEG-75C, and was wired to a Daytronic 3270 Signal Conditioner with Digital Indicator. Two leads were connected as a one-arm bridge, with black lead to white terminal, and red lead to red terminal.

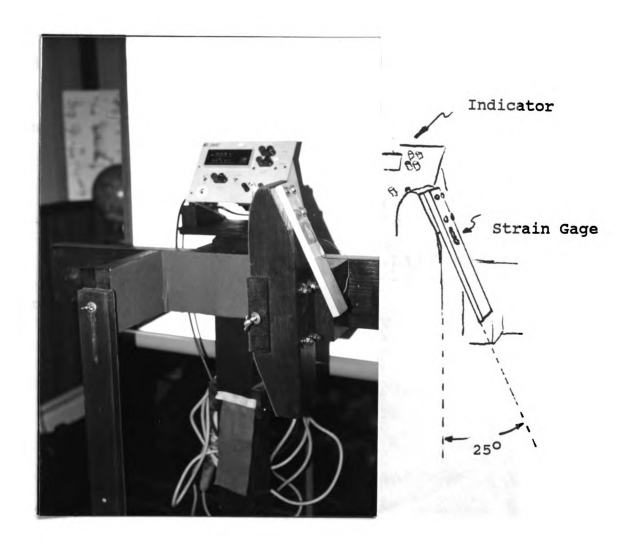
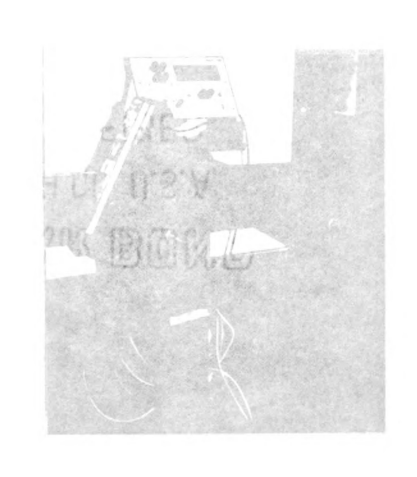


Figure 3.3 Test Apparatus - Aluminum Bar/Strain Gage



The size of the aluminum bar was determined using various formulae. To do so, an initial "rough estimate" of arm adduction force was made. A free-weight pulley arm exercise mechanism was adapted in the following manner: two rings from the adjacent weight systems were placed at the operator's elbow and the arm subsequently adducted. One-hundred and fifty pounds were lifted by the 5'11", 165 pound mesomorphic male. Based on this, the initial maximum adduction for this body habitus was estimated to be 200 pounds. The aluminum bar size, as a cantilevered beam, was then calculated, using the following formulae:

```
(3.7)
M = Pl.
               where M = Moment
                       P = load
                       l = length
I = \underline{bh}^{3},
               where b = width of cross section
                                                        (3.8)
                      h = thickness "
                       I = moment of inertia *
and
\sigma = \underline{MC} ,
I
               where I and M are from
                                                        (3.9)
               previous formulae,
                       \sigma = stress
                       c = distance from
```

The aluminum bar was then reduced to 2x10x0.5 inches in size, with three of the ten inches used to anchor the bar to the test apparatus. The strain gage was fixed one-half inch from the fulcrum point, on the contact surface that would stress the gage in tension. It was calibrated by first

cross section

centerline to top of

fixing the bar/gage combination on a bench. Again, an estimate of the maximum range of adduction force was attempted, only with the same operator lying on his side, adducting the elbow against the bar from above. This time, a maximum of approximately seventy pounds was achieved. Next, weights used for the calibration procedure were then loaded onto a hanger at the end of the bar. Five, ten, and twenty pound increments were used to a maximum of 120 pounds. A constant meter drift of 0.1 to 0.2 pounds was noted within thirty to forty-five seconds of loading. signal conditioner "CAL" function was used to verify calibration, once balance and span were set using both coarse and fine adjustments. The indicator, set at fullscale + 5000, was set with the decimal point to yield 0.1 microstrain increments. Thus, the digital readout linearly reflected the force of adduction in pounds, as the calibration was done originally with 100 pounds equal to 100 microstrains, with one pound giving one microstrain, two pounds giving two microstrains, and so forth.

The curvature of the bar supporting mechanism was shaped to fit along the anatomic contour of the flank from axilla to iliac crest. This adjustment mitigated the need for the subject to "lean into" the bar in order to contract against it. Adjustment of each subject's height, using spacers under the feet, enabled each to fit his axilla over the mechanism comfortably. Otherwise, some would stretch

along the strain gage bar to increase the leverage needed for the adducting arm contraction, causing impingement of the scapula against the device. As a result, distortion and posterior displacement might occur without the experimental contraction.

The strain gage data conditioner and digital readout unit was attached to the jig to allow visualization by the subject without having to stretch and distort the upper thorax and the scapular mechanism.

Finally, a white motion picture screen was affixed to the jig as a background and was supported perpendicular to the camera axis.

## 3.4.2 Subjects

Three subjects were used for the study, after the necessary Human Use Committee approval was obtained. All had been advised of the protocol and potential risks. Those electing to participate signed a consent form (Appendix C, page 128). The subjects stated that they were not inconvenienced regarding time and distance travelled.

From preliminary work, it was noted that mesomorphic males had more surface contrast produced by parascapular muscle contraction than did their female counterparts. In addition, the former might feel more at ease in baring their posterior thoraces for photography. Thus, male subjects, ages twenty-five to sixty-five who were right handed, non-

manual laborers and were approximately the same height, weight, and mesomorphic body habitus were chosen. All had received perfunctory physical examination with brief medical histories taken by the same physician. None had a history of chronic medication use, musculoskeletal disorder, injury, or surgery to the area of interest. All had good function and range of motion of the thorax and appendages, with no gross kyphoscoliosis noted upon exam. All had little body hair on the back, which provided a "cleaner" optical surface. In addition, the basic anthropometric data as age, height, weight, and the distance from the end of the aluminum bar to medial epicondyle were recorded for each person.

## 3.4.3 Protocol

To mark the point of interest, the inferior scapular angle, an "X" was drawn on the skin surface (Figure 3.4). These inferior angle sites were readily reproduceable, as they were located over boney prominences that were easily palpated. A short horizontal was placed using water-soluble ink, with oblique lines then placed to intersect them. These points were visible in the photographs and permitted digitization.

The subjects were placed in the test apparatus, whose clamping devices minimized body and positional change and, when adjusted to subject height, permitted comfortable

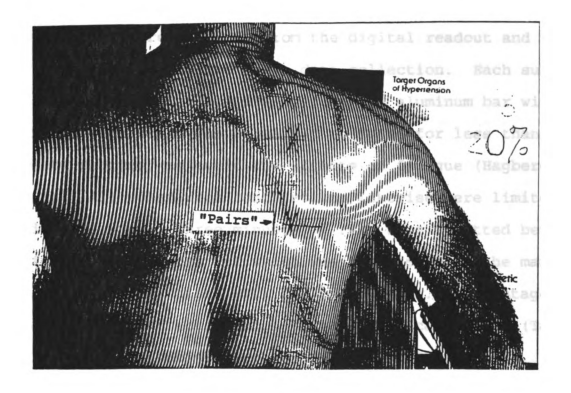


Figure 3.4 Subject Labelling and Landmark "Pairs"

placement of the axilla over the bar, without compression and displacement of the scapula. The subjects' extended arms were maintained at a twenty-five degree angle of abduction from their torsos against the fixed strain gage bar. Contact with the aluminum bar, to which was attached the strain gage transducer, was at the right medial epicondyle, with adduction force roughly perpendicular to the arm's long axis. The strain gage bar resisted this adduction and thus allowed for an isometric contraction of the arm.

Maximum voluntary arm contraction values for each participant were recorded from the digital readout and determined prior to the moire data collection. Each subject was asked to adduct his arm against the aluminum bar with maximum effort and was permitted to do so for less than twenty seconds, to avoid the affects of fatique (Hagberg, 1981). All subsequent contractions likewise were limited to this time span. Three minutes of rest were allotted between efforts, the greatest of which was considered as the maximum voluntary contraction (MVC) for the subject. Percentages of the maximum contraction amounts were then calculated (Table 3.1), and each subject was asked to maintain these increments during exposure of film for that level. A datum card was included in the field of view, so that subject number and contraction strength level could be recorded in each photograph. Each subject was asked to report from the indicator the range of digital readout fluctuation noted as they maintained contractions at the various levels. For the first contractions, these ranges were ± 0.5 to 1 pound and with more strenuous contractions, variations of  $\pm$  1-1.5 pounds were noted.

Table 3.1

\*MVC Values (in Pounds)

			Select		
		MVC's	MVC	<b>%MVC</b>	Force (pounds)
Subject	1			10	4.9
•		47.8		20	9.8
		49.0	49.0	30	14.7
		44.5		40	19.6
				50	24.5
				60	<b>29.4</b>
				70	34.3
Subject	2			10	4.0
	_	34.4		20	7.9
		35.5	39.6	30	11.9
		39.6		40	15.8
				50	19.8
				60	23.8
				70	27.7
Subject	3			10	5.0
		49.8		20	10.0
		47.4	49.8	30	14.9
		47.6		40	19.9
				50	24.9
				60	29.9
				70	34.9

## 3.4.4 Photographic Methods

The projected grating pitch pattern, measured from edge to edge for adjacent lines, was measured on the skin surface after the camera and projector axes were aligned at the scapular inferior angle, and was found to be the same for all subjects.

The subjects were given their individual "percentage of MVC" values, from 10% to 70% of MVC. They were then asked to contract at these ten percent increments, matching as closely as possible the values as displayed on the transducer meter. The smaller contraction intervals were chosen, as 75% of maximum voluntary contraction was difficult for the participant to maintain at a constant level for the four to five second exposures.

The first half of each subject's data collecting double-exposure was made at each of these levels with the subject at rest. The second half was made with the subject contracting the arm in isometric adduction at these precalculated amounts. Each full exposure was taken at two fstops: 11 and 16, to allow for the selection of the photograph having the highest contrast. Thus, each subject provided seven photographs for raw data, with an approximate participation time of one hour per subject. All photos were taken at approximately the same time of day (early nightfall) and in the same room, which had a constant temperature of approximately 21.25 degrees C.

Negatives were processed in the manner described in Chapter II. Using high contrast methods, they were first developed, enlarged to eight inches by ten inches, and then printed, using the exposure (f-stop) that yielded the greatest sharpness and clarity for each individual

contraction increments. The prints were then photocopied, a technique which further increased fringe contrast.

## 3.4.5 Data Processing

The centers of each moire fringe along its length were estimated and sketched onto the 10% MVC photographs.

Subsequent contraction level fringes were traced in the same manner, only onto clear plastic so that superimposed overlays could be made and fringe progression monitored.

After fringe centers were marked on the copies, a vertical line was drawn at the midline of the subject's image. Generally, these lines approximated the vertebral spinous processes and bisected a horizontal at the neck, dividing the neck into two equal halves. In instances of even mild rotoscoliosis, this would not have been the case, and symmetry would be lost. Films displaying such asymmetry were not processed. Lines were then drawn perpendicular to the midline, bisecting the scapular landmark point "pair" (Figure 3.4, page 43). Each pair was formed as a result of the double-exposure of a single, inferior scapular angle mark, shifted from its original position at rest to a position displaced with contraction.

## 3.4.6 Displacement Calculations

Distances on the parafrontal plane of the back from the midline to the scapular inferior angle's position before and

after contraction were measured and repeated. These distances,  $\mathbf{x}_{\infty}$  (undisplaced) and  $\mathbf{x}$  (displaced), were scaled prior to inclusion in the displacement formulae using a scaling factor which corrected for size changes from the projected grating pitch on the subject to that of enlarged 8"  $\mathbf{x}$  10" prints (Table 3.2). Over the scapula, the distance between each vertical projected grating line was 3.5mm edgeto-edge, while that on the photographic prints was 1.25mm.

The inferior angle in-plane values,  $\mathbf{x}_{so}$  and  $\mathbf{x}$  (in millimeters, Table 3.3) were then used in the out-of-plane displacement calculations, formulae 3.3, 3.4, 3.6. listed in the Geometry section and Table 3.4. Values for undisplaced points  $(\mathbf{x}_{so})$  were then used to determine w (Table 3.5), and those for displaced points  $(\mathbf{x})$  used to calculate  $\mathbf{w}_d$ , both of which are in millimeters.

## Table 3.2

#### Raw Data Scaling Factor

Pitch (Projected) - Full Scale 3.5mm

Pitch - 8 x 10 1.25mm

Scaling Factor: 3.5mm = 1.25mm(x)

x = 3.5mm 1.25mm

x = 2.8

Table 3.3

x<sub>10</sub>, x, and N Values

	* MVC	x <sub>so</sub> (mm)	x(mm)	<u>N</u>
Subject 1	10	116.9	115.5	0.5
•	20	118.3	116.9	0.5
	30	118.3		1.0
	40	123.9		1.0
	50	119.7		1.0
	60	122.5		1.5
	70	117.6		2.0
Subject 2	10	121.1	120.4	0.5
	20	121.1		0.5
	30	122.5		1.5
	40	124.6		1.5
	50	126.7		2.5
	60	125.3		2.5
	70	122.5	109.9	3.0
Cubdoct 2	10	107 1	102.0	1 0
Subject 3	10	107.1	102.9	1.0
	20	106.4		1.5
	30	109.2		2.0
	40	111.3		2.0
	50	113.4		2.0
	60 70	118.3	107.8	2.5
	70	120.4	112.7	2.5

## Table 3.4

## Formulae

```
w = -\frac{mx \sin \theta}{m \cos \theta - x \sin \theta}, where m = 3800mm \theta = 21.5^{\circ}
                                                                 \theta = 21.5^{\circ}
                                                                    \sin \theta = 0.3665
                                                                      \cos \theta = 0.9304
                                                                      \tan \theta = 0.3939
                                                                               x = x_n (measured from
                                                                                                8 x 10's and
                                                                                                scaled)
                 \frac{3800 \text{mm} (\mathbf{x}_{so}) \ 0.3665}{3800 \text{mm} (0.9304) - \mathbf{x}_{so} (0.3665)}
w_{d} = w + \frac{Np}{\sin \theta} \left[ \left( \begin{array}{cccc} 1 - \frac{2w}{s} \cos \theta - \frac{Np}{s \tan \theta} \right) - \frac{x}{s \sin \theta} \\ \left( \begin{array}{cccc} \underline{s} & \cos \theta & -\cos 2 \theta \end{array} \right) \right]
                        where w = calculated
                                                    = measured from 8 x 10's and scaled
                                       \begin{array}{ccc} p & = 3.5 mm \\ \theta & = 21.5^{\circ} \end{array}
                                       \sin \theta = 0.3665
                                                     = 4085 mm
                                       \cos \theta = 0.9304
```

$$w_d = w + \frac{N(3.5 \text{mm})}{0.3665} \left[ \begin{pmatrix} 1 - \frac{2w}{4085 \text{mm}} & 0.9304 - \frac{N(3.5 \text{mm})}{1609.08 \text{mm}} \end{pmatrix} - \frac{x}{1497.15 \text{mm}} \right]$$

 $\cos 2\theta = \cos 43 = 0.2689$ 

x = measured from 8 x 10's and scaled

m = camera/subject plane distance

 $tan \theta = 0.3939$ 

Table 3.5

w. w<sub>4</sub>, d. and d/N Values

	<u>*</u>	MVC	w (mm)	w <sub>d</sub> (mm)	d(mm)	d/N(mm)
Subject	1	10 20 30 40 50 60	-46.61 -47.18 -47.18 -49.44 -47.47 -48.88 -46.90	-42.01 -42.58 -37.99 -40.24 -38.22 -35.08 -28.49	4.60 4.59 9.19 9.20 9.25 13.79 18.41	9.20 9.19 9.19 9.20 9.25 9.19 9.21
Subject	2	10 20 30 40 50 60	-48.31 -48.88 -49.73 -50.58 -50.00 -48.88	-43.72 -43.72 -35.10 -35.96 -27.67 -27.11 -21.32	4.59 4.59 13.78 13.77 22.91 22.89 27.56	9.19 9.19 9.19 9.18 9.16 9.16
Subject	3	10 20 30 40 50 60	-42.66 -42.38 -43.51 -44.35 -45.20 -47.18 -48.03	-33.43 -28.55 -25.06 -25.92 -26.79 -24.18 -25.08	9.23 13.83 18.45 18.44 18.41 23.00 22.95	9.23 9.22 9.22 9.22 9.21 9.20 9.18

Fringe order N, a dimensionless value, was assigned based upon fringe progression determined from the

overlapped, serial mylar tracings of the original photographs. The zero order fringe was that which appeared earliest in the contraction sequence, varied the least, and had minimal motion over the increments of contraction (Figure 3.5). Subsequent fringes were numbered center-to-center incrementally as 1, 2, 3, and so forth. Distances between these whole-numbered fringe centers were subdivided into fractions of N to the tenths' place.

At the periphery, the highest order fringes appeared in the suprascapular and lateral thoracic regions, becoming more dramatic as the surface topographic changed. Hence, fringe numbers increased from the scapula to suprascapular and from scapula to lateral thoracic, with lower order fringes closer to the zero-order (N=0) fringe. Both suprascapular and lateral thoracic fringe series were given a positive value, to match protruding topographic change noted to take place. In contrast, if variations in topography yielded "gullies", the fringe series number be negative. The N-values used in the formulae were those defining the fringes which contained the inferior scapular angle landmark "X's" at each of the double-exposures.

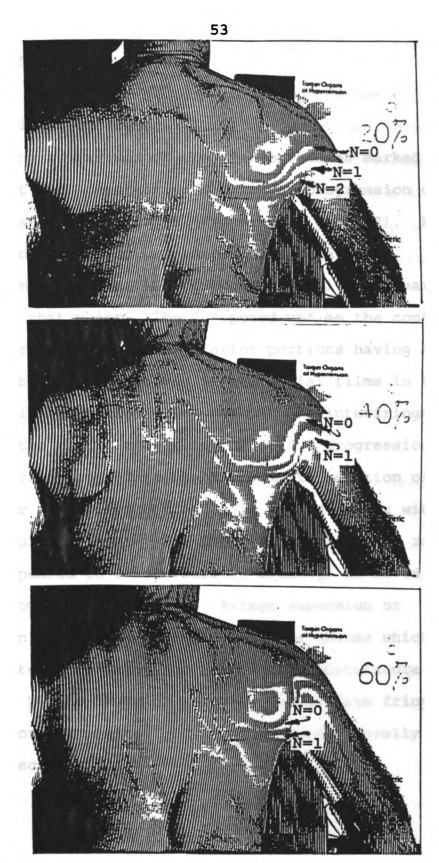


Figure 3.5 Fringe Progression and Fringe Values (N)

#### 3.5 RESULTS

## 3.5.1 Fringe Patterns

During comparison of the transparencies marked with the fringes at each contraction level, the progression of fringes was in a "C" shape (Figure 3.5, page 52). Fringes of this configuration originated at the lateral thoracolumbar region. The fringes themselves appeared Cshaped at that point. The C "opened up" as the contraction level increased, with the inferior portions having a greater distance between themselves in sequential films in the superomedial direction. The greater the interfringe distance, the faster the "rate" of fringe progression. medial portion seemed to blend the medial portion of the zero order fringe and continued in an arc to mix with the suprascapular fringes. The lateral aspect of the zero order fringe appeared to remain intact, although it moved cephalad and was compressed somewhat. Fringe expansion or "migration" was in a "C" shape, along a course which appeared to approximate the contracting musculature as reflected by the changing surface. Paramedian fringes changed more dramatically than those more laterally located over the scapula and deltoid muscle.

## 3.5.2 Displacement Graphs

Graphs were made of the dependent variables  $x_{\infty}$ , x, w,  $w_d$ , N, and finally, displacement, d versus the independent variable %MVC (Figures 3.6 to 3.11). The resemblence between the graphs of  $x_{\infty}$  versus %MVC and w versus %MVC reflected their interrelationship in the formulae used to calculate d. In a similar manner, d versus %MVC results were directly proportional to those of N versus %MVC, largely by virtue of the factor  $[N(p)]/\sin \theta$ .

#### 3.6 DISCUSSION

## 3.6.1 Apparatus and Protocol

Originally, three gradations of MVC were measured. Gradients of thirty-three percent, sixty-six percent, and seventy-five percent of MVC were photographed at each f-stop. Contraction increments of 33% MVC were too large to track the fringe sequence progression on the photographs and even allow assignment of the zero order fringe (N=0). In earlier moire trials, it was noted that the centers of the X's were unclear following contraction and double-exposure, and that the singular points were thus difficult to pick out. In these instances, lines were redrawn on the photocopies of the enlarged prints from the undistorted peripheral portions of the original marks.

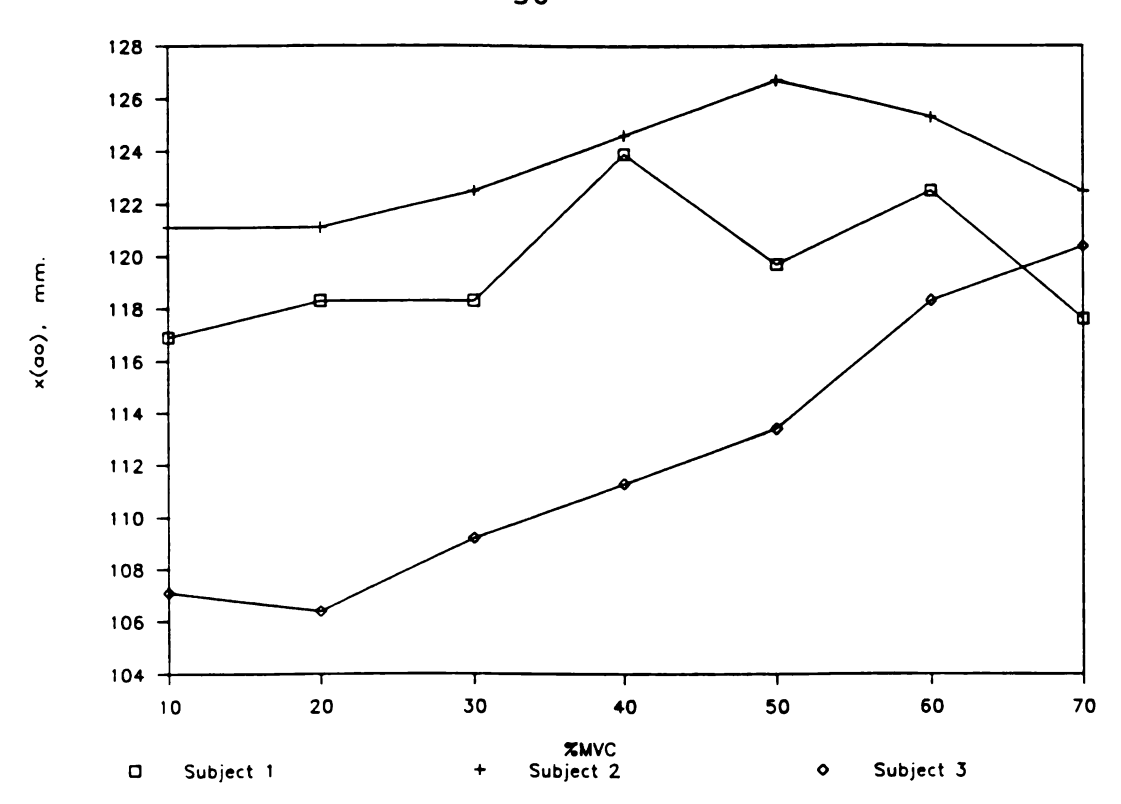


Figure 3.6 x<sub>ao</sub> vs. %MVC

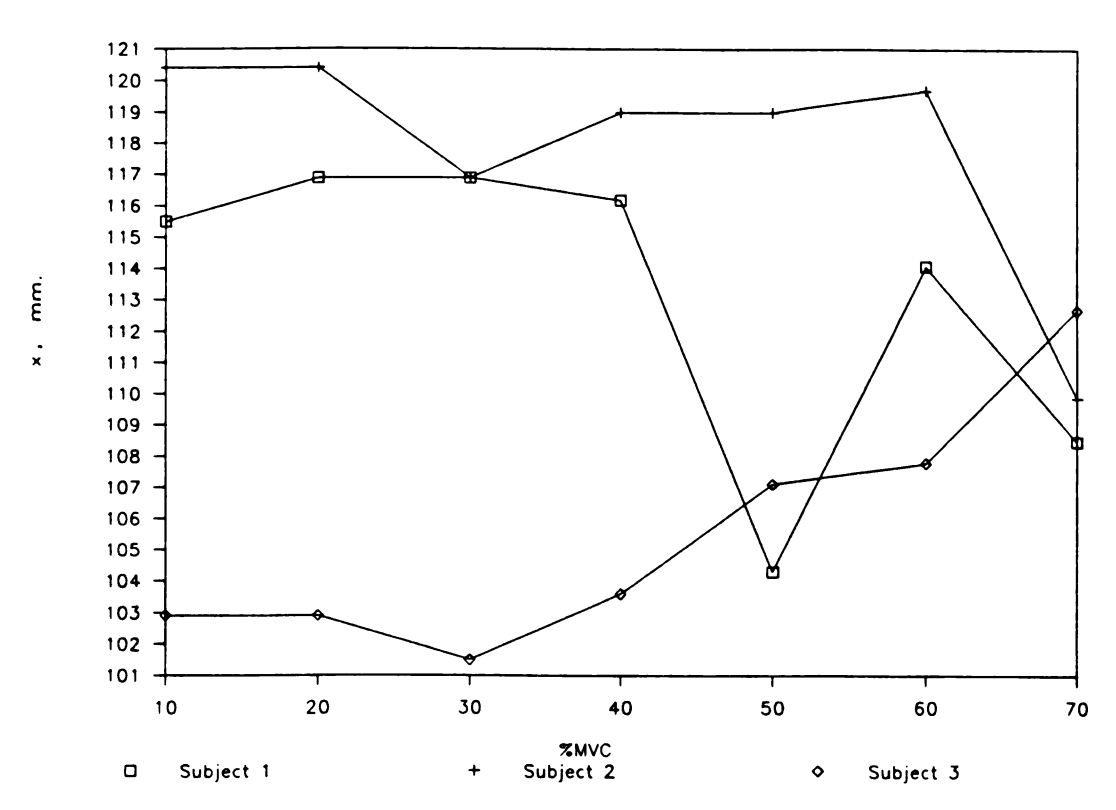


Figure 3.7 x vs. %MVC

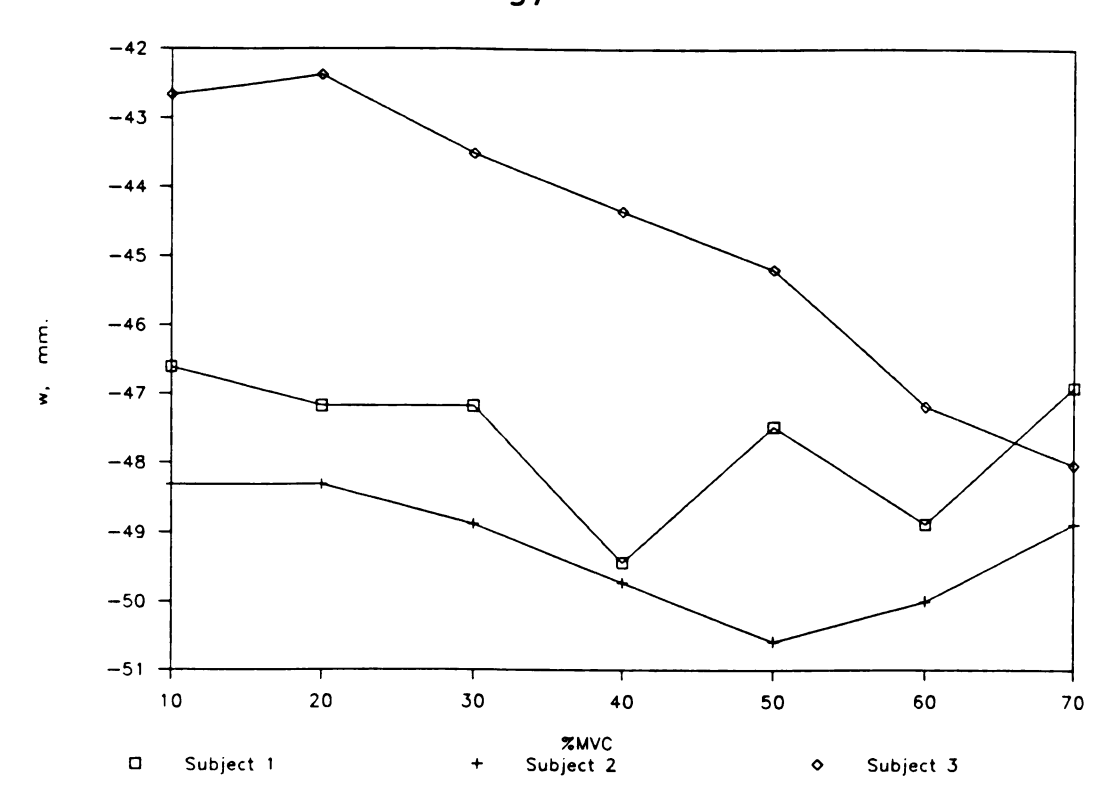


Figure 3.8 w vs. %MVC

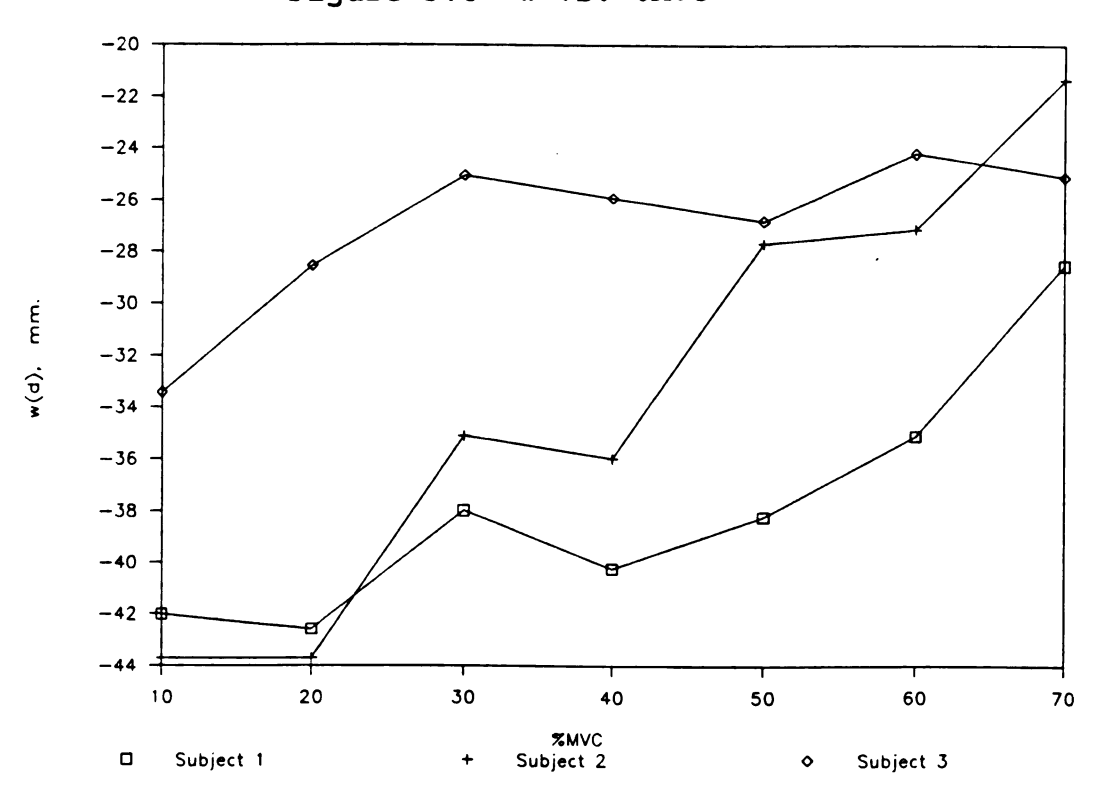
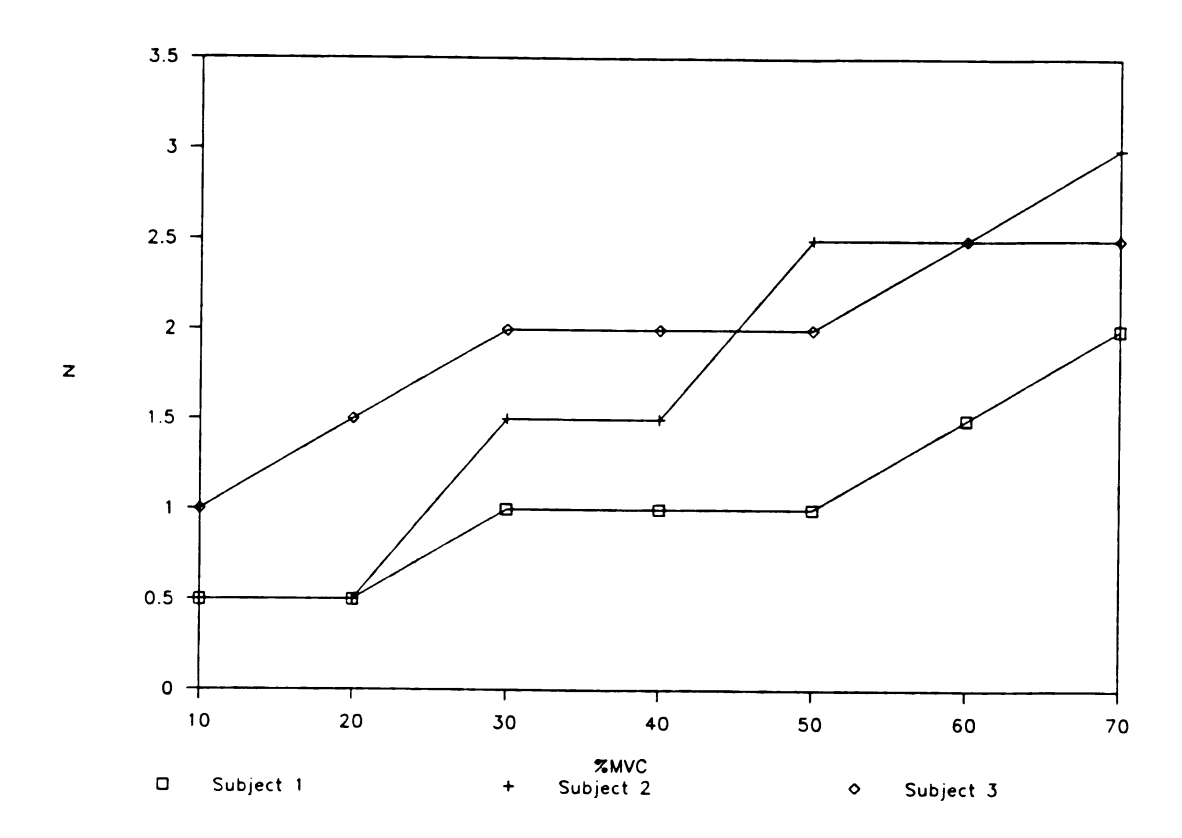
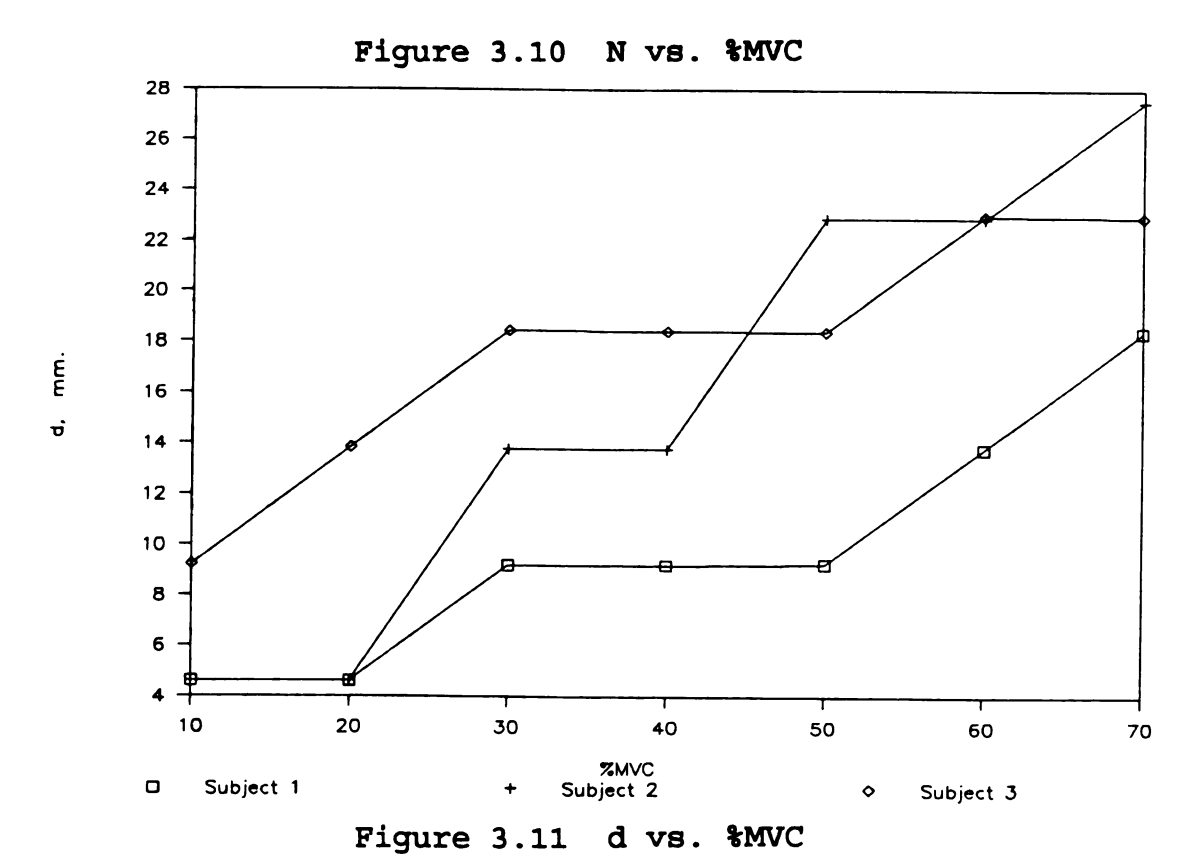


Figure 3.9 w<sub>d</sub> vs. %MVC





The angle of the bar and strain gage pair was originally set at 45 degrees in abduction. It was estimated that this angle would allow maximum force production from maximum muscle contraction, and, as a result, maximum topographic contrast. However, after the initial data collection, the fringe contrast level was found to be poor, despite the high contrast film processing methods.

Readjustment of the arm angle to twenty-five degrees yielded photographic moire fringes that were more prominent and sharp, because of more pronounced contraction changes.

With subjects standing, a maximum arm adduction of approximately forty-nine pounds in adduction was noted. This was somewhat smaller than the 70 or 200 pound values estimated when first establishing the adductor bar dimension. The latter was indeed an overestimation, primarily as the mechanical advantage of the device used for the original estimate was not taken into account. However, the resulting size and stiffness of the bar gave an increased resistance to arm adduction, providing good sensitivity to strain gage tension, especially at increased loads. It also was appropriate as a "target" for the humeral epicondyles of the arms of various subjects. One drawback was that a higher gain was required, potentially introducing additional noise into the system.

An ideal test apparatus would have had an auxillary strain gage transducer readout within the camera field to

record on film the contraction force at the time of exposure. Such an arrangement would require an auxillary light emitting diode (L.E.D.) display in addition to the primary meter, which had to be located within the subject's visual field to permit viewing with head held upright, looking straight ahead. Otherwise, changing of the posture and subsequent contraction would produce spurious fringes. Also, this readout could be "on" only for second half of exposure. If not, two readings would be superimposed and unintelligible following the double-exposure process.

# 3.6.2 Graphs

In the graphs of N and d versus %MVC, it appeared that the general displacement of the inferior scapular angle rose steadily. Because of the relationship of N to d in the formulae, d at higher contraction levels were the product of d at 10% MVC and fringe value N multiples. For example, d at 60% MVC was approximately equal to d at 10% MVC times the multiple of N at 10% MVC relative to 60% MVC. Thus, at 60% MVC, d calculated from 10% MVC values alone was equal to 4.60mm (10% MVC)  $\times$  3 (N of 1.5 compared with 0.5) or 13.81mm. The experimental value of d at that level was This means that, at sixty percent MVC, subject 1's 13.80mm. inferior angle was displaced 13.80mm posteriorly from its resting position. For subject 1, d doubled at thirty percent (30%) MVC, tripled at sixty percent (60%) and

quadrupled at seventy percent (70%), to a maximum of 18.41mm. For subject 2, d tripled at thirty percent (30%), increased five-fold at fifty percent (50%), and six-fold at seventy percent (70%) to 27.56mm. For subject 3, d increased by half at twenty percent (20%) MVC, doubled at thirty percent (30%), and increased by two and one-half times at sixty percent (60%), to a maximum of 23.001mm. The seventy percent (70%) value was only slightly less at 22.95mm.

Values of out-of-plane displacement d along the z-axis increased with increasing percentages of maximum voluntary contraction. Gross visual and palpatory examination of the scapula during incremental adduction detected movement of the medial border toward the midline with protrusion of the inferior angle. This corresponded well with the aforementioned literature, and appeared to be the case also in the comparisons of values of  $x_m$  and x.

Finally, values of d/N for all three subjects equalled approximately 9.2mm (Table 3.5, page 53, rounded to 0.01mm).

# 3.6.3 Measurement Variation

Variation in the measurement of the  $x_{so}$  and x positions was not great, and did not have a large impact on the graphs. Measurement error was found to be, in the initial raw data, in the range of  $\pm$  0.25 to  $\pm$  0.75mm. When

multiplied by the scaling factor, this variation expanded to  $\pm$  0.7 to  $\pm$  2.1mm. The singular 2.1mm value was the result of a hazy fiduciary mark caused by the formation of a fringe directly over it. Of the remaining forty-one measurements, four had measurement errors of  $\pm$  1.4mm and eighteen had variations of  $\pm$  0.7mm.

A 0.25mm difference in the original measurement of  $\mathbf{x}_{so}$  alone in the raw data at the same N yielded a difference in d of approximately 0.001 to 0.003mm. The measurement errors of  $\mathbf{x}$  only gave changes of -0.002 to -0.005mm. A difference of 0.25mm in both  $\mathbf{x}_{so}$  and  $\mathbf{x}$  became a 0.051mm change in displacement, d. Thus, raw data measurement variations of 0.25mm (0.7mm scaled) did not appear to make a great change either in calculations or graphed results.

In contrast, variations of fringe order N estimations were in the range of 0.05 to 0.1. These multiplied to an error range of approximately  $\pm 0.91$ mm in the final d values.

#### 3.6.4 Reassignment of N

Originally, N was assigned in increments of 0.5 between the whole-numbered, fringe center values. Based upon moire fringe progression during incremented contractions, it was felt that the landmark displaced within the portion between, for example, fringes 1.5 and 2, were not under the same stress or contraction force if it were closer to the fringe center (N=2) than to the mid-fringe region (N=1.5). Unless

an adjustment of the fringe assignment system was made, a point in either extreme would still, incorrectly and non-physiologically, have the same N-value assigned to it.

Therefore, the estimates for N were reviewed, and "fine-tuned" to increments of less than 0.5. Displacement was then recalculated according to earlier methods and listed in Table 3.2. New values for N and d were now plotted versus %MVC (Figures 3.12 & 3.13). With the more accurate assignment technique, it was found that the graphs now had a more linear slope than previously, reflecting more concisely the hypothetical physiologic function.

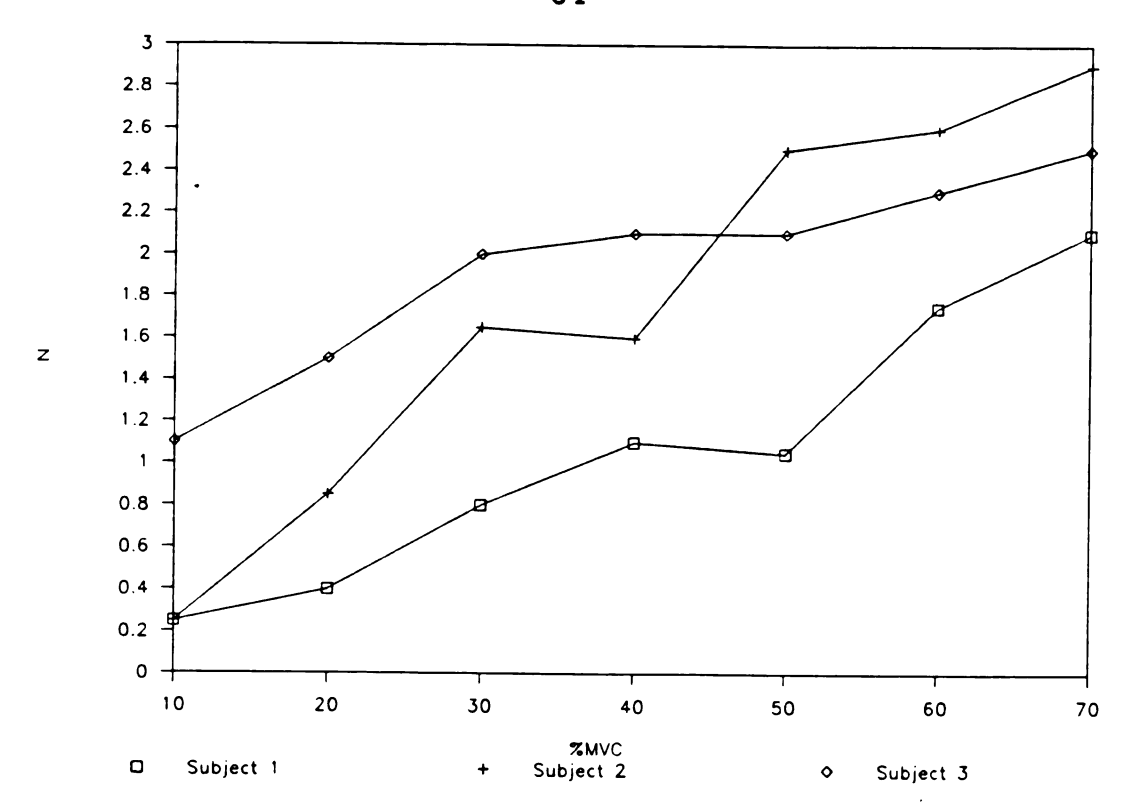


Figure 3.12 N (Re-estimated) vs. %MVC

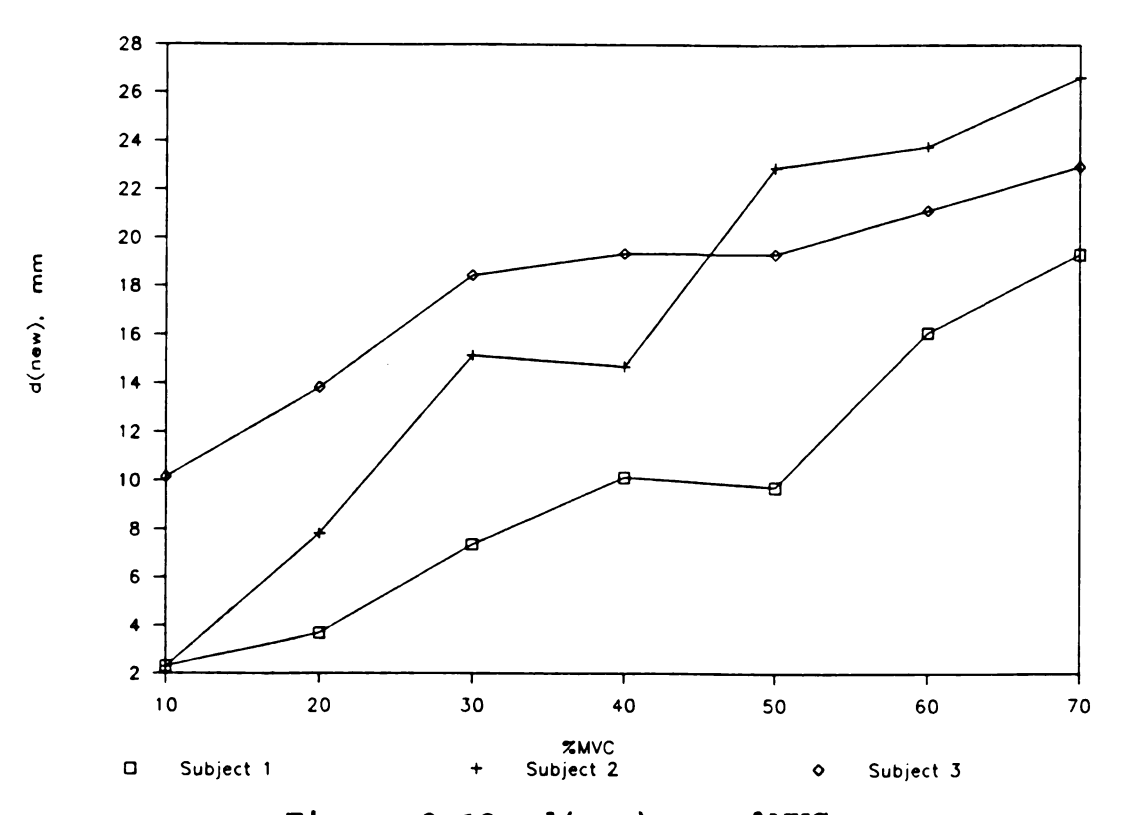


Figure 3.13 d(new) vs. %MVC

#### 3.7 CONCLUSIONS

It was hypothesized that the point labelled on the inferior scapular angle would be displaced in graded quantities corresponding to the amount of incremented percentages of maximal voluntary contraction of the arm. To study this motion, a non-invasive, non-contact method of optical metrology was adapted and applied. Single-source, differential, projection moire methods were used along with double-exposure photography to determine both the in-plane and out-of plane displacement of the scapular landmark.

The scapular landmark was found to be displaced in a step-wise fashion proportional to the intensity of the adducting contractions. It was noted on the digitized photographs that as fringe values, N, increased with increasing contraction force, so did the values of the out-of-plane displacement, d, in the anteroposterior, z-axis direction for a distance of 23mm,  $\pm 0.91\text{mm}$  at 70% MVC. Inplane displacement of the inferior scapular angle was likewise seen for all subjects, but in the mediolateral or x-axis direction, and, at 70% MVC, for an average distance of 9.8mm.

The exact influence that parascapular and shoulder muscles had on scapular and inferior angle displacement may depend upon several factors, such as shifts in axes of

motion, changes in muscle force and leverage, and even the order of muscle recruitment (Appendix: Kinematics, page 69).

# 3.7.1 Suggestions: Further Study

"Steps" were noted at thirty, forty and fifty percent These are discussed at length in Chapter V. Estimation of neutral fringe N values to fractions less than 0.5, and multiplication by d values at ten percent MVC smoothed the graphs but did not remove the steps. were similar shifts at ten percent for subject 1 and at sixty percent MVC for subject 3. Perhaps these regions of inferior angle point stabilization along the z-axis represent periods of "balance" between scapular adductors, axis shifts, or a combination of these. Further investigation at finer intervals of percentages of MVC, perhaps with EMG, might help to more accurately define scapular motion this finding. It is estimated that d versus %MVC or N versus %MVC might yield smoother graphs, but still contain step functions.

Comparisons were made of the d (displacement) values of each subject, relative to actual contraction strength and to individual height and weight (Table 3.6, page 68). With a greater subject population, it would be possible to expand upon these and develop regression equations and even nomograms for these parameters. This might help to define an average scapular activity for a given population, which

may potentially be applied to the clinical setting to help in the diagnosis and management of injury or disease. Some of the processes which may involve the scapular mechanism are reviewed in Appendix B, Pathology, on page 122.

Table 3.6

d and Force, Height, Weight, Age, Moment

Force	(Pounds)	6.3	11.3	16.2	21.2	26.2	31.2	36.2	5'9.5"	160 lbs.	63 Years	Lean-Muscular	2 4/16"	4 8/16"	49.8 lbs.	n.e	$\frac{+}{-}$ 1-2 lbs.
	Subject 3	10,1558	13.8334	18.4470	19,3533	19.3267	21.1701	22.9524		S.	ırs	/ Obese	=	4 3/16"	lbs.	-	.s.
	ZI	1.1	1.5	2.0	2.1	2.1	2.3	2.5	5'10"	17 06 1	31 Ye	11111)	9/16	1 3/16	39.6	1 3/8	+ 3 lbs.
Force	(Pounds)	5.3	9.2	13.2	17.1	21.1	25.1	29.0	u,	-	.,						Τ1
	Subject 2	2.2983	7.8036	15.1517	14.6845	22.9076	23,8028	26.6497		170 lbs.	28 Years	n-Muscular	/16"	3 10/16"	0 lbs.		<u>+</u> 3 lbs.
	zi	0.25	0.85	1.65	1.60	2.50	2.60	2.90	.9	170	78	Lea	3	3 1	49.	0	
Force	(Pounds)		11.2	16.1	21.0	25.9	30.8	35.7									y Subject
	Subject 1	2.3022	3.6806	7.3545	10.1199	9.7104	16.0892	19,3286					<del>.т</del> .				Range of Gage Reading by Subject
	zI	0.25	0.40	0.80	1.10	1.05	1.75	2.10			Age Body Habitus	Poin	٥,			of Gag	
	& MVC	10	20	8	<b>₹</b>	જ	8	20	Height	Weight	Age	Body Ha	Contact	Moment <sup>2</sup>	MVC	Lift <sup>3</sup>	Range c

[Note: Upper edge of strain gage 1/4" from fulcrum]

 $<sup>^1</sup>$  Elbow contact measured from distal end of strain gage bar.  $^2$  Length of bar from fulcrum to distal end (6 12/16") minus length of bar from elbow contact point to distal end.

Placed under subjects' feet to allow axilla to clear apparatus without contact, and thus, preventing scapular distortion.

#### 3.8 APPENDIX: Kinematics

Several ligaments of the shoulder complex are, to a large extent, responsible for scapular motion. The ligamentous attachments allow for the formation of axes about which the shoulder mechanism, and therefore scapula, move.

For example, the anchoring of the clavicle at both sternoclavicular and acromioclavicular joints lets the clavicle act as a transverse, or "x" axis in the frontal plane. A capsule and meniscus are present at either end of the clavicular strut. The medial articulation is further stabilized by an interclavicular ligament, sternoclavicular ligaments, and a costoclavicular ligament (Figure 3.8.1). The latter acts as a fulcrum for reciprocal motion with the acromioclavicular (A-C) joint in protraction and retraction, along with elevation and depression.

At the lateral aspect, the A-C joint is also anchored by the coracoacromial and coracoclavicular ligaments. The former has a transverse scapular component and the latter consists of trapezoid and conoid portions. The fiber orientation of these structures permits motion about three axes. The primary axis (Figure 3.8.2), at least in abduction and adduction, shifts according to the shoulder complex position in the range of motion (Dvir and Berme, 1978; Inman, 1944). Scapular protraction and retraction

# Coracoclavicular:

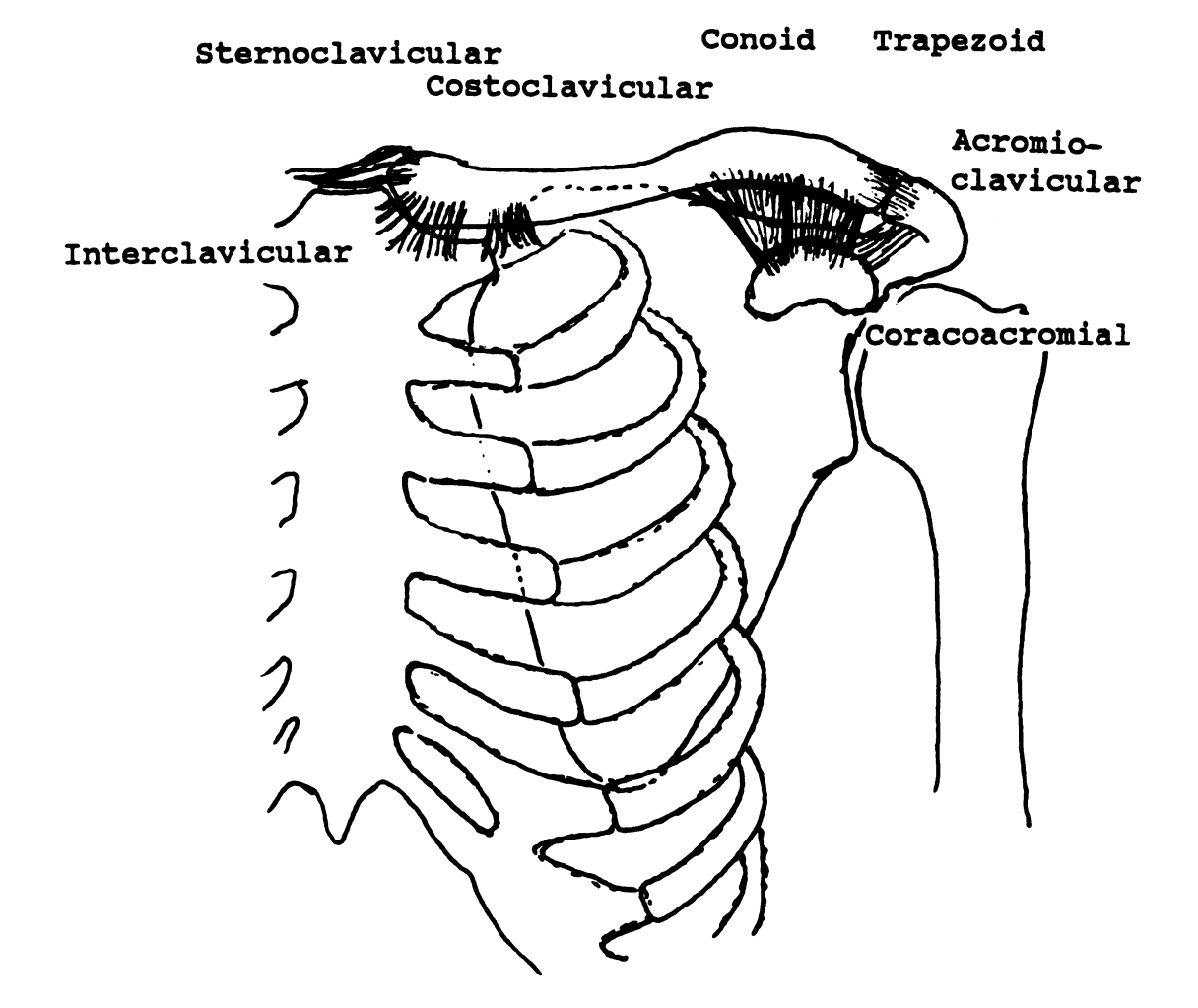


Figure 3.8.1 Clavicular Ligaments (adapted from Goss, 1974 and Warfel, 1974)

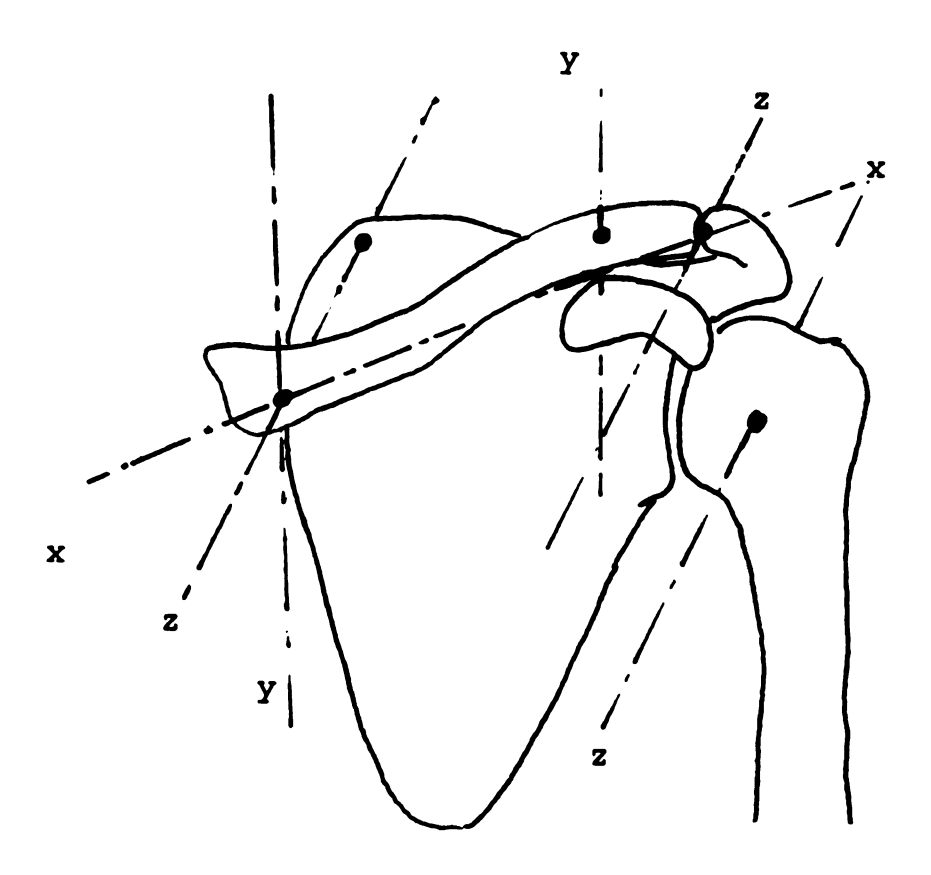


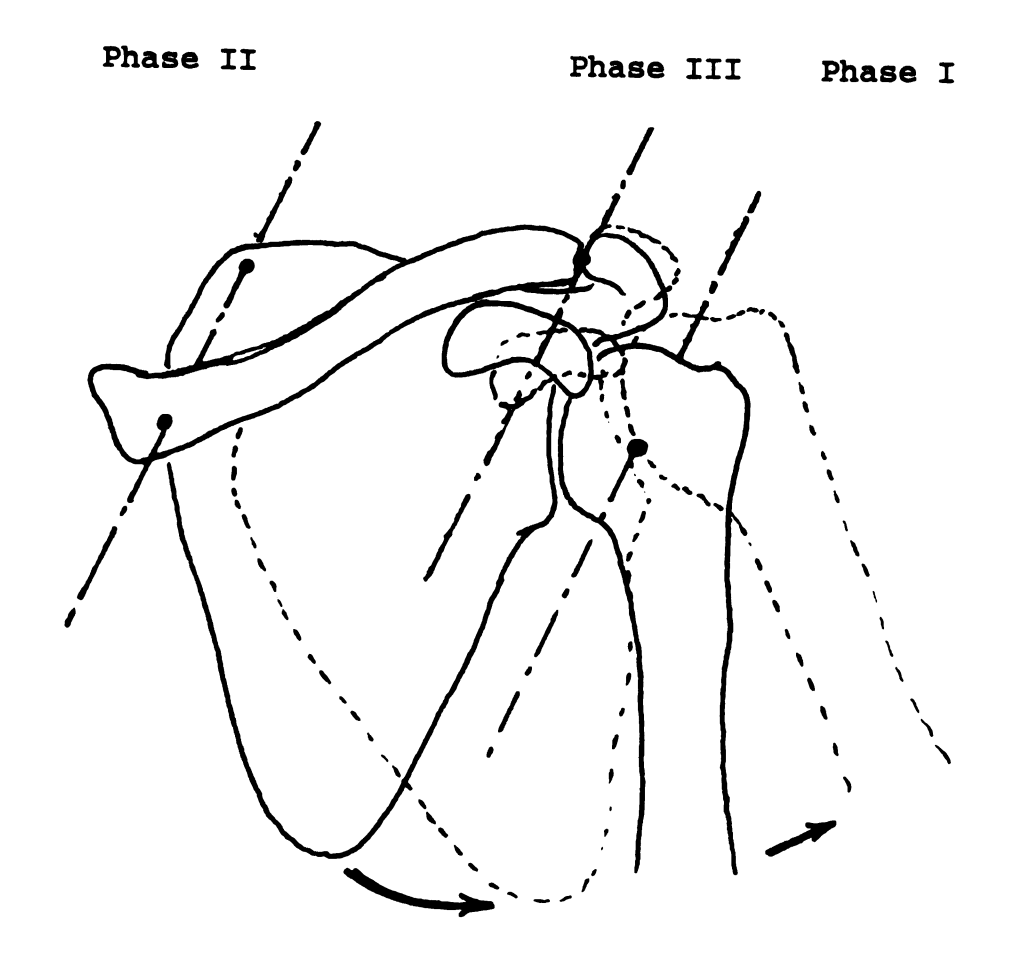
Figure 3.8.2 Shoulder Complex Axes (adapted from Nordin & Frankel, 1989)

occur about a superior-inferior, or "y-axis", centered at the conoid portion of the coracoclavicular ligament.

Protraction results in a type of voluntary "winging", with a prominence of both medial scapular border and inferior angle.

Likewise, rotation takes place likewise about the clavicle which is converted to an x-axis by the trapezoid portion of the coracoclavicular ligament. In addition, the scapula itself has an x-axis projected mediolaterally through the glenoid fossa, about which another type of rotation occurs. Anterior rotation, or scapular gliding along the contours of the thoracic wall, results in an elevation of the scapula, and prominence of the inferior angle.

Finally, the antero-posterior, or "z-axis", serves as the focus for abduction and adduction. The medial axis runs through the sternoclavicular articulation to the superior scapular angle. At a certain point in abduction, the rotational A-P or z-axis shifts laterally to the acromioclavicular joint. In addition, the inferior angle will move laterally, as depicted in Figure 3.8.3 (Poppen & Walker, 1976). Intuitively, movement in adduction of the scapula secondary to the many shifts in multi-axial motion should be the opposite of abduction.



Inferior Scapular Angle

Figure 3.8.3 Inferior Angle Displacement and Z-axis Motion in Abduction (adapted from Dvir & Berme, 1978 and Nordin & Frankel, 1989)

# 3.9 REFERENCES FOR CHAPTER III

- Andonian, A.T. Detection of stimulated back muscle contractions by moire topography. <u>J. Biomechanics</u>. 17(9): 653-661, 1984.
- Dally, J., and Riley, W. <u>Experimental Stress Analysis</u>. (pp. 380-405). New York: McGraw-Hill, 1978.
- Dvir, Z., and Berme, N. The shoulder complex in elevation of the arm: a mechanism approach. <u>J. Biomechanics</u>. 11:219-225, 1978.
- Hagberg, M. Muscular endurance and surface electromyogram in isometric and dynamic exercise. <u>J. Appl. Physiol.</u>, Respirat. Environ. Exercise Physiol. 51(1): 1-7, 1981.
- Inman, V.T., Saunders, J.R. de C.M., and Abbott, L.C. Observations on the function of the shoulder joint. <u>J. Bone Joint Surg.</u> 26 A:1. 1944.
- Khetan, R.P. <u>Theory and Applications of Projection Moire</u> <u>Methods</u> - Doctoral Dissertation, Department of Mechanics, State University of New York at Stony Brook, 1975.
- Livnat, A., and Kafri, O. Slope and deformation mapping by grating projection technique. <u>Optical Engineering.</u> 24(1): 150-152, 1985.
- Moga, P.J. and Cloud, G.L. A study of scapular displacement by differential moire methods. <u>Proc. Soc. Experimental Mech.</u> Milwaukee, WI. Spring, 1991.
- Nordin, M. and Frankel, V.H. <u>Basic Biomechanics of the Musculoskeletal System.</u> Lea & Febiger, Phila. 1989.
- Poppen, N.K. and Walker, P.S. Normal and abnormal motion of the shoulder. <u>J. Bone Joint Surg.</u> 58 A:195, 1976.
- Roger, R.E., Stokes, I.A.F., Harris, J.D., Frymoyer, J.W., and Ruiz, C. Monitoring adolescent idiopathic scoliosis with moire fringe photography. <u>Engineering in Medicine</u>. 8(3): 119-127, 1979.
- Takasaki, H. Moire topography. Applied Optics. 9(6): 1457-1472, 1970.

#### CHAPTER IV

# SCAPULAR OUT-OF-PLANE DISPLACEMENT IN LATERAL BENDING USING DIFFERENTIAL MOIRE

#### 4.1 ABSTRACT

Normal scapular function may be altered by trauma, developmental abnormalities, or neuromuscular pathology. To help quantify this, single-source projection differential moire fringe methods were applied to the study of the motion of the human inferior scapular angle. The method uses a grating of parallel, alternating lines and spaces of equal thickness that are projected onto the subject's back. Double-exposure photography captures the increments of surface change due to muscular contraction of the surface. It compares these gradations of contractions, ultimately generating moire fringes which may be digitized and mathematically processed to yield the in-plane and out-of-plane displacement of the scapular point.

To differentiate the accurate displacement results from the "noise" of rigid body motion, lateral bending was purposefully added to the subjects posture, within the confines of the test apparatus, in an attempt to introduce spurious motion into the data. Scapular landmark displacement at 30% of maximal voluntary arm adduction for both neutral and lateral bending positions were of the same

magnitude, with x-axis values of 7.7mm and 8.4mm, and z-axis figures of 18.47mm and 18.26 mm, respectively. This suggests that if a small amount of lateral bending occurs in the frontal plane, then little change of the displacement values occurs.

KEY WORDS: Moire, scapular displacement, scapular kinematics.

### 4.2 INTRODUCTION

The goals of this study were twofold. First, it was necessary to determine which of the possible extremes of motion permitted by the test apparatus used previously produced fringes most like those of neutral. Once that posture was identified, an incremented percent of maximal voluntary contraction study was needed to ascertain the extent of possible raw data contamination by the fringes produced by the subject while in this position.

In the "neutral study" (Chapter III) for all three subjects, "contaminating", superfluous fringes generally did not appear on the subjects' left scapular region until higher percentages of maximal voluntary contraction. Did the moire fringe data represent scapular out-of-plane displacement or were they the result of rigid body motion from rotation, lateral bending, or extension, or a combination of these? The rigid body fringes were thought

to form over the areas of non-contraction or non-motion, in addition to the experimental movement at the right scapula. For subjects 1 and 3, spurious, left-sided fringe formation occurred at forty percent MVC, while for subject 2 they were noted at fifty percent MVC.

The contralateral fringe production may have been the result of an anatomic positional change taking place at the higher contraction levels. With the subject's right arm fixed in the apparatus, scapular muscles were contracted and the inferior scapular angle was both medially and posteriorly displaced. With additional amounts of muscular contraction, the midline was likewise displaced, only to the right. That is, midthoracic, vertebral, left lateral bending may have been induced because that portion of the spine was relatively free while the arm and scapula were restricted by the apparatus. This component of upper thoracic midline shift had been demonstrated by the displacement of a vertical line drawn along the spinous processes of the subjects' backs. The soft tissue and musculoskeletal shift may have been enough to account for spurious fringe formation. As an indicator of this excessive positioning, "tell-tale" skin folds increased at the clamping portion of the apparatus.

As mentioned earlier, the test apparatus was designed to minimize subject motion in directions other than that experimentally required. It restricted the lower thorax and

thus made it difficult for the subject to flex, extend, rotate, or laterally bend the trunk. Rotation was restricted by the clamping action of both horizontal and posterior thoracic supports (Chapter II, Figure 2.6, page 20). Flexion was limited by the center post and horizontal brackets. The aluminum/strain gage bar had been located perpendicular to the mid-thoracic transverse plane, so rotation of the upper body would likewise disturb optimal leverage, with the subject potentially losing contact with it in right rotation. The addition of the bar bracket, which protruded snugly into the axilla, made right lateral bending extremely difficult. Left lateral bending would move the right epicondyle further up the contact bar, decreasing the moment arm in adduction and increasing the difficulty in achieving %MVC's. In addition to strain gage/bar placement, the LED readout was centered on the vertical post, which required subject visual attention to be straight ahead and slightly nodded. Of all motions, upper thoracic extension was the range which potentially had the greatest freedom of movement. As a result of the inherent subject motion control by the test platform, it was hypothesized that if the superfluous motion of lateral bending was indeed in a purely coronal plane, and if %MVC's similar to those in neutral were developed, then not much additional in-plane or out-of-plane displacement would occur.

#### 4.3 MATERIALS AND METHODS

#### 4.3.1 Protocol

In the first part of this investigation, a subject from the neutral study was placed in the test apparatus for additional data collection. He was instructed to attempt torso flexion, extension, bilateral rotation and lateral bending, in as much as the device permitted. Once at the greatest ranges possible, maximum voluntary contractions were determined. Double-exposure photographs using single-source, projection moire methods were then made at 20%, 40%, and 60% MVC, in the same manner as in previous chapters, at rest and with incremental contractions. This proceedure superimposed the projected grating patterns and obtained the necessary moire fringes. The photographic negatives were then enlarged, printed, and photocopied for maximum fringe contrast.

When the raw photographic data were compared with those in neutral, only the lateral bending results displayed fringes that closely resembled the neutral raw data. It was this posture that was used for the remainder of the study because of fringe similarities and the potential for inappropriate data.

The subject was then place in the widest possible range of lateral bending to both right and left sides. Using a goniometer, the angles of the maximum ranges of upper

thoracic left and right lateral bending, within the confines of the apparatus, were found. The goniometer device was simply an inverted protractor with a string-and-weight pendulum, and was affixed to the flat, left suprascapular portion of the back, which permitted unobstructed motion of the pendulum (Figure 4.1). This region was selected as it was thought to have the least deformation during arm adduction which would not interfere with the fringe patterns of the moving right parascapular mechanism.

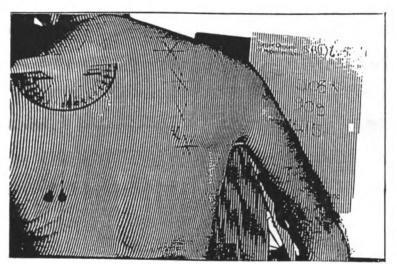


Figure 4.1 Goniometer

The left and right lateral bending ranges were then each divided into 25% portions. At each of these portions, maximum voluntary arm adduction quantities were determined following the protocol established in Chapter III.

Subsequently, portions of these MVC's were calculated 10%, 30%, and 50% of MVC. At full (100%) left and right lateral bending, 40% and 60% MVC were used. Double-exposure

photographs were then made at these increments with the subject first at rest and then contracting. Enlargements of the 35mm negatives were made and then printed, and points digitized and fringe patterns studied. Pictures showing obvious thoracic motion as shown by rigid body movement were discounted, as the intent of this portion of the study was to compare neutral with photographically contaminated data, but not with subject posture varying grossly from those in neutral. As in the manner of the previous studies, the midline of the back was demarkated and distances x, and x from the midline to the inferior scapular angle landmark measured and scaled (Table 4.1). Values for fringe order N were then estimated first at increments of 0.5 and then to the 0.01 place. These values, together the x-axis displacement figures, were used to calculate w,  $w_d$ , and d were calculated (Table 4.2).

# 4.4 RESULTS

The total range for lateral bending to both sides permitted by the apparatus for the singular test subject was thirty-eight degrees, thirteen to the left and twenty-five to the right, as measured by the goniometer. Further left bending was limited largely by the need to maintain medial epicondyle contact with the aluminum bar to monitor

Table 4.1

x<sub>20</sub>, x, and N Values

	x <sub>so</sub> (mm)	x(mm)	x(mm)	N
10% MVC				
L25 R100	135.1 149.1	132.3 148.4	2.8	1.25 0.50
30% MVC L25 50 75	142.1 138.6 137.9	133.7 132.3 131.6	8.4 6.3 6.3	2.00 1.50 1.50
100 R25 50 75	136.5 136.5 140.0 146.3	129.5 135.1 138.6 142.1	7.0 1.4 1.4 4.2	1.80 0.90 0.90 1.50
100 40% MVC	146.3	144.9	1.4	1.50
L100 R100	133.0 141.4	119.0 111.3	14.0 30.1	1.80 1.50
50% MVC L25 50 75	140.7 140.7 137.9	133.7 136.5 127.4	7.0 4.2 10.5	2.50 1.60 1.80
100 R25 50 75	143.5 136.5 143.5 149.8	137.9 132.3 138.6 144.2	5.6 4.2 4.9 5.6	2.00 2.00 1.70 1.75
100 60% MVC L100	148.4	142.8	5.6 14.7	2.80
R100	142.1	114.8	27.3	2.20

<pre>% MVC</pre>	<u> </u>	w <sub>d</sub> (mm)	d(mm)	d/N(mm)
Subject 1				
10	0.25	-44.31	2.30	9.21
20	0.40	-43.49	3.68	9.20
30	0.80	-39.83	7.36	9.19
40	1.10	-39.32	10.12	9.19
50	1.05	-37.76	9.71	9.25
60	1.75	-32.79	16.09	9.19
70	2.10	-27.57	19.33	9.20
Subject 2				
10	0.25	-46.01	2.29	9.19
20	0.85	-40.51	7.80	9.18
30	1.65	-33.73	15.15	9.18
40	1.60	-35.05	14.69	9.18
50	2.50	-27.67	22.91	9.16
60	2.60	-26.19	23.80	9.16
70	2.90	-22.23	26.65	9.19
Subject 3				
10	1.10	-32.50	10.16	9.23
20	1.50	-28.55	13.83	9.22
30	2.00	-25.06	18.45	9.22
40	2.10	-24.99	19.35	9.22
50	2.10	-25.87	19.33	9.20
60	2.30	-26.01	21.17	9.20
70	2.50	-25.08	22.95	9.18

contraction strength. An adequate contact distance from the fulcrum had to be maintained to provide enough of a mechanical advantage (moment arm) to enable effective contraction.

# 4.4.1 Fringe Patterns

Flexion generated a series of horizontal and parallel fringes (Figure 4.2). These fringes moved across the entire back and were roughly horizontal, except for the area over the scapula, where concentric circles were produced. With graduated levels of contraction, the fringes became less straight and more undulating. Fringe order did not progress as it did in "neutral" adduction. Extension produced a similar appearance of fringes, with concentric patterns now noted over both scapulae (Figure 4.3). Poor fringe progression was also seen, with N = 0 appearing as a reversed "C", rather than the upward "C" shape of the neutral position. Rotation to the right yielded a series of parallel, vertical fringes over the left hemithorax. At the right scapula, "C" shaped fringes were present. "Compression" of these with adduction occured at the inferior aspect of the right side. However, fringes did not originate and progress from axilla around the scapula as did those from neutral (Figure 4.4). Rotation to the opposite side produced similar vertical fringes. These were now more

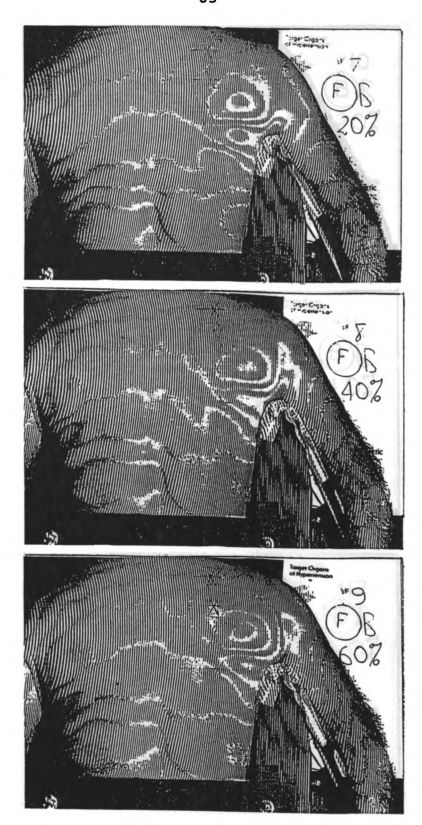


Figure 4.2 Fringe Progression in Flexion

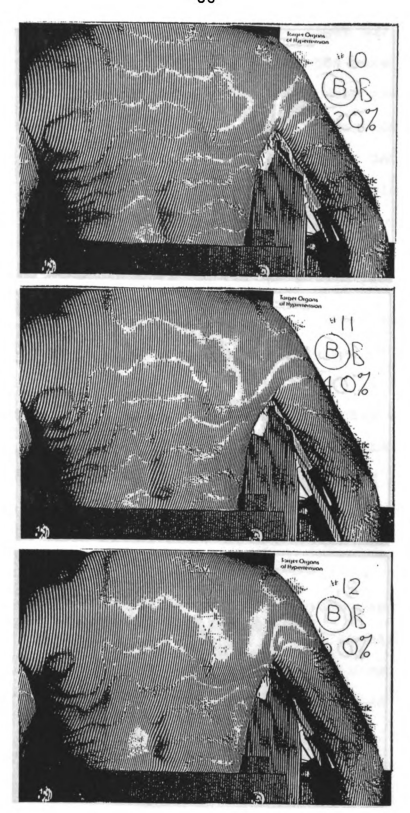


Figure 4.3 Fringe Progression in Extension

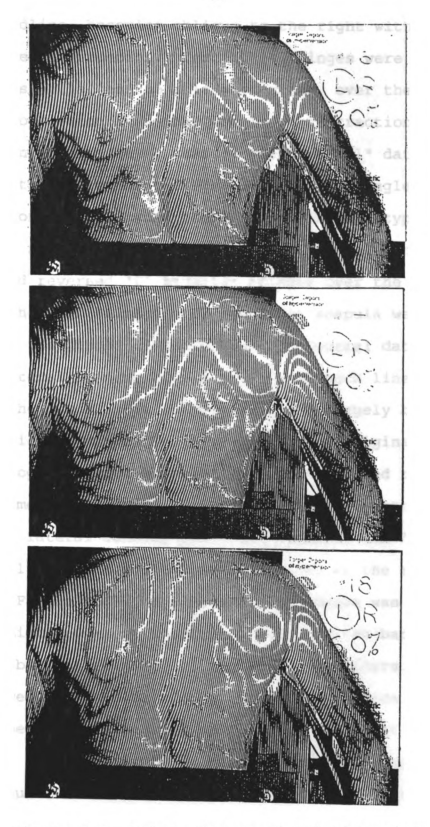


Figure 4.4 Fringe Progression in Rotation

at the midline, becoming oblique to the right with incremented contraction. Concentric fringes were noted over the left scapula, and to a lesser extent, over the right. Fringe progression at higher levels of contraction became similar in appearance to that of the "neutral" data. However, the motion of the scapular inferior angle landmark was horizontal and toward the left, unlike the typical motion of neutral contractions. Right lateral bending introduced reversed "C" parallel fringes over the left lateral thorax. Fringes over the right scapula were different than those obtained from the neutral data and any of the lateral bending curves containing such lines were not used in the study. Not surprisingly and largely because of the restrictive apparatus, very few of the original neutral data photographs of the three subjects contained this spurious motion, as shown by tell-tale fringe patterns.

Left lateral bending produced, perhaps, the fringes most similar to those obtained in neutral at the right scapula (Figure 4.5). A prominent difference was that a few fringes migrated along the entire width of the back, either from mid-back inferiorly, or across the shoulders. These fringes were slanted in the direction of the side to which lateral bending was positioned. Except for right and left rotation, the parallel fringes appeared to be roughly perpendicular to the direction of motion. With left lateral

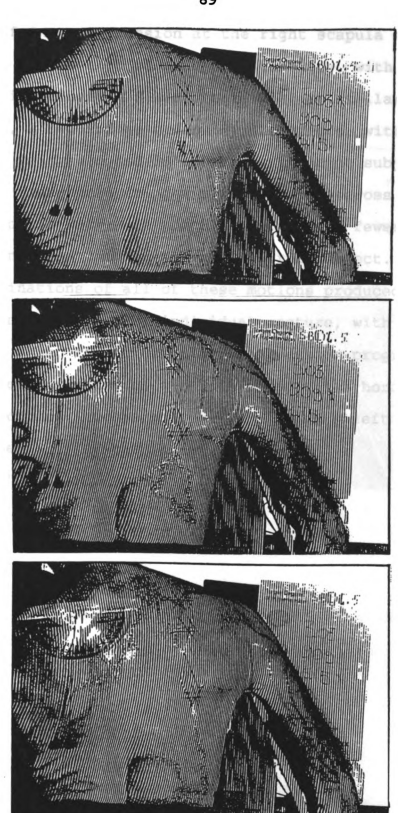


Figure 4.5 Fringe Progression in Left Lateral Bending, with Pendulum Goniometer

bending, fringe progression at the right scapula appeared to basically follow that of neutral adductions, with two primary differences. First, there was, at similar levels of adduction, a two fringe-order (N) difference, with a larger number of fringes noted in the laterally-bent subject. Secondly, transverse fringes that migrated across the midline to the left were roughly horizontal, fewer in number, and less complete in the neutral subject.

Combinations of all of these motions produced the distortions seen in each individual posture, with additive effects. Thus, right rotation and extension progressed in an inferior direction as a series of parallel horizontal lines, becoming increasingly vertical with a left to right slope superiorly (Figure 4.6).

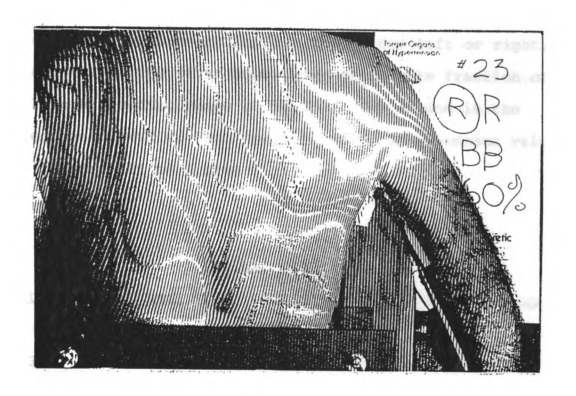


Figure 4.6 Fringe Progression in a Combination of Postures

## 4.4.2 Displacement Values

The results of the digitization and processing of the moire fringe patterns are listed below for the percentages of the lateral bending range of motion. The displacement value position abbreviations are L or R for left or right, respectively. The first number represents the fraction of the lateral bending range of motion. The second is the percentage of MVC at that position. The displacement values were rounded off to 0.01mm.

Latera	l Be	nding
--------	------	-------

Position	<u>x.o-x(mm)</u>	<u>N</u>	d(mm)	d/N(mm)	Force (pounds)
L25/30%	8.4	2.0	18.26	9.13	8.8
L25/50%	7.0	2.5	23.80	9.52	15.3
L50/30%	6.3	1.5	13.53	9.02	8.8
L50/50%	4.2	1.6	14.60	9.12	15.3
R25/30%	1.4	0.9	8.22	9.14	8.8
R25/50%	4.2	2.0	18.25	9.13	15.3

Comparable neutral values for the same subject at the same percentages of MVC are shown for comparison:

N	e	u'	t	r	а	1

Position	$x_{\infty}$ - $x$ (mm)	<u>N</u>	d(mm)	d/N(mm)	Force (pounds)
30%	7.7	2.0	18.47	9.23	16.2
50%	6.3	2.1	19.39	9.23	26.2

Lateral bending left at an angle of 3.25° at 30% MVC (L25/30%) and right of 6.25° at 50% MVC (R25/30%) produced results most similar to neutral data. Left lateral bending of 3.25°/50% MVC (L25/50%), 6.5° at 30% (L50/30%) and 50% MVC (L50/50%), and right of 6.25° at 30% (R25/30%) yielded N and d values that were fractions or multiples of neutral data. The L25/50% value was greater because with the shorter moment arm, more effort was required. However, values at L50/30% and 50% were less than those at neutral, as were R25/30% and 50%.

As in the neutral data, fringe order values, N, increased with rising contraction force. The range increase in neutral was 0.25 to 2.9, and that of incremented lateral bending was 0.5 to 2.8. Similarly, d increased with contraction strength as it did in the neutral data. The change in d for the neutral data ranged from 9.23 to 23.00mm. For sidebending photographs of similar appearance, it was 8.22 to 23.80mm. Plotting N versus %MVC and d versus %MVC (Chapter III, Figures 3.12 & 3.13, page 64) yielded similar graphs, which suggested a direct proportionality (Figures 4.7 and 4.8), as in the neutral data. Values of d were greatly influenced by those of N. This is largely due to the factor  $[N(p)]/\sin\theta$  (Chapter III, Table 3.6, page 68).

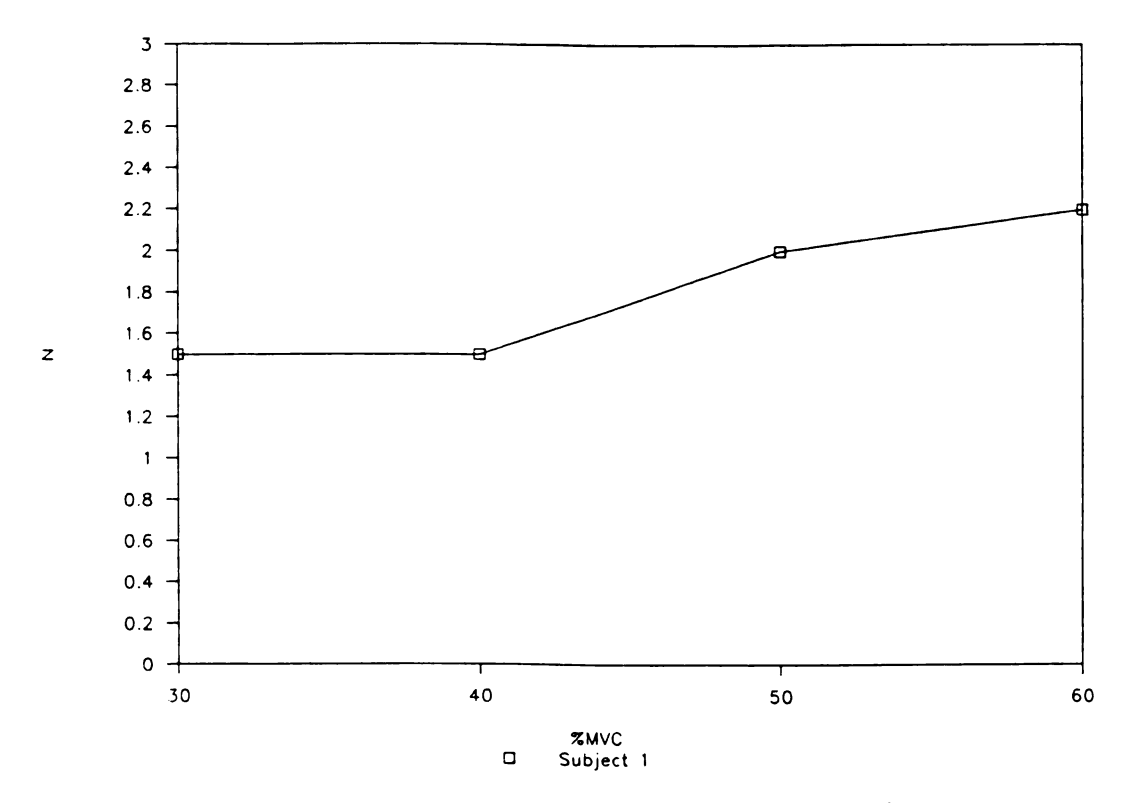


Figure 4.7 N vs. %MVC (Lateral Bending)

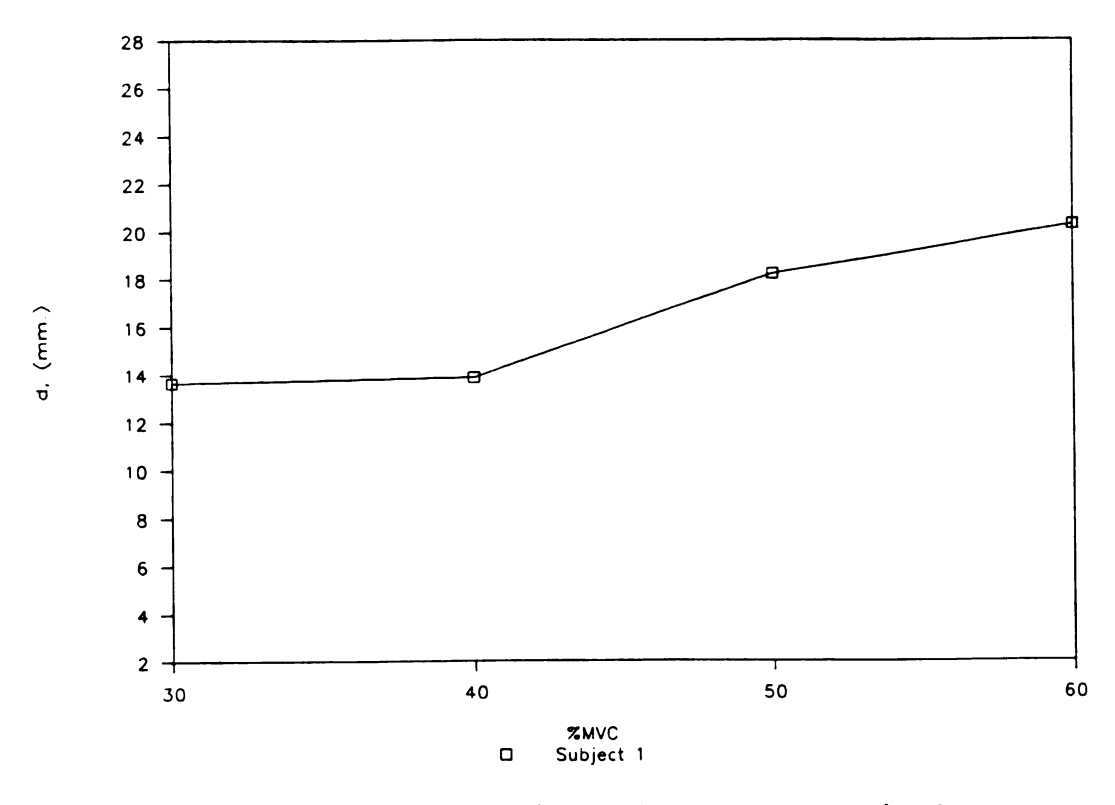


Figure 4.8 d vs. %MVC (Lateral Bending)

#### 4.5 DISCUSSION

Substantial differences were noted for values of x and x between neutral and laterally bent data (Table 4.3). For  $x_m$ , this range was 21.7 to 37.1mm, for x, 15.4 to 43.4mm. It was felt that several factors were responsible for the variations of inferior angle distance from the midline. First, shifts of the epicondyle along the aluminum bar/strain gage device changed the moment arm. Because of a shorter moment arm, more force would be needed in left lateral bending to give the same %MVC and perhaps less in right lateral bending, due to the longer moment arm. Because of the restrictions designed into the test apparatus, any lateral bending would have to take place from approximately T-6 cephalad. The scapular adductors rhomboideus major and minor attach at these levels. Changes of orientation of the muscles and their fibers would alter the efficiency and mechanical relation of these adductors, in terms of muscle force lines-of-action. Hypothetically, left lateral bending stretched and straightened the rhomboids' fibers along the horizontal, whereas right lateral bending increased the vertical orientation.

"Steps" such as those noted in the neutral data were seen at the same percentages of MVC, another characteristic which might be related to the above listed mechanisms.

Table 4.3

x<sub>20</sub>, x Values: Neutral vs. Lateral Bending

	Sideben x. (mm)	t <u>Neutral</u> x <sub>no</sub> (mm)	x <sub>so</sub> (mm)	Sidebent x(mm)		<u>x(mm)</u>	
10% M	<u>VC</u> 135.1	107.1	28.0	132.3	102.9	29.4	
R100	149.1	107.1	42.0		102.9	45.5*	
20% M	VC		106.4			102.9	
30% M	<u>VC</u>						
L25	142.1	109.2	32.9	133.7	101.5	32.2	
50	138.6		29.4	132.3		30.8	
75	137.9		28.7	131.6		30.1	
100	136.5		27.3	129.5		28.0	
R25	136.5		27.3	135.1		33.6	
50	140.0		30.8	138.6		37.1	
75	146.3		37.1	142.1		40.6	
100	146.3		37.1	144.9		43.4	
40% M	VC						
L100	133.0	111.3	21.7	119.0	103.6	15.4	
R100	141.4		30.1	111.3		7.7*	
50% M	v.C						
L25	140.7	113.4	27.3	133.7	107.1	26 6	
50	140.7	113.4	27.3	136.5	107.1	29.4	
75	137.9		24.5	127.4		20.3	
100	143.5		30.1	137.9		30.8	
R25	136.5		23.1	137.3		25.2	
50	143.5		30.1	138.6		31.5	
75	149.8		36.4	144.2		37.1	
100	148.4		35.0	142.8		35.7	
60% MVC							
L100	135.1	118.3	16.8	120.4	107.8	12.6*	
R100	142.1	110.0	23.8	114.8	_0,.0	7.0*	
70% M	70% MVC						
	-	112.7			112.7		

<sup>\*</sup> Fringes Contaminated by Rotational Component

Values for d/N calculated for neutral and lateral bending data had the value of approximately 9.2, which was essentially constant throughout. Such results were seen in the analysis of the neutral data of subjects 1 and 2. It appeared that d values were multiples or fractions of 9.2 based upon fringe order, N.

It is tempting to say that this value may be used as an index, and that variation from it might indicate data contamination by spurious motions or rigid body movement. However, lateral bending photographs at R100/40%, which were noticeably influenced by rotation, had d/N closer to 9.2 than those which showed minimal contamination, as L50/30%. Perhaps ranges of d/N are "individualized" and each subject might have his own unique value. This suggestion, and its application, is yet to be demonstrated, which would surely require a larger sample size.

## 4.6 CONCLUSIONS

Attempts were made to contaminate the data with incremented contractions at various degrees of flexion, extension, rotation and lateral bending. Lateral bending fringe patterns were the most similar to neutral data and thus, this position was used for further studies. Photographs were made at increments of left and right bending and at percentages of MVC. Those that displayed

rigid body rotation or flexion and extension were not processed, as was the case with those exhibiting grossly obvious lateral bending. The reduced data were compared to the MVC percentages of the same subject in neutral.

The ratio d/N remained constant, perhaps as a "check" suggesting that the overall magnitudes were in the same range. Both N and d values for right lateral bending were less than those at neutral. This may have been a result of a reduction in muscle contraction and topographic change. Recall that, in the lateral bending position, the subject contacts the strain gage bar farther from the fulcrum. This mechanical advantage requires less adduction effort to generate gage values of magnitudes similar to those from the neutral (upright) stance. Smaller values of fringe order N and d, therefore, were proportional to less effort. Again, the N values and d values were fractions of the neutral data of identical magnitude.

These changes may be biomechanically related to muscle fiber orientation, or scapular, humeral, and thoracic spine axial alignment. Maintenance of the elbow position along the strain gage bar assisted in retaining the subjects' erect posture and consistent data. In contrast, lateral bending forced the repositioning of the elbow from its resting contact point and the inferior angle away from the original lens focus point. Perhaps this shift from the

original point was optically significant and was partially responsible for changes in the data.

Intuitively, in-plane (coronal plane) sidebending should not affect z-axis displacement of the inferior scapular angle, provided that forces in adduction needed to generate the displacement and net mechanical relationships (torques) are unchanged. The data suggested that this may be the case. Neutral and lateral bending photographs yielded, independently, displacement and fringe order values of the same magnitude and progression. It was surmised that increases of mechanical advantage merely shifted the graphs of d vs. %MVC to lower corresponding %MVC values and toward the origin. This hypothesis is tempting, but proof requires complete study with closer contraction increments and more subjects.

### CHAPTER V

#### CONCLUDING REMARKS AND SUMMARY

## 5.1 DATA DISPLACEMENT PLATEAUX

An effort was made to explain the "steps" noted in each of the three graphs of d versus %MVC. The "displacement plateaux" or steps were noted at 40-50% MVC for subjects 1 and 3, and at 30-40% MVC for subject 2. Values for contraction forces were approximately the same for subjects 1 and 3. Displacements, d, were less for the former until a higher %MVC was reached. This may be explained by difference in moment arm, a concept that may be challenged when looking at displacement data for subject 2 at 50%, 60%, and 70% MVC. Here, the person has less gage force and greater d than the other two. Certainly, height, weight, age, body habitus and MVC did not seem to be apparent factors.

In all three subjects, contralateral fringes appeared at approximately the same intervals as the plateaux in the graphs of d vs. \*MVC. For subject 1, these occurred at 40% MVC. Subject 2 had slight formation at 10% and pronounced changes at 50% MVC, while subject three also had a few

spurious fringes at the same lower level and significant fringes again at 40% MVC. Quite possibly, the steps are related to the involvement of the left thoracic musculature to provide the contraction force necessary especially at higher MVC's.

Dvir and Berme (1978) applied anatomic relationships to their work and described several phases in which scapular motion occurred (Chapter III, Appendix, Figure 3.8.3, page 73). During the various phases of abduction, three z-axis, parasagittal rotational axes were described as being at the scapular spine root and sternoclavicular joint medially and through the acromioclavicular and glenohumeral articulations laterally. With abduction, the inferior scapular angle is displaced laterally during shoulder complex motion about these axes. Perhaps a portion of step-like appearance of the graphs is due to the shift of scapular rotation about these axes, relocation of the primary axis, or a change in the relative contribution of each of these axes.

The "steps" at approximately 40-50% MVC in the data may represent not only axis of motion changes but muscle recruitment order and fiber orientation changes. If not a result of error propagation, which seems doubtful, they may represent physiologic muscle function at the various percentages of maximal voluntary contraction. Similar graph functions were noted in a review of related literature.

Orizio, et al.(1989), conducted a study using acoustic

myography (AMG), electromyography (EMG), and isometric contractions of biceps brachii in humans. AMG is a modality in which muscle sound, generated with contraction, is sensed, amplified, and recorded. The tool has many potential applications, from diagnosis of certain disease states to a feedback control in prosthetics (Barry, et al., 1986). AMG amplitude changes are quite sensitive to muscle fatigue and seem to be good indicators of excitation-contraction coupling (Barry and Geiringer, 1985).

In their experiment, the Orizio group had each subject contract at varying percentages of maximum voluntary contractions (%MVC), all to exhaustion (fatigue). It is interesting to note that, prior to fatigue, the sound amplitude increased linearly with contraction strength up to 40% MVC (Oster & Jaffe, 1980). At 40%, AMG fluctuated, and began to drop off (Figure 5.1). Freund (1983) felt this to be a level of "transition with respect to motor unit activation pattern and muscle perfusion". He thought that there may be changes occurring in the "muscle environment" that might be responsible.

Step intervals have also been noted on a microscopic level. Pollack, et al (1977), noted that, during contraction, sarcomere shortening occurred in a series of successive bursts. This group also used an optical method and found that the shortening bursts were punctuated by

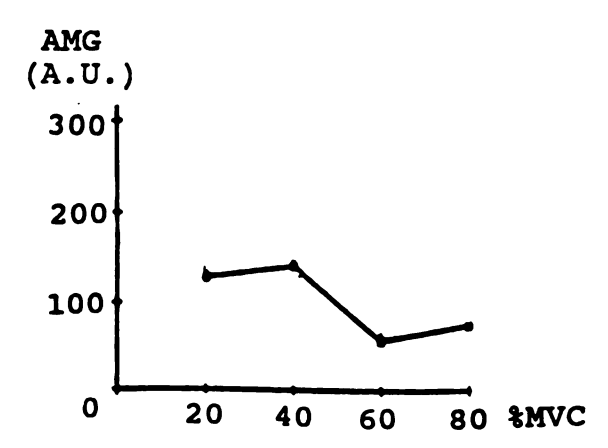


Figure 5.1 AMG Amplitude vs. %MVC (adapted from Orizio et al, 1989)

well-defined periods during which motion "virtually ceased". If, as suggested by DeLuca (1984), motor units, which are single motor nerves and the muscle fibers that they innervate, synchronized during contraction, this pattern would be seen in many contiguous sarcomeres. As a result, shortening, various levels of tension (Ford, et al., 1981), and plateaus of non-shortening (resting), would be noted. This phenomenon was found especially in the early phase of contraction.

The "transition or settling points" may also represent the "migration of activity between different muscles" (Viitasalo & Komi, 1977). During sustained contractions, this is a result of the recruitment of new motor units to replace those that are fatiguing.

Graphs of the data of Viitasalo & Komi show some interesting

results comparing percent MVC to either electromyographic amplitude or frequency (Figures 5.2 and 5.3). EMG signal amplitude is generally directly proportional to contraction force, while signal frequency typically drops off with fatigue. Alterations of the EMG signal begin even at the onset of contraction. The drop in the median frequency interestingly is at a maximum at 50% MVC (Stulen, 1980), while the amplitude increase is also the greatest at the same percentage (Clamann & Broeker, 1979). Assuming that changes in impulse conduction are related to the pH of the tissues, and that lactic acid influences the pH, it is easy to appreciate that maximum lactate levels are also noted at 50% MVC (Tesch & Karlsson, 1977).

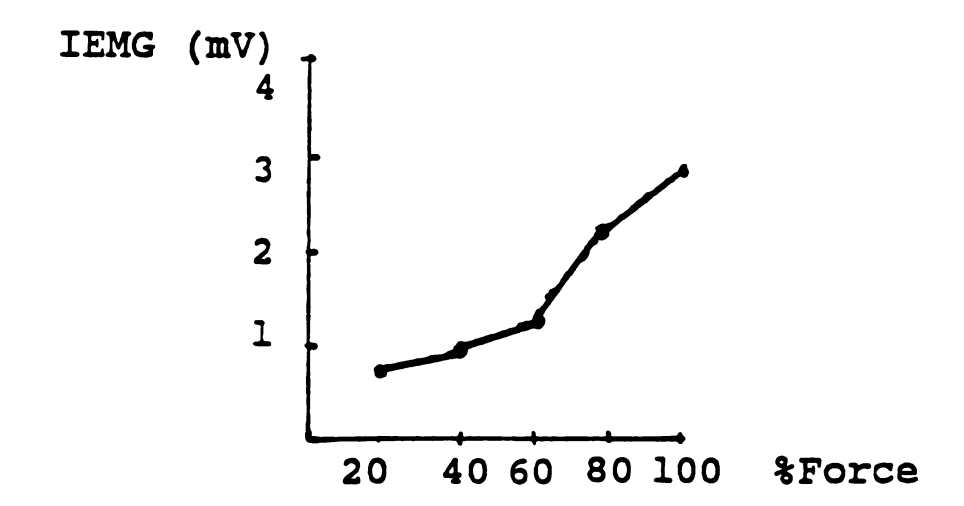


Figure 5.2 Integrated EMG vs. %Force (adapted from Viitasalo & Komi, 1977)

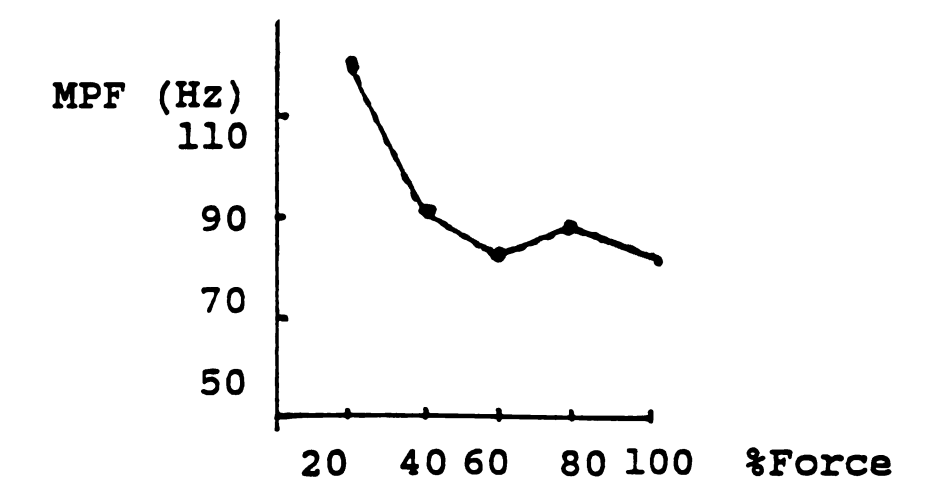


Figure 5.3 MPF vs. %Force (adapted from Viitasalo & Komi, 1977)

Recruitment of muscle fiber types within a muscle may also be a part of this observation. Gydikov, et al (1976), suggested that the threshold for slow motor units (in biceps) was from 0 to 80% MVC. That of fast motor units, which, incidently, fatigue first (Maton, 1981), are from 30 to 80% of MVC. If thresholds of synchronously contracting, homogeneous groups of fibers are reached, plateaus might also be seen. The time interval may not be of the same magnitude in the moire experiments, but shifts of recruitment and firing order not only within individual

muscles but between groups of adductors may be responsible for the data steps.

In addition to recruitment order and according to Bigland-Ritchie & Woods (1984), different muscles have different firing rates, as well as twitch contraction and relaxation times, with motorneuron firing rates geared to match the contractile requirements of the individual muscles. For efficiency, excitation rates stay at the minimum needed to yield the maximum force, a "safeguard" against neuromuscular transmission failure. Displacement plateaux may be due, in part, to a rate adjustment to force requisites, secondary to fatigue and contractile "fall-off".

Of course, with the short contractions of the moire study, fatigue does not maximize. Also, many of these experiments were with muscles other than the parascapular groups. Yet, the aforementioned are interesting observations made by several authors at levels of voluntary contraction roughly corresponding to those at which stepping has been seen in the moire results.

### 5.2 EXPERIMENTAL DESIGN

Initial study showed that, at rest, no fringes were formed. Furthermore, in the absence of rigid body motion, if double exposures were made on subjects not contracting the parascapular musculature, no incremental alteration of

topography was produced and no fringes were formed. Thus, there was to be no treatment or comparison group as each subject underwent two sets of similar contractions in the study and thus each served as his own control.

Many extraneous variables were present in the study. Some individual variation was noted in body size, weight, age, strength of contraction, and moment arm size (humerus length). Reaction time and the ability to maintain a submaximal voluntary contraction during photographic exposure would also, more than likely, be characteristics unique to each individual. Attempts were made to control these differences, including a standardized perfunctory history and physical examination performed by the same physician and the use of the same test apparatus and protocol. Because the participants, all having similar histories, had approximately the same physiques and muscular distribution, their motion while in the test apparatus would be restricted to the same degree.

Photographic techniques, film, apparatus distances and exposure times were held constant for all participants. All anthropometric and digitization measurements were done by the same person, as were the photographic exposures in an attempt to keep data acquisition consistent. Film processing and printing were done by the same two establishments.

### 5.3 ASSUMPTIONS AND LIMITATIONS

Assumptions of the research plan were manifold. Primarily, it was assumed that subjects were able to understand instructions, that they had motor control enough to be able to maintain contractions at a relatively constant value, and that they could estimate a range of variation from that value. A portion of these abilities were estimated from history and physical examination. Also, the subjects were assumed to be unbiased, and were honest and complete in their medical history. It was believed that the photographic emulsions, chemicals and papers were relatively uniform, and that they provided similarly reliable results. It was also presumed that the electric apparatus had a relatively constant power supply during the experiment, and that gage readout fluctuation was not primarily due to gross changes in household current.

Limitations of the proposed plan were of several types. Optical sensitivity was limited in part by the resolution of the image by lenses of the photographic and projection systems, the quality of which was restricted by cost.

Manual digitization of photographic enlargement by visual means limited the accuracy of the method, but again, was restricted by finances. The use of strain gage and gage signal processing equipment had its own inherent problems, as calibration, zeroing, and so forth.

Perhaps the greatest limitation of the method was the application of the technique to human study. Despite the use of a restraining apparatus, subjects could not be as positionally rigid as an inert body. Also, the ability of the subject to transiently maintain a contraction at a constant, predetermined level placed some restrictions into the design. However, given the resources of time, money and available manpower, most of these limitations (and perhaps sources of error) were addressed.

### 5.4 SUMMARY

It was hypothesized that the point labeled on the inferior scapular angle would be displaced in graded quantities corresponding to the amount of submaximal voluntary contraction. Formulae to determine displacement in terms of z-axis shifting of the digitized point (d=w<sub>d</sub>-w, Formula 3.3, page 35) were used to process moire fringe raw data and yielded z-coordinates of the point. Appropriate scaling relationships to quantify landmark point changes secondary to photographic enlargement were incorporated prior to the final calculations.

Towards this end, the paper demonstrates the adaptation and application of a non-invasive, non-contact method of optical metrology. The technique itself is relatively inexpensive, and offers some portability. Use of the

single-source, differential moire projection method yielded both in-plane and out-of-plane displacement information of surface landmarks of human subjects. Double-exposure photography of the parascapular musculature of subjects isometrically contracting provided the different moire fringe raw data. Surface marker distances from the midline were ascertained and fringe values assigned and digitized for the series of graded contractions, with a digitization measurement error of approximately ±1.5-2mm. The resulting figures were then processed using formulae developed by Khetan (1975) especially for single light source applications.

The scapular landmark was found to be displaced in a incremented fashion proportional to the intensity of the adducting contractions. These displacements were along the mediolateral (x-axis) and anteroposterior (z-axis) directions. Along the former axis, at 70% MVC, the in-plane displacement distances were 9.1, 12.6, and 7.7mm for subjects 1, 2, and 3, respectively. The average x-axis motion was 9.8mm. The 70% MVC, out-of-plane displacement (z-axis) values were 18.4, 23, and 27.6 mm, with an average of 23mm.

Upon gross examination, it appeared that the inferior scapular angle became more prominent and moved medially upon scapular adduction (Nordin & Frankel, 1989). These observations were corroborated by trends in the data. The

medial motion was shown both by inspection and measurements of the double-exposures. The former was demonstrated in two First, N values, estimated in tenths, increased with increasing contraction force, with ranges for the three subjects from 0.25 to 2.10, 0.25 to 2.90, and 1.10 to 2.50. Greater age, conditioning, and muscle tone may have accounted for the difference in the initial values. On the photographs, fringes formed and migrated, increasing in density as percentages of maximum voluntary contraction increased. Likewise, values of d also grew larger. exact influence that parascapular and shoulder muscles had on scapular and inferior angle displacement may depend upon several factors, as muscle force, leverage, order of recruitment, and scapular fossa contour relative to posterior chest wall curvature.

### 5.5 SUGGESTIONS FOR FURTHER STUDY

Several improvements on the current apparatus could be made. The addition of a fiberglass "cast" contoured to the left hemithorax might help to further fix subject position. This, coupled with a refined adjustable epicondylar contact point on the strain gage bar should assist in reducing data contamination by spurious movement from additional posturing.

Because of the aluminum bar thickness, the gain was set relatively high. This gave a high signal-to-noise ratio but also increased the MVC signal sensing capacity. To reduce signal-to-noise ratio, a thinner bar of decreased width and thickness would have been required, which would have decreased the resistance to arm contraction and increased bar deformation at higher loads. The bar deformation at the point of contact would be only a few millimeters, however. So, to decrease gain, one must decrease bar size, and lose a portion of arm contraction isometricity.

Of course, finer gratings, camera/projector optics, and more exact lens nodal point positioning would improve resolution and sensitivity. Reference mark adjustable templates for standardization would be desirable, as would computerized digitization techniques and computer algorithms for data reduction. Indeed, computerized camera/monitor systems would be convenient not only for static work, but to possibly permit dynamic testing.

Further studies investigating d at finer increments would improve data results by being a more concise evaluation of fringe progression. Finer increments of contraction about the "stepped areas" might help to better define z-axis shifts as they are related to fringe development.

Corroboration of the photographic data may be obtained by affixing a linear variable differential transformer (L.V.D.T.) to the apparatus contacting the point of the inferior scapular angle. An appropriate design would allow the measurement of physical displacement, independent of position of the scapula in three-dimensional space.

Digitization of more data points about the scapular border would enlarge the data base and expand the knowledge of scapular motion. The addition of y-axis data to the x-and z-axis figures would improve the accuracy of three-dimensional depiction.

With larger subject populations, more concise statistical analyses, such as regression of results on variables as height, weight, body habitus, moment length, and age, could be done to improve predictability. Likewise, randomization of percentages of MVC in both neutral and lateral bending test protocols would improve the reliability of the conclusions.

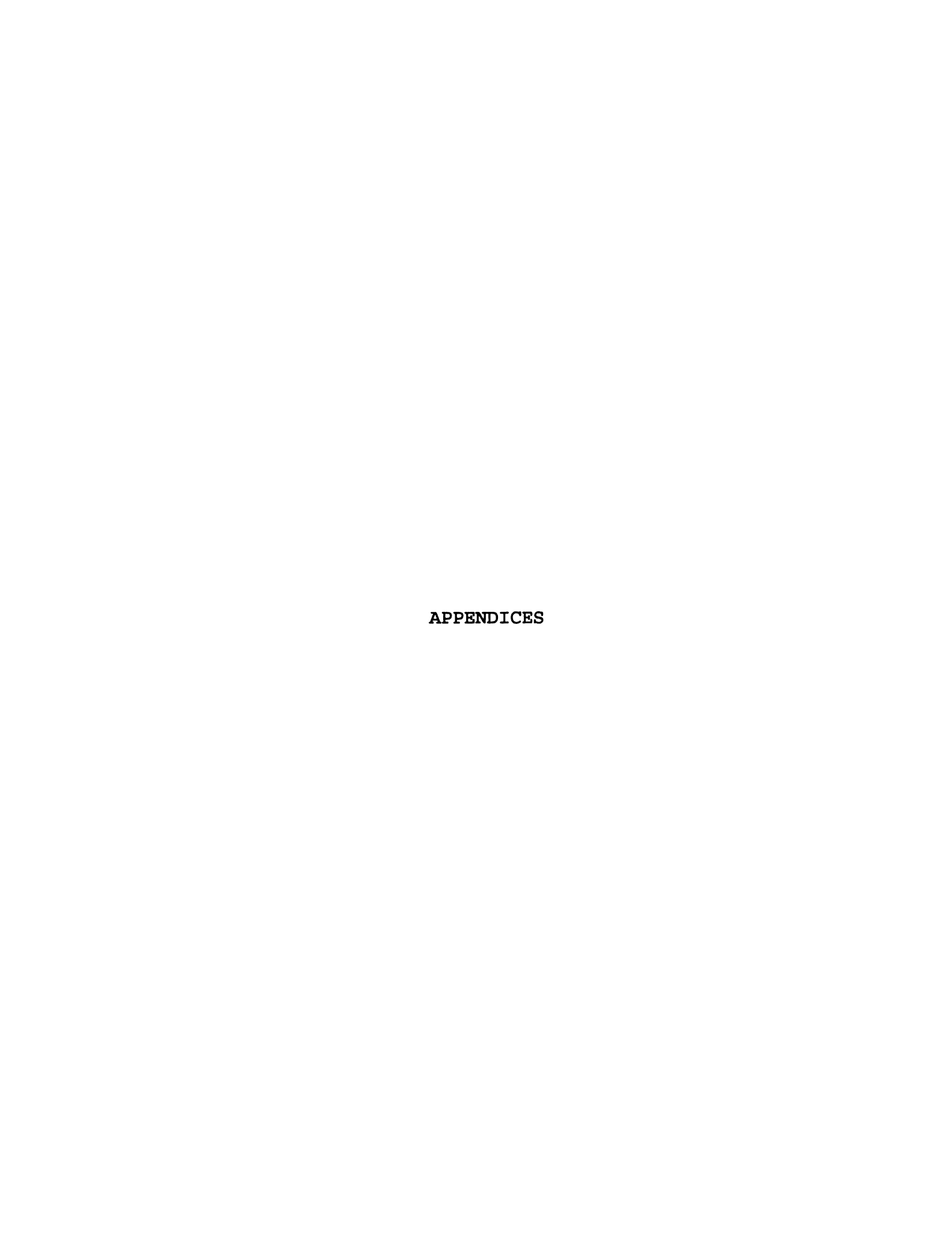
The incorporation of parascapular EMG to ascertain strength and parascapular muscle recruitment sequence might augment the kinesiologic picture. Muscle activation order, fiber orientation, or lever arm length may play a large part in the data steps. If available, information on the percentage of slow and fast muscle fibers of each muscle would be of value to define recruitment speed relative to the electromyographic data at these steps.

#### 5.6 APPLICATIONS

Previous biological applications have primarily utilized absolute topography to determine surface contours scoliotic curves. Occasionally, specific angles between surface curves were measured using geometric relationships.

Differential methods have been used less frequently. In this study, fringe patterns were compared at sequential increments of muscular contraction at two different postures to yield both in-plane and out-of-plane point displacement information.

Single-source, differential moire fringe projection method may be applied to other musculoskeletal sites to further expand the body of kinesiologic and clinical information. Expansion of this information into a larger data set may be used to construct tables of "normal" values. Once nomograms are developed and the three-dimensional motion of healthy scapulae established, application to injury or illness may be made. Diagnosis, treatment, and the progress of injury rehabilitation may be facilitated by this knowledge.



### APPENDIX A

#### **ANATOMY**

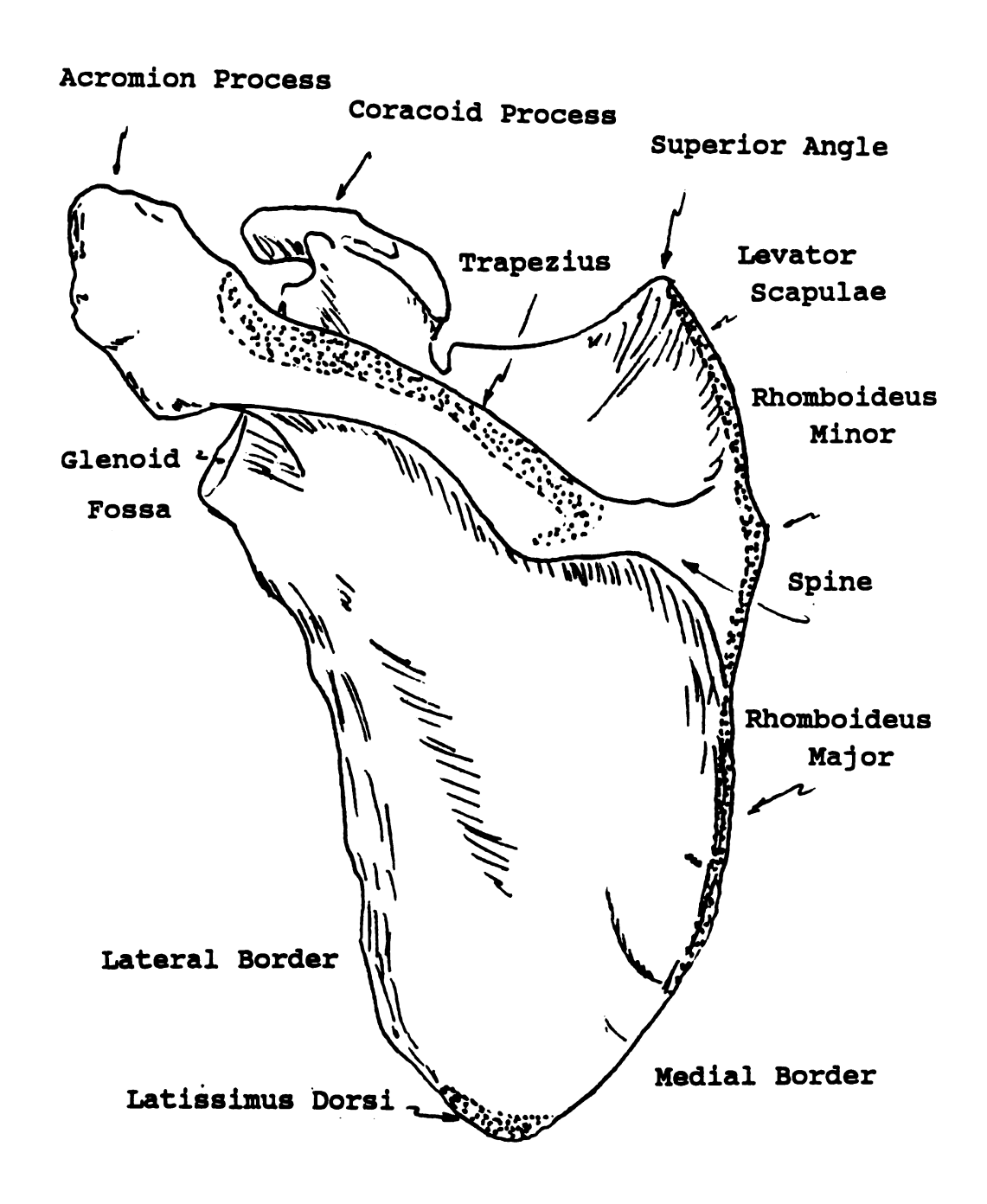
#### A.1 OSTEOLOGY

The shoulder complex consists of the clavicle, scapula, and humerus. With the addition of muscles and ligaments, the following articulations are formed: glenohumeral, acromioclavicular, sternoclavicular, and scapulothoracic, with the latter being a non-synovial, muscular articulation.

The scapula is essentially an elongated boney triangle, with base cephalad and apex, or inferior angle, caudad. It provides a "seat" for the humeral head and arm and sites for muscular attachment (Figure A.1). The humerus is the proximal portion of the upper extremity, and it moves through its range of motion within a ligamentous capsule. Finally, the elongated, cylindrical clavicle acts as a strut, supporting the scapulohumeral unit.

### A.2 MUSCULATURE

The muscles of the scapulothoracic articulation responsible for scapular adduction are arranged in



Inferior Angle

Figure A.1 Scapular Osteology and Adductor Attachments (adapted from Goss, 1974)

superficial and deep layers. Superficially, the primary muscles are the trapezius and latissimus dorsi. The deeper muscle are the rhomboidei major and minor, and the levator scapulae. The latter muscles of each group are less influential than the former. The anatomic relationships of these muscles, along with their fiber orientation, may be noted in Figure A.2. Muscle fiber direction, coupled with muscle size, origin and insertion relative to the scapula, determine the direction and quality of adduction. General muscle anatomy, that is, origin, insertion, and nerve supplies are noted in Table A.1, with variations documented elsewhere (Goss, 1974). The attachment sites of the scapular adductors, those muscles that connect the scapula to the vertebral column, are illustrated in Figure A.1. Although the trapezius and latissimus dorsi may blend with fibers, aponeuroses, tendons, or fasciae of other structures, their scapular involvement is the primary consideration.

When the scapula is fixed, the actions of several muscles change, primarily acting to rotate the head or to bend the neck generally in the direction of fiber orientation. In contrast, with thorax and arm fixed, and with the latter isometrically adducting, the scapular inferior angle will be displaced posteromedially (Nordin & Frankel, 1989).

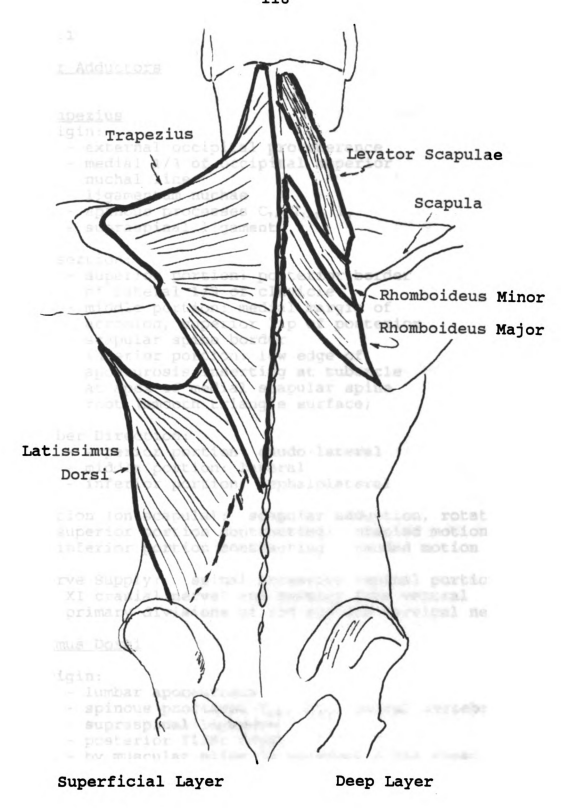


Figure A.2 Parascapular Muscles (adapted from Goss, 1974)

#### Table A.1

# Scapular Adductors

# Trapezius

## Origin:

- external occipital protuberance
- medial 1/3 of occipital superior nuchal line
- ligamentum nuchae
- spinous processes C<sub>7</sub>, T<sub>1-12</sub>, L<sub>1</sub>
- supraspinal ligament

## Insertion:

- superior portion: posterior border of lateral 1/3 of clavicle
- middle portion: medial margin of acromion, superior lip of posterior scapular spine border
- inferior portion: low edge of aponeurosis inserting at tubercle at apex of medial scapular spine root (smooth triangle surface)

#### Fiber Direction:

- superior portion: caudo-lateral
- middle portion: lateral
- inferior portion: cephalolateral

Action (on scapula): scapular adduction, rotation superior portion contracting: craniad motion inferior portion contracting: caudad motion

Nerve Supply: spinal accessory (spinal portion of XI cranial nerve) and sensory from ventral primary divisions of 3rd and 4th cervical nerves

### Latissimus Dorsi

# Origin:

- lumbar aponeurosis
- spinous processes  $T_{6-12}$ ,  $L_{1-5}$ , sacral vertebrae
- supraspinal ligament
- posterior iliac crest
- by muscular slips to external iliac crest, caudal aspects ribs 3 and 4
- interdigitates with obliquus externus abdominis

## Table A.1 (cont.)

#### Insertion:

- fibers converge, twist upon themselves, forming a quadrilateral tendon which inserts at humeral intertubercular groove
- upper horizontal fibers passing under inferior scapular angle are joined by fasciculi arising out of scapula
- occasionally, this is separated by a bursa

# Fiber Orientation:

- superolateral

#### Action:

- adduction, extension and medial rotation of arm
- moves scapula, shoulder medial/caudad

# Nerve Supply:

thoracodorsal (long subscapular)
 from the brachial plexus, with
 fibers from 6th, 7th, 8th cervical

# Rhomboideus major

## Origin:

- tendinous fibers from spinous processes T<sub>2-5</sub> (as trapezius, but deep to it)
- supraspinal ligament

## Insertion:

 cephalad: narrow tendinous arch to inferior portion of triangular smooth surface of scapular spine root caudad: inferior angle

# Rhomboideus minor

## Origin:

- inferior ligamentum nuchae
- spinous processes C<sub>7</sub>, T<sub>1</sub>

### Insertion:

- base of triangular smooth surface at root of scapular spine

### Fiber Orientation:

- superomedial

## Table A.1 (cont.)

## Action:

- adduction, slightly craniad motion and depression of lateral angle

# Nerve Supply:

- dorsal scapular from brachial plexus, containing fibers from 5th cervical

# Levator Scapulae

## Origin:

- tendinous slips from lateral bodies  $C_{1\cdot 2}$
- posterior tubercles of lateral bodies C<sub>3.4</sub>

## Insertion:

 vertebral aspect of scapular border, between superior angle and triangular smooth surface at scapular spine root

### Fiber Orientation:

 essentially cephalad, with slight medial component

## Action:

 medial rotation of scapula, with elevation to lower lateral angle

## Nerve Supply:

- branches of 3rd, 4th cervical from cervical plexus
- lower portion of branch of dorsal scapular nerve (frequently), containing fibers from 5th cervical

#### APPENDIX B

#### **PATHOLOGY**

Abnormalities of neuromusculoskeletal tissue interfere with anatomic motion. This interruption of normal function potentially could be detected and quantified by moire methods, perhaps in early stages of onset and development.

Congenital defects certainly prevent normal scapular function. Sprengel's deformity or "high scapula" is an example, a condition which results from failure of the embroyonic stage descent of the scapula. Concomitant abnormalities may be present, as an omovertebral ligament or bone. The latter results from the ossification of a congenital ligament between the medial scapular border and the distal cervical vertebral spinous processes. The scapula is reduced in size and is in an adducted, inferiorly rotated position, resulting in the restriction of abduction.

Motion is also restricted by limitations of the clavicular strut and parascapular musculature. The former may be a result of clavicular fracture. This, added to scapular fracture with poor fragment alignment, may result in the development of muscular fibrosities and in

alterations of muscle mechanics. Muscle dysfunction might also be a result of contusion or acute or chronic strain. Bursitis may cause local irritation and restriction of motion. Even avulsion of the adductors, especially at the tenuous insertion of latissimus dorsi to the inferior angle, may result in obvious motion interference.

Injury to the nerve supply of parascapular musculature can result in paresis or paralysis and changes of scapular position and function. With nerve supply compromised, the muscles regulated by these nerves might also function poorly. Antagonisitic muscles may override those involved muscles. For example, spinal accessory nerve injury by many mechanisms, as pressure from neoplasms or from "posterior triangle" surgery, may result in trapezius palsy. In such an instance, the scapular superior border is externally rotated by the still-active rhomboids, with the resulting "winging" noted especially in horizontal abduction. An additional etiology of winging is long thoracic nerve trauma, as from stab wounds, surgery, or supraclavicular pressure. Serratus anterior muscle weakness ensues, again with persistent rhomboideus or levator tension. Thus, the inferior angle is medially approximated, again accompanied by external rotation and projection of the superior border. In a similar manner, motor component paresis effects both supraspinatus and infraspinatus muscle function, resulting in external arm rotation. Dorsal scapular nerve entrapment

results in a neuritis which may be associated with scapular winging in wide abduction and pain along the C5-6 nerve distribution.

Weakness, cramps, and fasciculations may characterize nerve root or cervical plexus lesions. Direct trauma, compression, inflammation, or tumor may be responsible. Cervical spondylosis, nucleus pulposis herniation, as C5 radicular compression causing interscapular pain, or root avulsion are other potential etiologies. Pain could also be parascapular in nature, following compressive lesions of the sensory component of the suprascapular nerve.

There are many neurological disease processes resulting in muscular weakness and change in function. Parascapular weakness might be a non-specific sequela of many of these processes. For instance, poly-neuropathies may result in parascapular muscle weakness and changes in surface topography. These neuropathies may result from a wide variety of conditions, as general medical disease or infection (Table B.1). They may also be inherited, or may result from nutritional deficits. Other pathologic states which effect muscle function include lower motor neuron disease, neuro-muscular junction deficits, or disorders of neuromuscular transmission.

Finally, the muscles themselves can also be diseased. Such myopathies include the muscular dystrophies, causing parascapular muscle wasting and thus, changes in scapular

position. Some types, as scapulo-peroneal syndrome may cause scapular winging or elevation (Beeson & McDermott, 1975). An abbreviated list may be found in Table B.2.

#### Table B.1

# Neuropathies - An Abbreviated List

Polyneuropathies from General Medical Conditions as

Diabetes Mellitus Amyloid

Alcoholism Periarteritis Nodosa

Uremia Sarcoid

Malignancies Paraproteinemia

Infections and Post Infectious Neuropathies

Guillain-Barre Leprosy

Diptheric

Metabolic Neuropathies

Nutritional Deficits Toxic Ingestions

Inherited Neuropathies

Charcot-Marie-Tooth

Frederich's Ataxia

Acute Intermittent Porphyria Liproprotein

Fabry's Disease

Hereditary Ataxic Neuropathy Hereditary Neuropathy Hereditary Sensory

Pressure-Sensitive

Giant Axonal

Cerebral Liposis

Lower Motor Neuron Disease

Neuromuscular Junction Pathologies

Disorders of Neuromuscular Transmission

Myasthenia Gravis Botulism

Myasthenic Syndrome Tick Paralysis Neonatal Myasthenia Drug Associated

Congenital Myasthenia

#### Table B.2

## Myopathies - An Abbreviated List

## Muscular Dystrophies

Duchenne Limb-Girdle Becker Myotonic

Facioscapulohumeral Scapuloperoneal Syndrome

## Congenital Myopathies

Central Core Myotubular

Nemaline Fiber Type Disproportion

Centro Nuclear

### Metabolic Myopathies

Acid Maltase Deficiency (Type II Glycogenosis)
Debrancher Deficiency (Type III Glycogenosis)
Muscle Phosphorylase Deficiency (Type V Glycogenosis)

## Metabolic Myopathies

Muscle Phosphofructokinase Deficiency (Type VII Glycogenosis) Disorders of Lipid Metabolism Mitochondrial Disease Malignant Hyperpyrexia or Hyperthermia

## Endocrine Myopathies

Thyroid Adrenal Parathyroid Pituitary

## Myositis

Dermatomyositis Infectious Agents Polymyositis

#### APPENDIX C

## REQUEST FOR APPROVAL OF HUMAN PARTICIPATION IN RESEARCH

PROJECT TITLE: A Study of Scapular Displacement by Differential Moire Methods

PRINCIPAL INVESTIGATOR: Paul J. Moga, D.O., Graduate Student, Department of Biomechanics

ADVISOR: Gary L. Cloud, Ph.D., Professor, Department of Mechanics and Materials Science

#### **ABSTRACT**

A pilot study has been designed to study out-of- plane displacement of the scapula and parascapular musculature using projecton moire. The moire fringe phenomenon is a result of the optical interference produced by superimposition of two uniform gratings. A grating is projected onto the subject in both unstressed and stressed states. In this experiment, "unstressed" is at rest and "stressed" is with muscles at various contracted incremented percentages of maximum voluntary contraction (MVC). The patterns that result on the thirty-five 35 millimeter (35mm) double-exposed negative may then be digitized. The resulting values may be processed using various formulae and geometric relations to determine displacement of a point on the body using a point on the body using a non-invasive, optical method of metrology.

#### SUBJECT POPULATION AND METHOD

Three male subjects, ages twenty-five (25) to sixty-five (65), will participate in the pilot study. All will have negative histories of systemic disease, injury or surgery to the scapular area, arm or thoracic spine. None chosen will be taking medication on a regular basis. Each will receive a perfunctory physical examination by the physician-investigator.

Each participant will perform a series of isometric adductions of the right arm. The subjects will be standing, with thoraces restricted by the test apparatus. In this way, rotation, sidebending, flexion, and extension is expected to be very limited. The arm is set at a twenty-five degree (25°) angle to the vertical, and rests against an aluminum plate affixed with a strain gage. Reference marks, in water-soluble ink, will be placed at three anatomical landmarks of the scapula.

All three will be asked to exert a maximal effort of less than twenty seconds in isometric adduction against the fixed plate. The greatest of three such efforts, as noted by digital strain gage indicator, shall be considered to be the MVC. An adequate rest period is scheduled between each contraction. Double-exposure photographs of the bared scapular region will be taken at rest, for the first portion of the exposure, and then at 10% increments of MVC, from ten to seventy percent. The photographs themselves will be of a

grating projected onto the subjects using a Kodak slide projector. Each grating consists of equidistant, alternating lines and spaces imprinted on the photographic emulsion of the glass slide. In essence, the distortion of the projected gratings occurring with the gradations of muscular contractions as recorded with double-exposure results in moire fringe production. To accumulate the desired raw data, two sets of films per subject will be obtained.

#### INFORMED CONSENT AND RISK

As the techniques that are used are non-contact, non-invasive, few risks are foreseen. Those that are might be parascapular muscular soreness or, at worst, strain. Perhaps discomfort at the points where the participants contact the felt-lined apparatus may occur (thorax and medial elbow). This would not appear to be a common occurrence at this point, however.

All potential subjects will be informed of the experimental procedures, objectives and risks, both verbally and in writing prior to participation. All will be well informed as to the voluntary nature of their participation and right to interrupt it at any time. Written information and consent forms are as attached.

#### PARTICIPANT INFORMATION

You have elected to take part in a study to investigate motion of the human shoulder blade (scapula) as detected by a non-invasive technique utilizing optical interferometry. The technique utilizes basic thirty-five millimeter (35mm) photographic methods to record the moire fringe phenomenon which results from the interference process.

You will stand against a device which, when adjusted snugly but comfortably against your chest (thorax), will limit motion of that area of your body. It will not restrict your breathing, however. Your right arm will rest at a twenty-five degree (25°) angle to your body on a plate and strain gage measuring device. You will be asked to press your arm, and thus, your elbow, toward your body in a downward fashion. Initially, a full effort (MVC or maximum voluntary contraction) reading will be determined.

Subsequently, you will be asked to be at rest, and then to contract the arm at various percentages of the full-effort MVC. The actual quantities of each requested contraction will be calculated from the MVC.

A digital readout will be in your visual range. You will be instructed to compress your arm to the value calculated above and to hold it at that level for no more than twenty seconds. A rest interval will be provided between contractions. Two separate sessions of

approximately six contractions per session will be required.

Each session will last about one hour.

You will be asked to stand in the apparatus with back (and thus, shoulder blades) exposed. For reference points, water-soluble ink marks will be placed over three landmarks on your shoulder blade. A slide consisting of equally spaced lines and gaps will be placed in an ordinary slide projector, using a standard white light bulb. The pattern from the slide will thus appear on your back.

The pattern appears differently at rest then with your muscles contracted. The pattern-change at each interval, when recorded by double-exposure photography, yields a new series of lines and spaces, or fringes. This is the desired raw data, which is to be processed to give the experimental results. Thus, your back will be photographed at rest and during various contraction levels.

Prior to your participation, you will be asked general health history questions regarding illness, injuries, and surgeries, with close attention to upper back and shoulder. A list of allergies and regularly-taken medication will also be part of the history. Subsequently, a basic examination will be performed by the physician-investigator, Paul Moga, D.O. Dr. Moga is a graduate student in the Department of Biomechanics, College of Osteopathic Medicine, of Michigan State University. He is also a Board-certified Osteopathic Family Practitioner, licensed to practice in Michigan.

Both history and physical examination are for the protection of both participant and investigator, in order to provide optimum scientific data while minimizing subject risk. It should be noted that all history and physical examination information as well as any experimental data taken will be held in STRICTEST CONFIDENCE. Presentation of scientific data will be done in a manner so as to PRESERVE PARTICIPANT ANONYMITY.

Because of the non-invasive nature of the experiment, little risk to you is anticipated. As the apparatus is rigid and is to be snugly adjusted, mild discomfort at the points of contact might transiently be noted. You will be asked to inform the investigator, so that readjustments may be made to eliminate discomfort. With PROLONGED, repeated muscle contractions to unconditioned muscles, one might experience temporary soreness. However, with so few contractions at such transient durations as are required by test protocol, the risk of this is low. Finally, in the extreme situation, there is a distant chance of strain of the muscles attached to the shoulder blade.

Participation in the research project is elective and voluntary. It must be understood that you have the right to discontinue participation at any time, or to advance questions and comments to the investigator.

Researcher: Paul J. Moga, D.O.
Department of Biomechanics
Michigan State University
East Lansing, Michigan
(517) 353-9110

#### CONSENT FORM

I have read the Participant Information Form for this project.

I understand the potential risks involved.

I have had all of my questions answered to my understanding and satisfaction.

I realize that I am free not to participate at all, or to discontinue participation at any time without penalty.

I realize that I may ask additional questions at any time.

I understand that results of history, physical examination, and any experimental data taken will be held in strictest confidence, and that anonymity will be preserved in any presentation of the results of this study.

I understand that no medical or other personal benefits are to be expected by me from participation in this study.

I understand that if I am injured as a result of my participation in this research project Michigan State University will provide emergency medical care if necessary, but these and any other medical expenses must be paid from my own health insurance program.

Thus, I freely elect to participate in this research project.

Participant: Witness:

Date: Date:

# 135 APPENDIX D

## PROPOSED BUDGET

Title of Proposed Study: A STUDY OF SCAPULAR DISPLACEMENT BY MOIRE METHODS

Proposed Study:	STOPT OF SCAPULA	· USPU	icelie i i	DI NOIRE	- 161700.	, 
Salaries and Wages:     % Full   Dollar Amounts (omit cents)						
<u> </u>		Total				I Cents)
Name	Position	Hours	Rate/hr	Sa <u>lary</u> Wages	Benefits	Totals
P.J. MOGA	Princ. Invest.	12013	Raie/iii	wages		101013
G.L. CLOUD	ADVISOR	36				
J. NOAKES	GRADUATE STUDENT	10				
K. ZIMMERMAN	GRADUATE STUDENT	3				
RESEARCH ASSISTANT		500	6.50	325000	813,00	4063,00
Forting to the course of the state of the st						
Equipment: MINOLTA X-370 \$175.00 MISC EQUIPMENT \$50.00						1275.00
200 mm lens 225,00 Datascope, 600,00						
PROJECT	Projector 100.00 Strain Gage/wire 20.00					
2 x exte	NDER 76.0			•		
Supplies: CART	\$7500	Pa	NT	430		410.00
	LUMBER 50.00 FILM, 24 ROLLS 70.00					
NARDWARE 15.00 \$ 2,90/Roll						
MAILING 30.00 PHOTO NEG, HOLDERS 15.00						
Misc.	100,00	PAP		14	0.00	
FILM PROCESSING 8 3/ROLL-24 ROLL-72.00 MED. EXAMS 0'25.00 EA. 75.00						
Services: PRNTS: 8410 03,50 x 40 PRINTS 210,00 TYPING 12500						1757.00
LABOR TO MACHINE BAR @ 2500 AR * 2 HR. 50.00 COMPUTER TIME 300.00						
LABOR TO BUILD APPARATUS & 20/18 × 24 HDS, 480.00 TELEPHONE 50.00						
SUBJECT FEES @ 15/SUBJECT X 3 45.00 ARTISTS FEES 175.00						
MISC. 100.00 LEAAL FEES TO REVIEW 75.00						
		.00.00		HT, COUSE		
0	44.00	1 6 AM 22				
Travel: PHOTO PROCE	SSING 24 ROLLS >				MILES	101,00
PHOTO PRINT	Travel: PHOTO PRINTING 3 ROLLS @ 30 MILES/TRIP X 3 90					
CONSTRUCTION / DELIVERY OF APPARATUS 210						
MISC. (504 TOTAL MILES @ 0.20/MILE 101.00) 60						
Alterations and Renovations:						
					1	
•					1	
Other Expenses:					Ì	
and I am fundament / I forestering						
TRADE JOURNAL SUBSCRIPTIONS (J. BIOMECHALICS,						150.00
APPLIED OPTICS, SPINE, ETC.						
		•	-	-	ĺ	
-			# UVO-	THETICAL		7755.00
Total Amount of Fine	ancial Support Reque	sted:	Actu		•	3700.00
- O I G I / WHOULIN OI / THE	Jacobol i Madae		. , . , . , .			

<sup>&</sup>lt;sup>1</sup>Full-time work for salaried persons is figured: (50 wk/yr)(40 hr/wk) = 2000 hr/yr.



#### COMPREHENSIVE LIST OF REFERENCES

- Adair, I.V., Van Wijk, M.C., and Armstrong, G.W.D. Moire topography in scoliosis screening. <u>Clinical Orthopaedics</u> and <u>Related Research</u>. 129: 165-171, 1977.
- Andonian, A.T. Detection of stimulated back muscle contractions by moire topography. <u>J. Biomechanics</u>. 17(9): 653-661, 1984.
- Barry, D.T., Geiringer, S.R., and Ball R.D. Acoustic myography: a noninvasive monitor of motor unit fatigue. Muscle & Nerve. 8:189-194. 1985.
- Barry, D.T., Leonard, J.A., Gitter, A.J., and Ball, R.D. Acoustic myography as a control signal for an externally powered prosthesis. <u>Arch. Phys. Med. Rehabil.</u> 67:267-269. 1986.
- Beeson, P.B., and McDermott, W. <u>Textbook of Medicine (14th ed.)</u>. (pp. 793-795). Philadelphia: Saunders, 1975.
- Benoit, P., Mathieu, E., and Thomas, A. Sign determination of contour lines. Optics Communications. 15(3): 392-395, 1975.
- Bigland-Ritchie, B. and Woods, J.J. Changes in muscle contractile properties and neural control during human muscular fatigue. <u>Muscle & Nerve.</u> 7:691-699, 1984.
- Brooks, R.E. and Heflinger, O. Moire gauging using optical interference patterns. <u>Applied Optics</u>. 8(5): 935-939, 1969.
- Clamann, H.P. and Broecker, M.S. Relation between force and fatigability of red and pale skelatal muscles in man. Am. J. Phys. Therapy. 58:70, 1979.
- Cox, A. <u>Photographic Optics</u>. (pp. 28-40). New York: Focal Press, 1971.
- Dally, J., and Riley, W. <u>Experimental Stress Analysis</u>. (pp. 380-405). New York: McGraw-Hill, 1978.
- De Luca, C.J. Myoelectrical manifestations of localized muscular fatigue in humans. <u>CRC Crit. Rev. in Biomed. Eng.</u> 11:251-279, 1984.

- Dvir, Z., and Berme, N. The shoulder complex in elevation of the arm: a mechanism approach. <u>J. Biomechanics</u>. 11:219-225, 1978.
- Ford, L.E., Huxley, A.F., and Simmons, R.M. The relation between stiffness and filament overlap in stimulated frog muscle fibres. <u>J. Physiol.</u> 311:219-249, 1981.
- Freund, H.J. Motor unit and muscle activity in voluntary motor control. Physiol. Rev. 63:387-436, 1983.
- Goss, C.M. (Ed.). Gray's Anatomy (29th ed.). (pp. 200, 445-449). Philadelphia: Lea & Febiger, 1974.
- Gydikov, A., Dimitrov, G., Kosarov, D., and Dimitrova, V. Functional differentiation of motor units in human opponens pollicis muscle. <u>Exp. Neurol.</u> 50:36-57, 1976.
- Hagberg, M. Muscular endurance and surface electromyogram in isometric and dynamic exercise. <u>J. Appl. Physiol.</u>, Respirat. Environ. Exercise Physiol. 51(1): 1-7, 1981.
- Hagberg, M. On Evaluation of Local Muscular Load and Fatigue By Electromyography. (Arbite Och Halsa 24). Umea University Medical Dissertations, 1981.
- Inman, V.T., Saunders, J.R. de C.M., and Abbott, L.C. Observations on the function of the shoulder joint. <u>J. Bone Joint Surg.</u> 26 A:1. 1944.
- Khetan, R.P. <u>Theory and Applications of Projection Moire</u> <u>Methods</u> - Doctoral Dissertation, Department of Mechanics, State University of New York at Stony Brook, 1975.
- Livnat, A., and Kafri, O. Slope and deformation mapping by grating projection technique. <u>Optical Engineering.</u> 24(1): 150-152, 1985.
- Lord Rayleigh. On the manufacture and theory of diffraction gratings, in his scientific papers, Cambridge University Press, Vol. 1, p. 209. <u>Philadelphia Magazine</u>. 47: 81-93, 193-205, 1874.
- Martin, L.P., and Ju, F.D. The moire method for measuring large plane, nonhomogeneous deformations. <u>Experimental</u> <u>Mechanics</u>. 10(12): 521-528, 1970.
- Maton, B. Human motor unit activity during the onset of muscle fatigue in submaximal isometric isotonic contraction. <u>Eur. J. Appl. Physiol.</u> 46:271-281, 1981.

- Meadows, D.M., Johnson, W.D., and Allen, J.B. Generation of surface contours by moire patterns. <u>Applied Optics</u>. 9(4): 942-947, 1970.
- Miles, C.A., and Speight, B.S. Recording the shape of animals by a moire method. <u>J. Phys. 'E'.</u> 8: 773-776, 1975.
- Moga, P.J. and Cloud, G.L. A study of scapular displacement by differential moire methods. <u>Proc. Soc. Experimental Mech.</u> Milwaukee, WI. Spring, 1991.
- Morse, S., Durelli, A.J., and Sciammarella, C.A. Geometry of moire fringes in strain analysis. <u>J. Eng. Mech. Div.</u>, <u>ASCE</u>. 86(EM-4): 105-126, 1960.
- Nordin, M. and Frankel, V.H. <u>Basic Biomechanics of the Musculoskeletal System.</u> Lea & Febiger, Phila. 1989.
- Orizio, C., Perini, R., and Veicsteinas, A. Changes of muscular sound during sustained isometric contraction up to exhaustion. <u>J. Appl. Physiol.</u> 66(4):1593-1598. Apr., 1989.
- Oster, G. and Jaffe, J.S. Low frequency sounds from sustained contraction of human skeletal muscle. <u>Biophys. J.</u> 30:119-128. Apr., 1980.
- Oster, G., and Nishijima, Y. Moire patterns. Sci. Amer. 208(54): 54-63, 1963.
- Pollack, G.H., Iwazumi, T., and ter Keurs, H.E.D.J. Sarcomere shortening in striated miuscle occurs in stepwise fashion. Nature. 268:757-759, 1977.
- Poppen, N.K. and Walker, P.S. Normal and abnormal motion of the shoulder. <u>J. Bone Joint Surg.</u> 58 A:195, 1976.
- Roger, R.E., Stokes, I.A.F., Harris, J.D., Frymoyer, J.W., and Ruiz, C. Monitoring adolescent idiopathic scoliosis with moire fringe photography. <u>Engineering in Medicine</u>. 8(3): 119-127, 1979.
- Stulen, F.B. A technique to monitor localized muscular fatigue using frequency domain analysis for the myoelectric signal. Ph.D Thesis. Massachusetts Institute of Technology. Cambridge, Mass. 1980.
- Takasaki, H. Moire topography. <u>Applied Optics</u>. 9(6): 1457-1472, 1970.
- Takasaki, H. Moire topography. Applied Optics. 12(4): 845-850, 1973.

- Tesch, P. and Karlsson, J. Lactate in fast and slow twitch skeletal muscle fibers of man dutring isometric contraction. Acta Physiol. Scand. 99:230, 1977.
- Theocaris, P.S. Moire fringes: a powerful measuring device. Applied Mechanics Reviews. 15(5): 333-337, 1962.
- Theocaris, P.S. Isopachic patterns by the moire method. <a href="Exp. Mech.">Exp. Mech.</a> 4(6): 153-159, 1964.
- Tollenaar, D. Moire: interferentieverschijnselen bij fasterdruk, <u>Amsterdam Instituut Vour Grafische Techniek</u>, 1945.
- Van Wijk, M.C. Moire contourograph an accuracy analysis. J. Biomechanics. 13: 605-613, 1980.
- Viitasalo, J.H.T. and Komi, P.V. Signal characteristics of emg during fatigue. <u>Eur. J. Appl. Physiol.</u> 37:111-121, 1977.
- Yatagai, T., Idesawa, M., Yamaashi, Y., and Suzuki, M. Interactive fringe analysis system: applications to moire contourgram and interferogram. Optical Engineering. 21(5): 901-906, 1982.

#### GENERAL REFERENCES

- Bigland-Ritchie, B., Donovan, E.F., and Roussos, L.S. Conduction velocity and EMG power spectrum changes in fatigue of sustained maximal effects. <u>J. Appl. Physiol.</u>: Respirat. Environ. Exercise Physiol. 51(5): 1300-1305, 1981.
- Boyd, W. <u>A Textbook of Pathology. (8th ed.).</u> (pp. 1192-1384). Philadelphia: Lea & Febiger, 1970.
- Figge, F.H.J. <u>Sobotta-Figge Atlas of Human Anatomy (Vol. 1)</u>. (Figures 149-150). New York: Hafner, 1968.
- Hovanesian, J.D., and Hung, Y.Y. Moire contour-sum contour difference and vibration analysis of arbitrary object.

  Applied Optics. 10(12): 2734-2738, 1971.
- Kadefors, R., Arvidsson, A., Herberts, P., and Petersen, I. EMG data processing in ergonomics, with emphasis on studies of shoulder muscle load, computer-aided electromyography. In J.E. Desmedt (Ed.), <u>Progress in Clinical Neurophysiology (Vol. 10)</u>. (pp. 273-286). Stuttgart: Karger-Basel, 1983.

- Kimura, J. <u>Electrodiagnosis in Diseases of Nerve and Muscle: Principles and Practice.</u> (pp. 491-492). Philadelphia: F.A. Davis, 1986.
- Lockett, A. In H.W. Lee (Ed.), <u>Camera Lenses (5th ed.)</u>. (pp. 32-33). New York: Pitman, 1950.
- O'Donoghue, D.H. <u>Treatment of Injuries to Athletes (3rd ed.)</u>. (pp. 300-330). Philadelphia: Saunders, 1976.
- Ohtsuka, Y., Shinoto, A., and Inoue, S. Application of moire topography and low-dose x-ray imaging to school screening program of scoliosis. In M.S. Moreland, M.H. Pope, and G.W.D. Armstrong (Eds.), Moire Fringe Topography and Spinal Deformity. (pp. 102-112). Elmsford, New York: Pergamon Press, 1981.
- Petrofsky, J.S. Computer analysis of the surface EMG during isometric exercise. <u>Computers in Biology and Medicine</u>. 10: 83-95, 1980.
- Pope, M., Moreland, M., Stokes, I., and Turner-Smith, A. Effects of pelvic tilt on moire fringe analysis. In M.S. Moreland, M.H. Pope, and G.W.D. Armstrong (Eds.), Moire Fringe Topography and Spinal Deformity. (pp. 132-137). Elmsford, New York: Pergamon Press, 1981.
- Salter, R.B. <u>Textbook of Disorders and Injuries of the Musculoskeletal System.</u> (pp. 111-112). Baltimore: Williams & Wilkins, 1970.
- Shinoto, A., Ohtsuka, Y., Inoue, S., Idesawa, M., and Yatagai, T. Quantification of analysis of scoliosis and kyphosis by moire method. In M.S. Moreland, M.H. Pope, and G.W.D. Armstrong (Eds.), Moire Fringe Topography and Spinal Deformity. (pp. 206-224). Elmsford, New York: Pergamon Press, 1981.
- Stokes, I.A., Cobb, I.C., and Moreland, M.S. Surface shape analysis of spinal deformity. <u>Automedica.</u> 6: 71-83, 1985.
- Suzuki, M., Kanaya, M., Suzuki, K., and Shokouchi, N. Projection type moire topography camera (FM-40) system used for early detection of scoliosis. In M.S. Moreland, M.H. Pope, and G.W.D. Armstrong (Eds.), Moire Fringe Topography and Spinal Deformity. (pp. 24-39). Elmsford, New York: Pergamon Press, 1981.
- Theocaris, P.S. Moire patterns of isopachics. <u>J. Sci.</u> Instrum. 41: 133-138, 1964.

Warfel, J.H. <u>The Extremities (4th ed.).</u> (pp. 12-16). Philadelphia: Lea & Febiger, 1974.

Wasowski, J. Moire topographic maps. Optics Communications. 2(7): 321-323, 1970.

MICHIGAN STATE UNIV. LIBRARIES
31293008775607